BERICHTE AUS DEM

ZENTRUM FÜR MEERES- UND KLIMAFORSCHUNG

Reihe A: Meteorologie

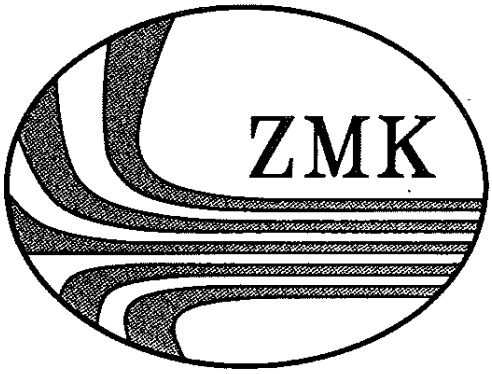

Nr. 3

ARKTIS 1991

Report on the Field Phase
with Examples of Measurements

Edited by

Burghard Brümmer

Zentrum für Meeres- und Klimaforschung der Universität Hamburg
Meteorologisches Institut
1992

Berichte aus dem Zentrum für Meeres- und Klimaforschung
Reihe A: Meteorologie

Nr. 3

ARKTIS 91

Report on the Field Phase with Examples of Measurements

Edited by

Burghard Brümmer

Meteorologisches Institut
Hamburg 1992

Die **"Berichte aus dem Zentrum für Meeres- und Klimaforschung"** erscheinen in 6 Reihen mit folgendem Inhalt:

Reihe A:	Meteorologie
Reihe B:	Ozeanographie
Reihe C:	Geophysik
Reihe D:	Biogeochemie und Meereschemie
Reihe E:	Hydrobiologie und Fischereiwissenschaft
Reihe Z:	Interdisziplinäre Zentrumsberichte

Alle Beiträge sind unredigiert und geben allein die Meinung des Verfassers wieder. Sie sollen in erster Linie dem sich mit dem jeweiligen Thema befassenden Personenkreis als Arbeitsunterlagen dienen und sind oft gleichzeitig Berichte für die Institutionen, die die betreffenden Arbeiten gefördert haben.

Exemplare dieser Arbeit können bezogen werden über:

Meteorologisches Institut
Bundesstr. 55
D-2000 Hamburg 13

ISSN 0936-949X

Zentrum für Meeres- und Klimaforschung der Universität Hamburg
Bundesstr. 55 - 2000 Hamburg 13

1. *Introduction*

(B. Brümmer, Meteorologisches Institut der Universität Hamburg)

1.1. *Scientific objectives*

The field experiment ARKTIS 1991 was an expedition planned by meteorologists of the Sonderforschungsbereich 318 entitled "Climatically relevant processes in the system ocean-atmosphere-ice" which is funded by the German Science Foundation and established at the University Hamburg. The expedition took place in the Norwegian Sea between Northern Norway, Bear Island and Jan Mayen during the period 17 February until 15 March 1991 (Figure 1.1).

The main aim of the experiment was the investigation of cold air outbreaks from the surrounding arctic ice sheets. During such weather episodes the air mass coming from the ice is rapidly modified over the water due to the contrasts in temperature, heat conduction, humidity and roughness between ice and water. This leads to the formation of a "new" boundary layer. Its depth, mean temperature and moisture increase with increasing distance from the ice edge mainly due to sensible and latent heat supply from the ocean (Figure 1.2).

Depending on the air-sea temperature difference and the wind speed the sensible heat flux from the ocean to the atmosphere is between 50 and several 100 W/m^2 in cold air outbreaks. This is considerably more than the sensible heat fluxes averaged over the whole Earth surface or over all ocean surfaces which are 20 W/m^2 and 15 W/m^2, respectively. It also stresses the climatological importance of cold air outbreaks for the energy budget of atmosphere and ocean. According to Budyko (1978) the world-wide largest annual mean value of the sensible heat flux over the ocean, namely about 60 W/m^2, occurs in the regions north of Northern Norway. The experimental area of ARKTIS 1991 was situated in the southern part of this region.

The cold air coming from the ice sheets is mostly cloud-free. Due to evaporation at the sea surface the moisture in the boundary layer increases and clouds will develop at some distance from the ice edge. In strong wind situations these clouds are organized in streets which mark the upwind lines of roll-like, nearly wind-parallel secondary circulations. Satellite images show that the cloud streets broaden with increasing distance from the ice edge and often change into open or closed cellular cloud patterns at several 100 km to 1000 km distance from the ice edge. This pattern transformation is accompanied by an

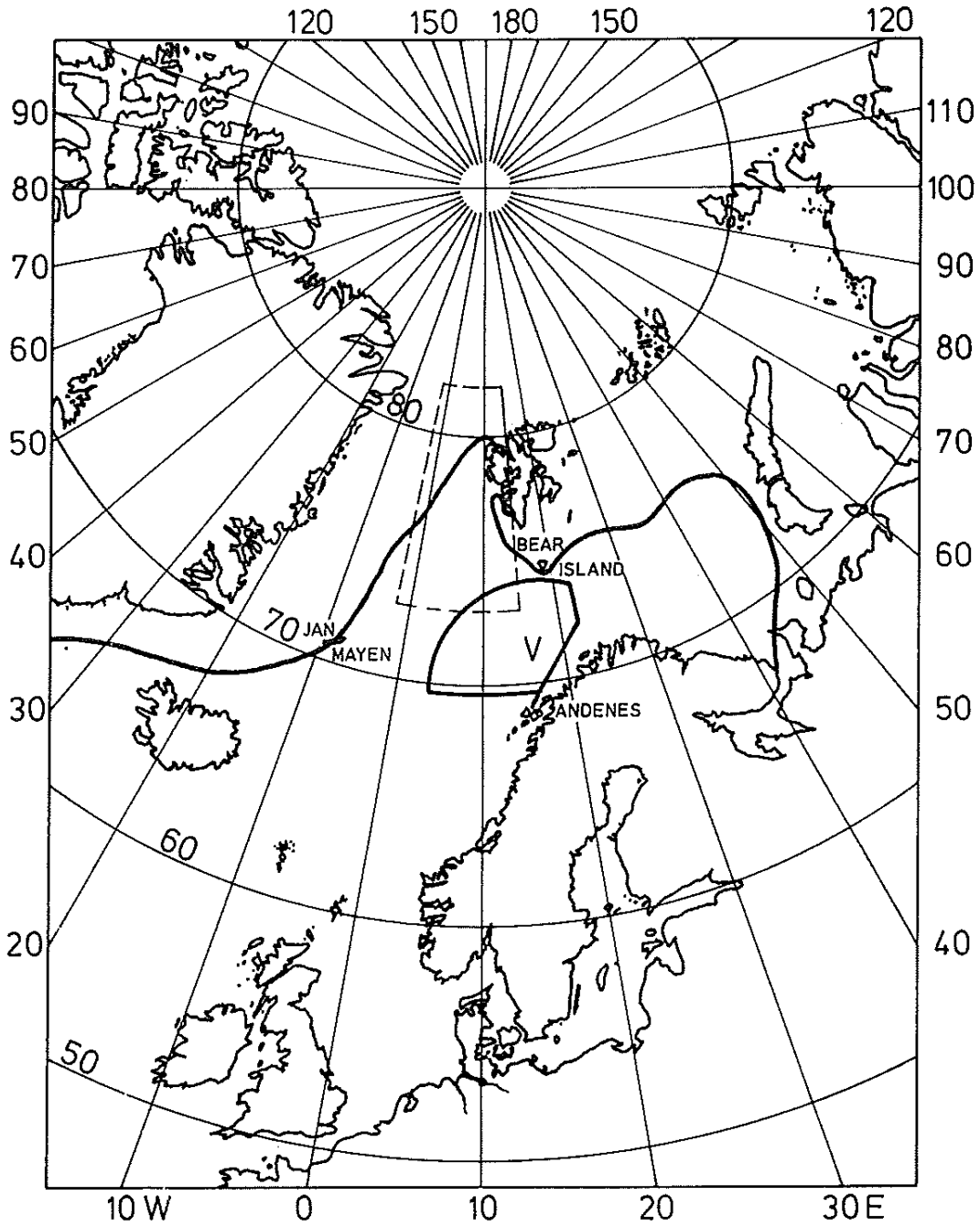

Figure 1.1: The experimental area of ARKTIS 1991 in the Norwegian Sea between Northern Norway, Bear Island and Jan Mayen is surrounded by a full line. The letter "V" marks the average position of research vessel VALDIVIA. The aircraft operation base was the airfield ANDENES. The thick full line shows the average ice edge. The experimental area of ARKTIS 1988 is surrounded by a dashed line.

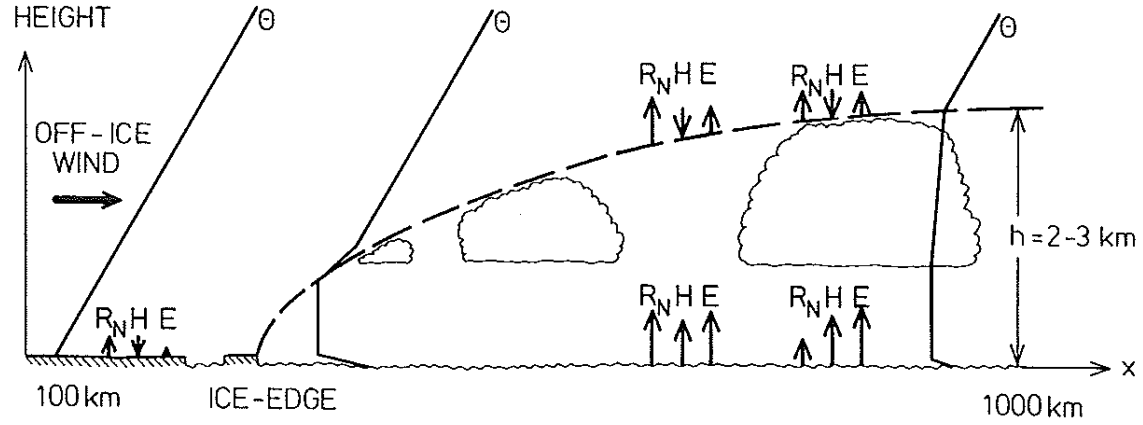

Figure 1.2: Schematic representation of boundary layer modification during a cold air outbreak from the sea-ice over the open water. Θ is potential temperature, R_N, H, E are the net radiative, sensible and latent heat flux, respectively.

increase of the aspect ratio between the horizontal wavelength and the vertical depth of the convective pattern.

Laboratory and numerical experiments have shown that several processes may be the reason for the convective pattern transition and aspect ratio increase in cold air outbreaks, as e.g. the mean vertical motion, turbulence exchange, latent heat release, density stratification above the boundary layer and others. However, a direct assignment of one or more of these processes in observed cases of transition from cloud streets to open or closed cells has not been made. Furthermore, it has not been investigated which consequences the pattern transition has for the vertical transports of heat, moisture and momentum by the secondary flows.

Closely connected with the problem of pattern transition is the problem of cloud coverage in cold air outbreaks. The total heat loss of the ocean depends to a large degree on the longwave radiative heat loss, which in turn depends on cloud cover. The radiative heat loss can vary between about 100 W/m^2 under clear sky conditions and about zero W/m^2 under overcast conditions. This is a considerable difference and will affect the formation of sea ice and convection in the water.

Beside the main aim of ARKTIS 1991, the investigation of cold air outbreaks, other aims of secondary priority had to be formulated because cold air outbreaks cannot be expected to occur permanently during a four weaks period and the expensive experimental infra-structure has to be used efficiently. The secondary goals were (a) the investigation of marine arctic stratus or stratocumulus, especially to study the conditions of its generation and dissolution, and (b) the detection and investigation of sub-synoptic scale vortices, so-called polar lows, developing in the cold air over the warm water. The weather conditions during the experiment were favourable so that each of these aims could be investigated.

References

Budyko, M.I. (1978): The heat balance of the Earth. in: Gribbin J. (ed.): Climatic Change. Cambridge University Press, 85-113.

1.2. Logistic considerations

The investigations of cold air outbreaks and arctic stratus by scientists of the Sonderforschungsbereich 318 began already three years ago with the field experiment ARKTIS 1988 which took place in May 1988 in the area west of Spitsbergen (see Figure 1.1). ARKTIS 1991 is an continuation of this work, this time under winterly weather conditions.

Since the cold air outbreaks during ARKTIS 1988 were relatively weak and could only be investigated at a few hundred kilometers distance from the ice edge, we decided to place ARKTIS 1991 in the winter season and further southward at longer distances from the ice edge. As in ARKTIS 1988 the research vessel VALDIVIA and the two research aircraft FALCON-20 of the DLR at Oberpfaffenhofen and DO-128 of the TU Braunschweig were at our disposal. The research icebreaker POLARSTERN was not available, because the POLARSTERN normally operates in the Antarctic region during this time of the year.

In order to obtain the initial conditions over the ice during a cold air outbreak, the meteorological station of the Norwegian Weather Service on Bear Island was incorporated into the experimental programme with three-hourly surface observations and six-hourly radiosonde ascents. In case of winds from north to northeast, it may be assumed that the conditions on Bear Island are representative of those over the ice, because the ice edge extends to the island or is not

far away from it during this time of the year. The ice charts in Appendix E show that this was also true in February and March 1991.

The downstream modification of the boundary layer, the formation of organized convection and clouds and the transition from one convective pattern to another were documented by the measurements at the RV VALDIVIA and of the two aircraft. VALDIVIA was situated about 400 km S/SW of Bear Island approximately in the center of the warm Western Norwegian current with sea surface temperatures around 6°C. Here, surface observations were made every hour, radiosonde ascents up to 15 km height and oceanographic profilings down to 500 m depth every four hours as well as continuous registrations of surface layer data at a meteorological mast and radiometric measurements of the sea surface temperature.

The two aircraft operated from the military airfield in Andenes on the Vesteralen island Andøya. This is an logistically excellent place because it is right at the edge of the experimental area. Depending on the weather conditions the flight missions were flown at different places in a direction sector between W and NE of Andenes (Appendix D). Since the processes under investigation occur over large horizontal distances the experimental flight strategy was to fly joint missions with both aircraft but at different distances from Andenes. According to the different flight specifications, the FALCON-20 operated at larger distances from Andenes and smaller distances to the ice edge whereas the DO-128 operated in an area downstream of the FALCON and at nearer distances from Andenes.

Andenes was also the place of the operation center for the whole ARKTIS 1991 campaign. The operation center was accommodated in the office of the Andøya Rocket Range which is part of the Norwegian Space Center. Aircraft operations were planned on the basis of weather forecasts received from the German and Norwegian Weather Service and on the basis of NOAA satellite images, received at the Tromsø Satellite Station, transmitted to Andenes by computer links and processed and printed in the operation center.

1.3. Participating institutions and acknowledgement

The expedition ARKTIS 1991 was initiated and organized by scientists of the Meteorological Institute of the University of Hamburg and the Max-Planck-Institute for Meteorology at Hamburg which work together in the Sonderforschungsbereich 318.

However, without the contributions and supports of other institutions an experiment of this size would not have been possible. These institutions were:
Deutsche Forschungsanstalt für Luft- und Raumfahrt (DLR), Oberpfaffenhofen,
Institut für Flugführung der Technischen Universität Braunschweig,
Institut für Meereskunde der Universität Hamburg,
Det Norske Meteorologiske Institutt (NMI) at Oslo and Tromsø,
Norwegian Space Center at Oslo, Tromsø and Andenes,
Norwegian Air Force at Andenes.

Particular thanks are referred to:
Prof. U. Schumann of the DLR and Prof. H. Schänzer of the TU Braunschweig, who agreed to use the FALCON-20 and DO-128, respectively. Prof. J. Meincke of the Institut für Meereskunde, who placed the Kieler Multisonde at our disposal, Profs. A. Eliassen and M. Lystad of the NMI in Oslo, who decided to support the experiment by additional radiosonde ascents on Bear Island, Dr. K. Wilhelmson of the NMI in Tromsø, who supported the logistic preparation of the experiment, Mr. K. Adolfsen of the Norwegian Space Center, who agreed to use Andøya Rocket Range as operation center and organized the allowance to use the airfield Andenes as operation base, and last but not least Major K. Alvheim of the military airfield Andenes, who organized the support of the aircraft operations.

2. *Measurements on board RV VALDIVIA*

(G. Kruspe, Max-Planck-Institut für Meteorologie, Hamburg)

2.1. *General Remarks*

2.1.1. *The Cruise*

The cruise "108" of the RV VALDIVIA was mainly dedicated to meteorological measurements of the planetary boundary layer within the ice free region of the European Polar Sea (Figure 2.1). VALDIVIA left Hamburg on 17 February 1991, to overtake its role as a mobile observational platform about 250 km north of the Vesteralen islands. The ship reached the observational area on 22 February 1991. From 5 March 1991 22 UT until 6 March 1991 22 UT VALDIVIA left the measuring area, to bunker engine fuel in Tromsø/Norway, however, without interrupting the aerological program for longer than 4 hours. When the coordinated field phase ended on 14 March 1991, VALDIVIA was already cruising to Reykjavik (Iceland) along a zonal path at 71°N latitude through a convective cloud field. The crew disembarked in Reykjavik on 16 March 1991.

2.1.2. *Participants*

The scientific crew involved in the measuring programs on board the VALDIVIA consisted of 11 members, seven of them were students of the Meteorological Institute of the University of Hamburg. They kept highly motivated all time regardless of the often very rough sea conditions. Two technicians were responsible for the meteorological and oceanographical instruments. The scientific programs were supported by the professional help of the chief master Klaaßen and his excellent crew.

The members of the scientific crew (Figure 2.2) were: Sven Anderson (cand. rer. nat., Aerological Routine), Werner Biselli (SFB 318, technician), Gabriele Fischer (cand. rer. nat., AR), Martin Fortmann (cand. rer. nat., AR), Dr. Gottfried Kruspe (Max-Planck-Institut für Meteorologie, chief scientist and cruise leader), Michael Offermann (University of Hamburg, technician), Paul Frank (cand. rer. nat, AR), Detlev Persson (cand. rer. nat. Oceanographic Routine), Dr. Peter Schlüssel, (University of Hamburg, scientist, especially KT4 experiments, OR), Jens Schumacher (cand. rer. nat., AR), Susanne Waszkewitz (cand. rer. nat., AR).

2.1.3. *Experimental Program*

The main experimental tasks of the VALDIVIA were to monitor continuously the mean vertical structure of the relevant meteorological quantities (wind, temperature and moisture) within the troposphere. The aerological sounding frequency was 6 per day, with the launch schedule 00, 04, 08, 12, 16, 20 UT. Oceanographic profiling of sea temperature and salinity down to 500 m depth followed also that 4-hourly schedule but one hour earlier for nautical reasons. All aerological and oceanographical soundings are listed in Table 2.1. The extensive vertical sounding of atmosphere and ocean was accompanied by continuous sampling of surface layer data on two meteorological masts to evaluate the relevant parameters of the air-sea interaction processes (stability parameter, heat, moisture and momentum fluxes). To relate the automatically measured quantities to the visible meteorological phenomena, intensive observations of cloud type, cloud cover, visibility and other weather phenomena were carried out at least every hour. An automatic APT-reception of polar orbiting satellites on board the VALDIVIA (System Technavia from Skyceiver Silver) allowed for identification of the cloud situation and the sea ice edges in the wider environment of the ship. Finally, a radiation thermometer KT4, measured continuously the sea skin temperature, which is important for the transfer of heat at the sea-air interface.

Table 2.1: Times, locaction and altitudes/depths of radiosonde and CTD soundings. First time is for CTD, second time for radiosonde.

Date	Sounding time [UT]	Longitude [°E]	Latitude [°N]	Radiosonde height [m]	CTD depth [m]
22 February	2300/0000	4.05	68.23	12876	500
	0300/0400	6.21	69.52	10963	500
	0700/0820	6.85	69.92	13266	500
	1050/1150	7.01	70.01	14010	500
	1500/1550	7.03	70.04	12648	490
	1900/1950	7.04	70.09	11074	500
	2300/0030	7.01	70.13	13102	
23 February	0300/0400	6.89	70.17	11860	500
	0700/0750	6.92	70.20	11486	510
	1100/1130	7.00	70.23	14446	520
	1500/1610	7.10	70.26	14316	490
	1900/2000	7.16	70.30	13030	500
	2300/0010	7.28	70.33	12439	500
24 February	0300/0420	7.68	70.39	13284	490
	0700/0750	8.87	70.46	12265	500
	1100/1150	10.07	70.56	15003	500
	1500/1550	10.96	70.61	13376	500
	1900/2020	12.35	70.66	13832	500
	2300/0050	13.81	70.77	10419	500

Date	Sounding time [UT]	Longitude [°E]	Latitude [°N]	Radiosonde height [m]	CTD depth [m]
25 February	0300/0350	13.94	71.23	15226	520
	0700/0750	14.04	71.50	14899	500
	1100/1150	14.16	71.53	14972	500
	1500/1550	14.13	71.53	15216	510
	1900/1950	15.09	71.50	15198	500
	2300/2340	14.20	71.44	14234	75
26 February	0300/0400	14.00	71.49	14503	500
	0700/0750	13.89	71.50	14046	500
	1100/1140	13.85	71.45	14835	500
	1500/1600	13.89	71.44	13086	510
	1900/2000	13.63	72.34	12937	500
	2300/2340	13.75	71.45	12715	500
27 February	0300/0350	13.90	71.40	11383	500
	0700/0750	14.02	71.35	13216	500
	1100/1140	14.10	71.31	15124	510
	1500/1620	13.94	71.27	13108	500
	1900/2000	13.80	71.22	12601	500
	2300/2350	13.75	71.17	14568	420
28 February	0300/0400	13.62	71.09	15025	500
	0700/0910	13.69	71.20	15004	500
	1100/1140	13.56	71.18	12681	510
	1500/1550	13.42	71.15	14606	500
	1900/1950	13.40	71.08	16513	500
	2300/2340	13.32	70.99	15695	
01 March	0300/0400	13.30	70.95	14849	500
	0700/0750	13.40	70.86	13865	500
	1100/1140	13.74	71.37	16354	500
	1500/1550	13.96	71.48	15675	500
	1900/2050	13.85	71.42	13511	500
	2300/2340	13.79	71.39	16870	500
02 March	0300/0350	13.78	71.39	15476	500
	0700/0800	13.84	71.36	16741	500
	1100/1150	13.87	71.33	16575	500
	1500/1550	13.86	71.33	13873	500
	1900/1950	14.00	71.33	16248	500
	2300/0050	14.09	71.25	15251	510
03 March	0300/0350	14.10	71.20	11987	500
	0700/0750	14.09	71.18	15504	500
	1100/1140	14.14	71.36	11524	520
	1500/1550	14.34	71.37	15574	500
	1900/1950	14.65	71.34	12868	520
	2300/0010	14.74	71.31	15424	500
04 March	0300/0350	14.93	71.30	15737	500
	0700/0740	15.08	71.31	15565	500
	1100/1150	14.96	71.32	16664	500
	1500/1550	15.01	71.33	11457	410
	1900/2000	15.08	71.39	15155	
	2300/2350	15.21	71.44	14292	500

Date	Sounding time [UT]	Longitude [°E]	Latitude [°N]	Radiosonde height [m]	CTD depth [m]
05 March	0300/0400	15.33	71.51	15339	500
	0700/0800	15.48	71.60	16432	520
	1100/1200	15.50	71.64	16833	510
	1500/1550	15.62	71.70	13869	500
	1900/2000	16.08	71.28	14343	520
	2300/0000	16.68	70.75	15165	500
06 March	0300/0400	17.41	70.06	14980	
	0700/0900	17.90	69.60	14860	
	2000/2030	17.77	69.68	13024	
	2300/2340	16.81	70.18	13029	510
07 March	0300/0350	15.87	70.63	13178	500
	0700/0800	14.91	71.10	14437	500
	1100/1150	13.90	71.50	16026	500
	1500/1600	14.08	71.51	14699	500
	1900/1950	14.41	71.52	12834	500
	2300/2340	14.75	71.54	15117	500
08 March	0300/0410	14.92	71.59	14726	500
	0700/0750	15.16	71.68	15507	500
	1100/1150	15.35	71.72	14425	500
	1500/1610	15.53	71.75	12560	500
	1900/1950	15.81	71.81	14572	450
	2300/2350	16.01	71.89	14919	400
09 March	0300/0350	16.19	71.93	13818	370
	0700/0800	16.40	71.94	16860	320
	1100/1140	15.11	71.60	9065	
	1500/1550	15.38	71.74	14710	
	1900/1950	15.70	71.78	8775	500
	2300/0000	16.16	71.81	15154	500
10 March	0300/0350	16.45	71.81	12900	500
	0700/0820	16.74	71.82	14512	290
	1100/1210	16.64	71.79	16979	330
	1500/1600	14.95	71.64	15807	500
	1900/2050	13.74	71.31	14940	510
	2300/2340	14.04	71.40	15762	500
11 March	0300/0350	12.80	71.12	14567	500
	0700/0820	11.52	70.89	15704	500
	1100/1150	10.87	70.76	16759	500
	1500/1550	9.48	70.50	13730	530
	1900/1950	7.85	70.28	15559	500
	2300/2350	6.29	70.22	12766	530
12 March	0300/0350	4.75	70.17	15073	500
	0700/0800	3.29	70.12	16437	500
	1100/1140	1.74	70.06	16889	520
	1500/1550	0.24	70.00	15886	510
	1900/1950	0.60	69.71	15626	510
	2300/0000	0.43	69.74	14787	520

Date	Sounding time [UT]	Longitude [°E]	Latitude [°N]	Radiosonde height [m]	CTD depth [m]
13 March	0300/0350	0.29	69.77	15280	500
	0700/0750	0.22	60.79	15898	500
	1100/1150	0.36	69.78	16182	490
	1500/1600	0.40	69.77	16265	510
	1900/1950	0.40	69.91	16111	500
	2300/2350	- 0.55	69.31	15679	
14 March	0300/0430	- 2.79	68.72	16463	
	0700/0750	- 3.73	68.31	15794	
	1100/1200	- 4.48	67.79	17382	
	1500/1540	- 5.16	67.30	16276	
	1900/2000	- 6.03	66.83	16021	
	2300/2350	- 8.94	66.38	15668	

2.1.4. Observational Strategy

VALDIVIA operated between 71° - 72°N and 12° - 17°E from 24 February 20 UT until 11 March 06 UT except for the short Tromsø break. For the position 71°N, 14°E, the distance from the mean ice edge was about 420 and 700 km in NE and NW direction, respectively. The experimental area fits the trajectory for the NE-sterly boundary layer flow from the ice margin near Bear Island satisfactorily. Daily two status reports were send by Telex to the operation center at Andenes to inform about the actual meteorological situation at VALDIVIA. Reports by telephone planned at fixed times normally failed due to the overall bad radio communication conditions. Two aerological soundings (00, 12 UT) were telegraphed as SHIP TEMP to the office of the Norwegian Weather Service at Tromsø to make them available for the routine forecasts.

2.1.5. Overview about instrumentation

The equipment used on board the VALDIVIA is summarized in Table 2.2 and partly photographically documented in Figures 2.3a-c.

Table 2.2: Measuring devices on board the VALDIVIA during ARKTIS '91.

A. Automatic Stations for Surface Layer	
Foredeck station (h = 15 m)	Afterdeck station (h = 8 m)
Pressure digiquartz	
Cup anemometer, wind vane	Cup anemometer, wind vane
Heated aspiration psychrometer	Heated aspiration psychrometer
Global shortwave radiation	
B. Additional Instrumentation for Surface Layer Data	
Hand-held ventilated psychrometer (h = ~ 5m)	
Hand-held cup anemometer	
Precision aneroid	
Bucket water temperature (~ - 0.3 m)	
Automatic sampling water thermometer (~ - 4 m)	
Nautical equipment	
MAGNOVAX-satellite navigation system	
Global positioning system navigation	
Anschütz compass	
SAGEM-LOG	
C. Upper Air	
Vaisala MicroCora System with Omega windfinding	
Radiosonde RS80 N15	
Height of start level: 5 m	
D. Surface Radiation Temperature	
KT4 thermometer with attached calibration equipment	
E. Subsurface Profiling	
CTD-sonde (Kieler Multisonde) of Institut für Meereskunde, Hamburg	
Temperature, conductivity, pressure	
Mean depth achieved: 500 m	
F. Polar Orbiting Satellite Reception	
Technavia System, manufactured by SKYCEIVER SILVER for APT- reception of NOAA images (VIS, IR)	

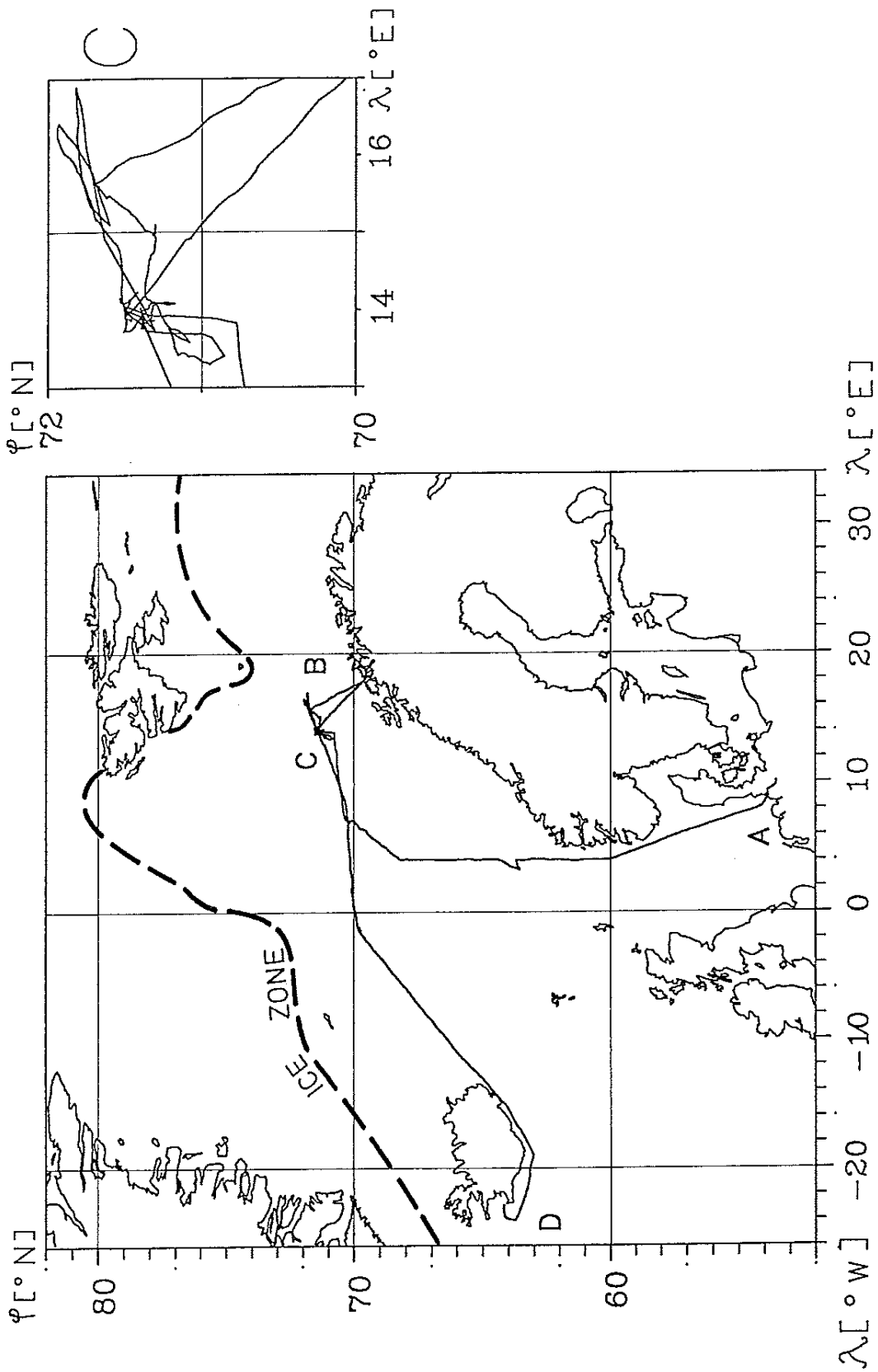

Figure 2.1: Cruise "108" of RV VALDIVIA: A: Departure from Hamburg 17 February 1991, 10 UT; B: Refueling in Tromsø 06 March 1991, 11-18 UT; C: Main experimental area: 70-72°N, 13-17°E; D: Disembarcation Reykjavik 16 March 1991.

Figure 2.2: The scientific crew of VALDIVIA during ARKTIS '91 (from left): D. Persson, J. Schumacher, S. Waskewitz, S. Anderson, P. Schlüssel, M. Offermann, G. Fischer, M. Fortmann, W. Biselli, P. Frank, G. Kruspe.

Figure 2.3a, b: Inflating and starting a balloon with radiosonde RS80/N15 by G. Fischer.

Figure 2.3c: Fore-deck station with aircraft DO-128 during a calibration flight.

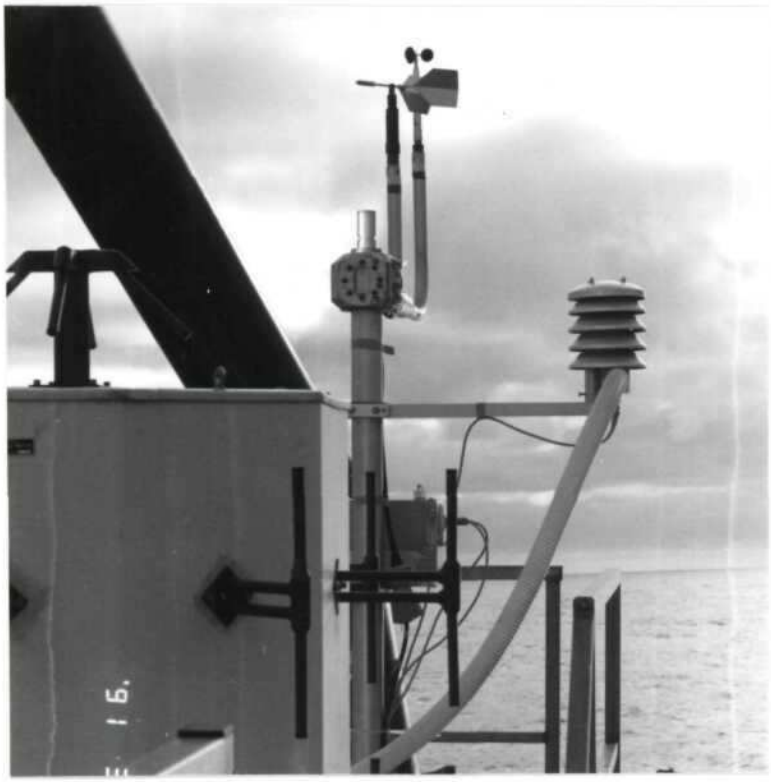

Figure 2.3d: After-deck station with meteorological sensors.

Figure 2.3e: The Kieler Multisonde (KMS) on deck.

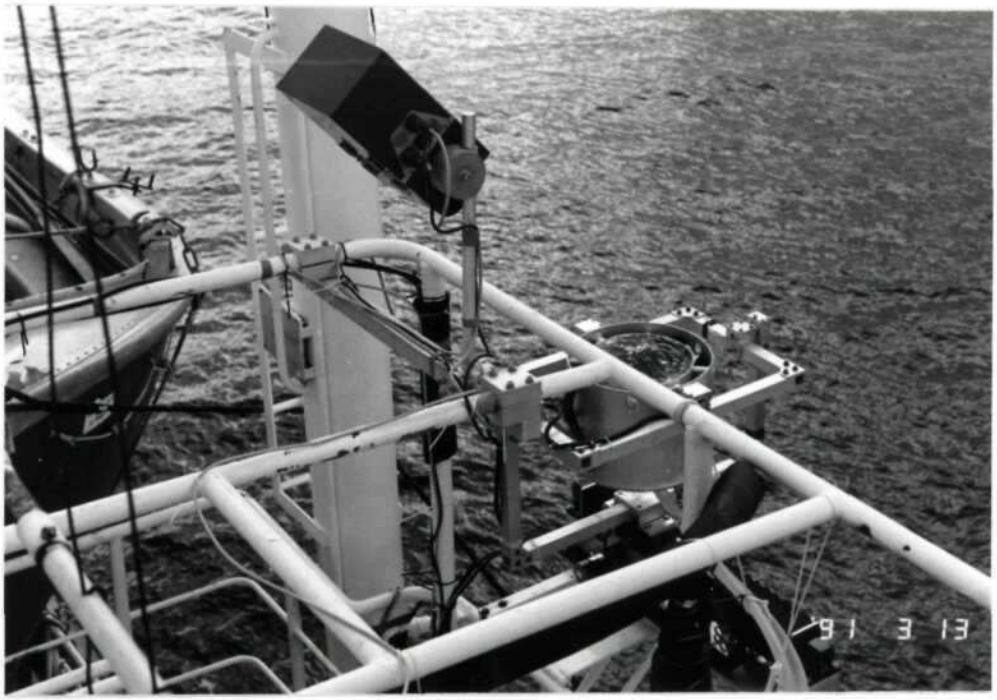

Figure 2.3f: Radiation thermometer KT4 with calibration device.

2.2. *Measurements in the Surface Layer*

(G. Kruspe, Max-Planck-Institut für Meteorologie, Hamburg)

2.2.1. *Experimental Set-up*

Two analogous systems, designed for continuous observations of the relevant meteorological surface parameters were mounted on the foredeck mast (Figure 2.3c) and on a afterdeck mast at port side (Figure 2.3d). The latter was placed on top of the balloon inflation container. The heights above sea level were 15 m and 8 m, respectively.

The two systems provided real wind data from nearly all wind directions relative to the ship, except for small direction sectors which are disturbed by the ship's superstructure. The wind was corrected for movements of the ship. Mean values of the various quantities, averaged over 30 seconds, were recorded on PC discs, simultaneously with the ship's heading and speed, the later relative to the water (SAGEM LOG). The automatically recorded data were checked twice the day by measurements with hand-held instruments.

Noticeable periods of data loss occurred due to malfunction of the cup anemometer on the foredeck mast, mishandling of the PC software for automatic recording of the data, and services of the sensors.

Table 2.3: Periods of malfunction of the automatic surface layer stations.

Periods of malfuction				Remarks
20 Feb.	04:00 UT	- 20 Feb.	10:30 UT	No continuous data
24 Feb.	09:30 UT	- 24 Feb.	20:00 UT	No continuous data
26 Feb.	09:00 UT	- 26 Feb.	10:00 UT	No continuous data
28 Feb.	21:00 UT	- 28 Feb.	23:30 UT	No continuous data
01 March	15:00 UT	- 03 March	16:00 UT	No continuous winds from the foremast
06 March	07:45 UT	- 06 March	08:15 UT	No continuous data
10 March	09:00 UT	- 10 March	10:00 UT	No continuous data

Figures 2.4a - 2.4c give an example of the daily data flow from the two automatic stations. The time series of cruise and heading (Figure 2.4c) also reflect the aerological and CTD sounding cycles: short spikes in the heading curve are ship maneuvers during the radiosonde launches and the about half an hour long interruptions of the cruise and heading curves indicate the times of CTD profiling. The wind difference between foremast (index m) and aftermast (index h) result apart from the different sensor heights mainly from the disturbing superstructures of the ship. To provide for sufficient ventilation of

the thermodynamic sensors during weak wind situations, the ship moved at moderate cruise speed.

Surface layer data were completed by hourly bucket measurements of the water temperature T_w.

2.2.2. Results

Hourly values of the automatic surface layer station and various quantities derived therefrom are shown in Figures 2.5a-c for the entire observational period. The data gaps, as listed in Table 2.3, could be closed by informations from paper records, data from the hand-held instruments, or in case of malfunction of the foredeck anemometer by the wind data of the afterdeck mast. The index "10" marks values reduced to 10 m height according to formulae which account for the stability in the surface layer. The specific humidity at the sea surface has been assumed as 98% of the saturation specific humidity q_s (T_w). The Monin-Obuchov stability parameter z/L is calculated from the Monin-Obuchov length L and the height z = 10 m. The lifting condensation level z_{LCL} is referred to 10 m height. The Bowen ratio B is the ratio of the sensible heat flux H to the latent heat flux E. The measured time series of the various quantities have to be seen in context with the synoptic situation and the distance from the ice edge. With respect to VALDIVIA's position in the experimental area, northeasterly wind components led to be most significant convective effects in the surface layer (Figure 2.6a). A comparison of the ice station Bear Island and open water station VALDIVIA is given in Section 3.

From 28 February until 10 March (neglecting the break in Tromsø) the air temperature steadily decreased from about 4°C to 0°C (long term tendency -0.4 K/day). This was accompanied with a long term negative pressure tendency of about -2 hPa/day. During this period, the prevailing wind direction changed from southerly to easterly directions implying increasing cold air advection from the ice region. The water temperature was relatively high around the 6°C level due to the influence of the Golf stream. The mean vertical air-sea temperature difference was about -5 K. Remarkable cold air outbreaks occurred on 25 February, 6 March and 13 March with DT10 values near -8 K.

Over the whole period, the stratification in the surface layer was unstable. During periods with wind speeds greater than 8 m/s a nearly adiabatic stratification ($-0.2 < z/L < 0$) was observed (forced convection). During the remaining time with FF < 4 m/s free convective conditions were predominant ($z/L \leq -5$).

The mean wind over the whole period was about 9 m/s. Three longer phases occurred, when the mean surface wind averaged over 10 minutes exceeded 15 m/s (maximum observed value 22 m/s), namely 19 February 19 UT - 21 February 01 UT with wind from SW (not shown in Figure 2.5a), 27 February 05 UT - 28 February 01 UT with wind from SSW, and 09 March 08 UT - 10 March 12 UT with wind from E. According to the histogram in Figure 2.6b winds from 22.5 - 67.5 degree (off ice flow) occurred in about 40% of the time. In nearly 15% of the measuring period wind directions from south as well as from north were observed.

The mean specific humidity and relative humidity over the whole period were about 3 g/kg and 70%, respectively. A long term decrease of the moisture content due to steadily increasing advection of relatively dry and cold air was observed from 1 March until 8 March. During this period, the specific humidity of the surface layer dropped from about 4 g/kg to 2.5 g/kg, accompanied with the longterm trend of the relative humidity from about 80% to 55%. Consequently, the course of the lifting condensation level follows inversely to that of the relative humidity. The mean value over the whole period was about 600 m.

The mean heat fluxes H and E averaged over the whole period were about 75 and 125 W/m^2, respectively, and the mean Bowen ratio B was about 0.6. B dropped to about 0.4 during periods of advection of relative warm atlantic air because of small temperature differences between air and water ($T_a - T_w \sim -2$ K). During the period 1 - 10 March H and E increased steadily from 50 to 150 W/m^2 and 75 to 200 W/m^2, respectively. The momentum flux is remarkable during the strong wind situations. Maximal values up to 0.7 N/m^2 were measured on 9 - 10 March.

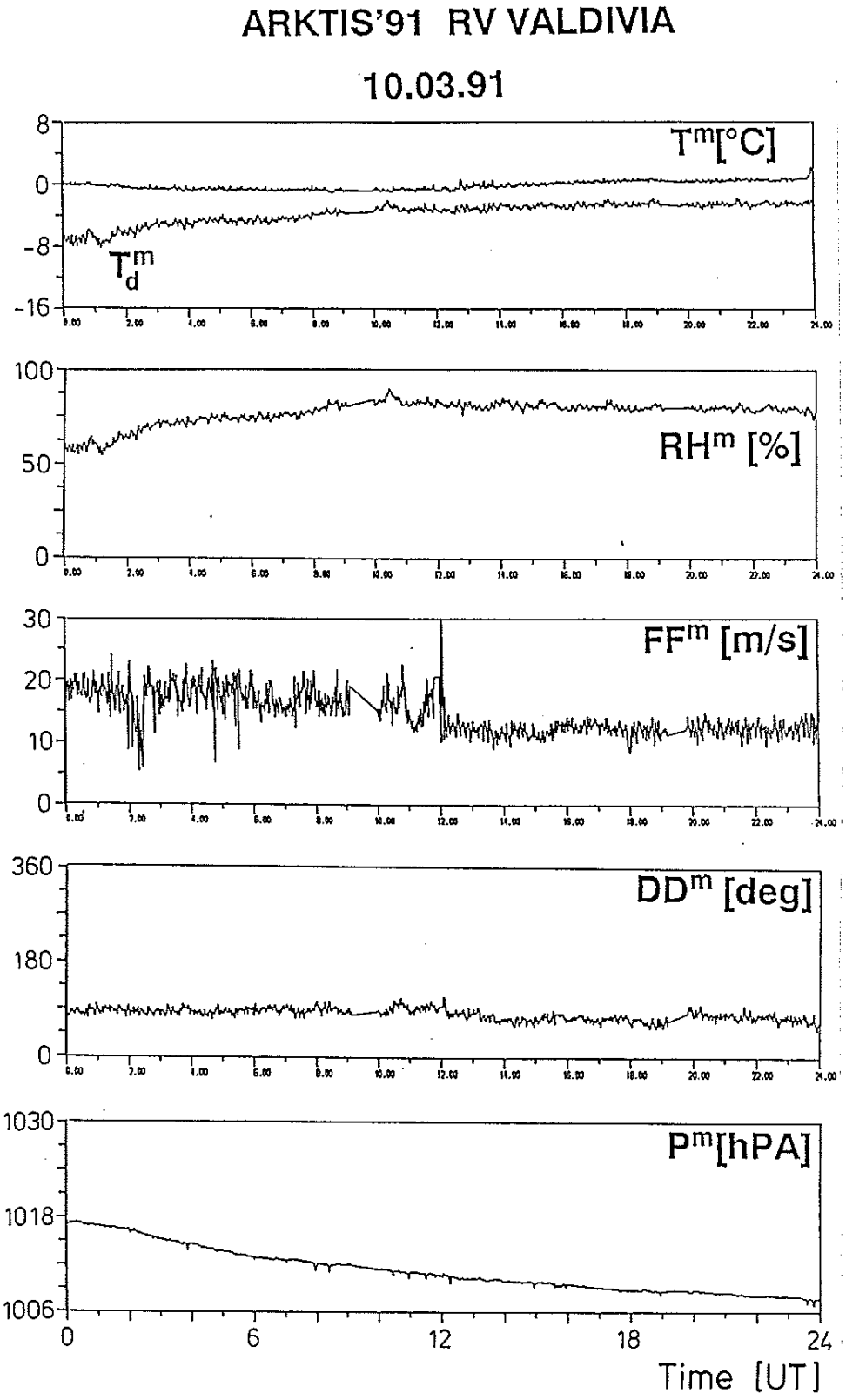

Figure 2.4a: The daily data flow from the fore-deck station (index m): Temperature T, dew-point T_D, relative humidity RH, wind speed FF, wind direction DD and pressure p; all at 15 m height.

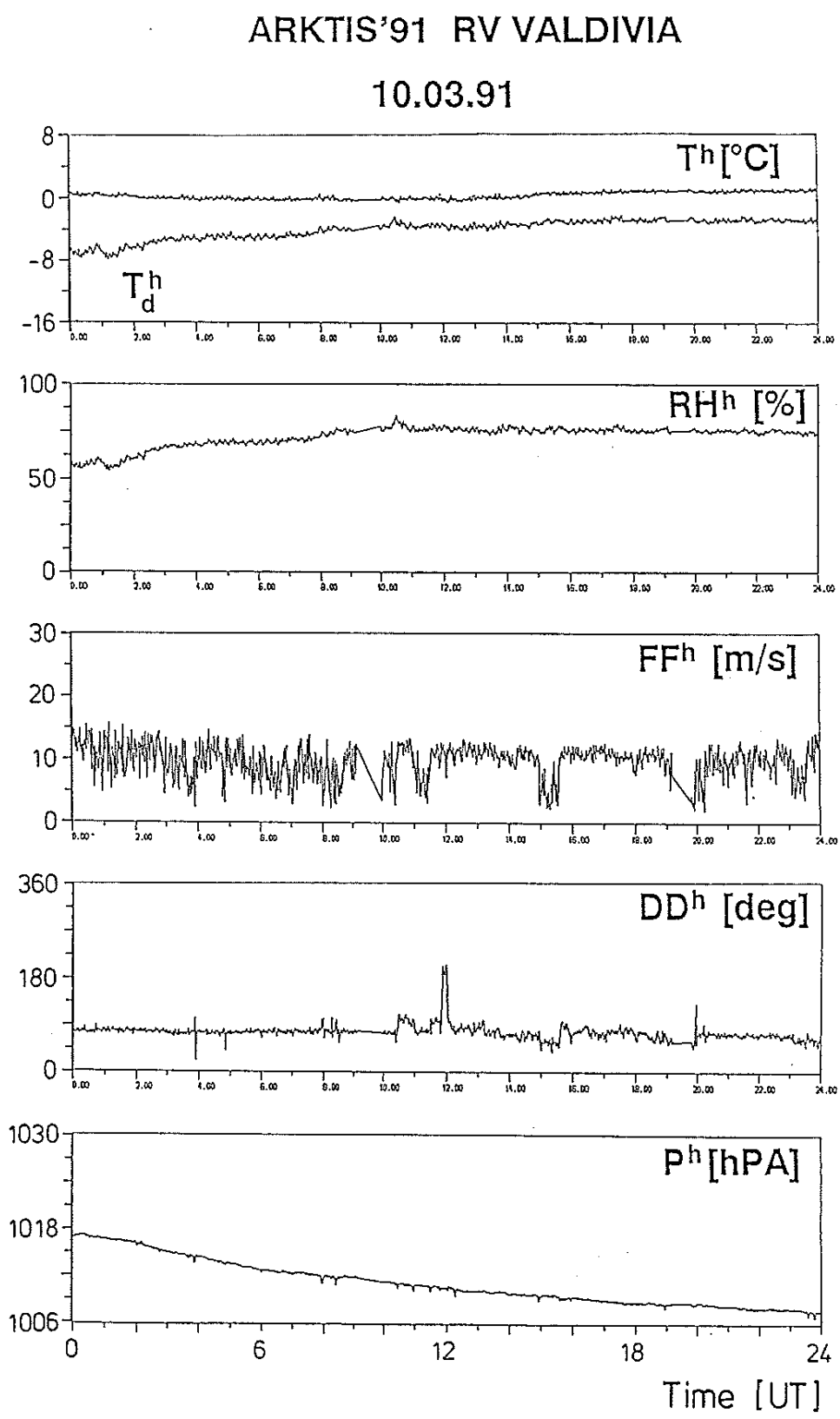

Figure 2.4b: As Figure 2.4a, but from after-deck station (index h).

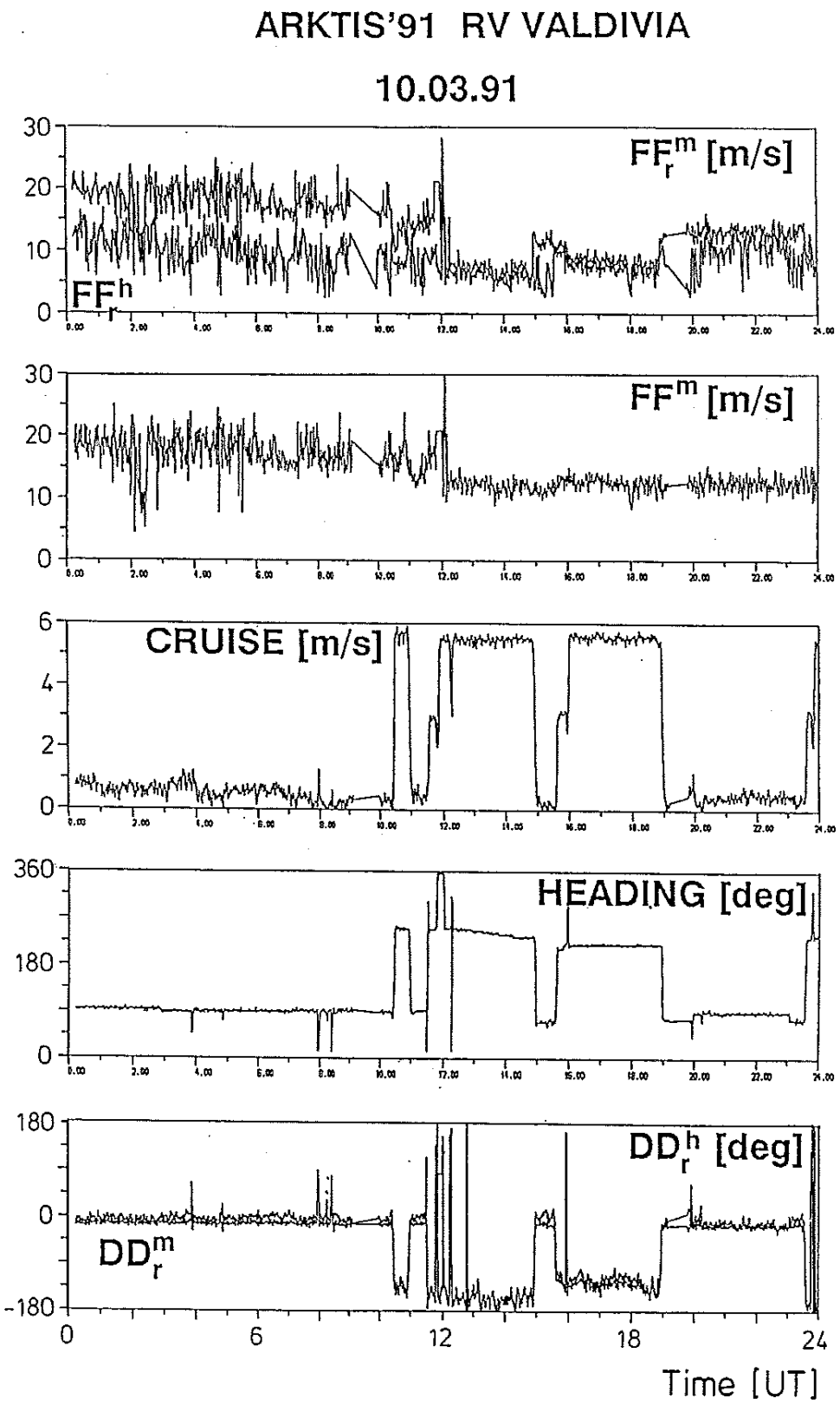

Figure 2.4c: Wind speed FF and direction DD relative (index r) to the ship at fore-deck station (m) and after-deck station (h) as well as ship's speed and heading.

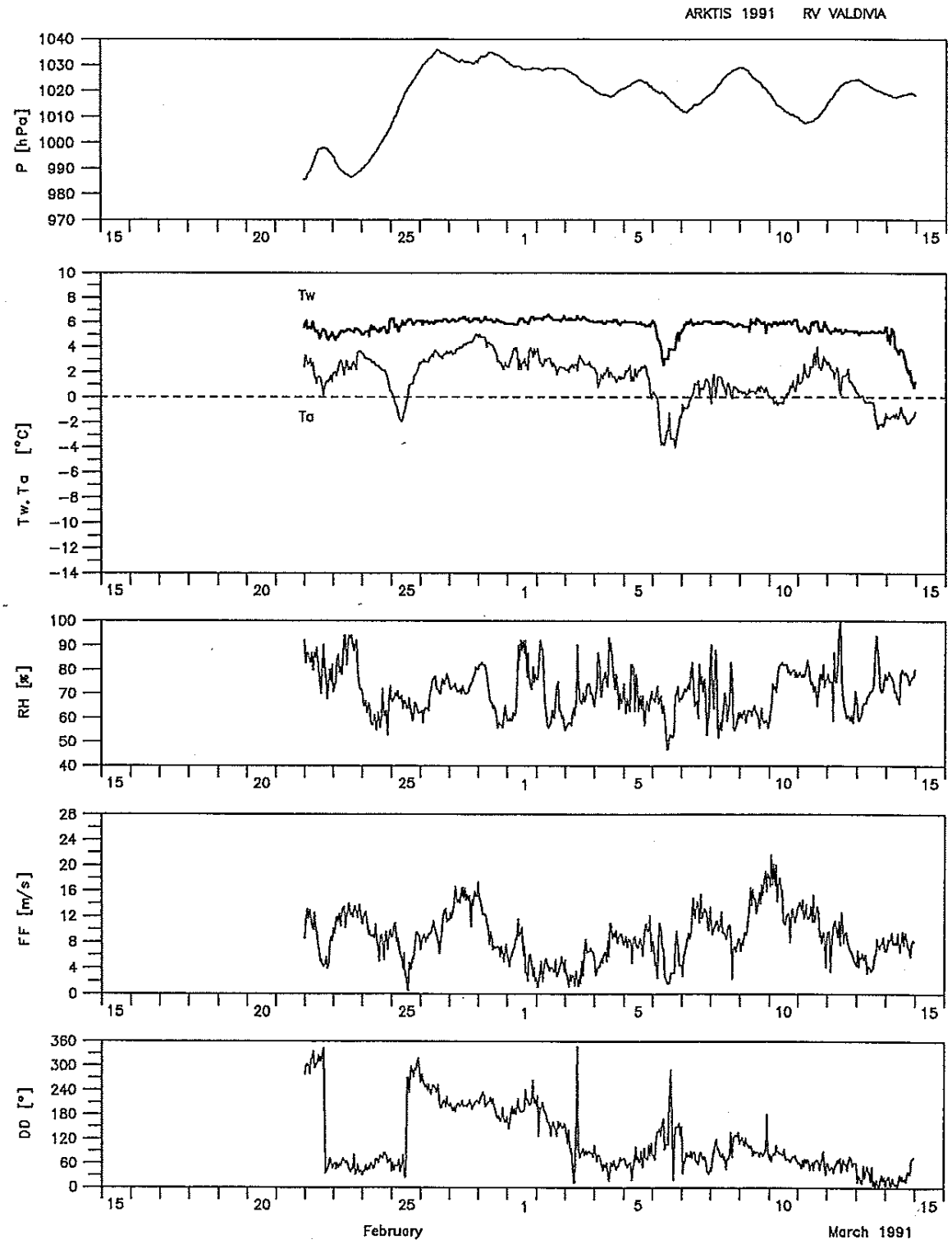

Figure 2.5a: Hourly values of pressure at sea level p, air temperature T_a reduced to 10 m height, water temperature T_w, relative humidity RH, wind speed FF and wind direction DD.

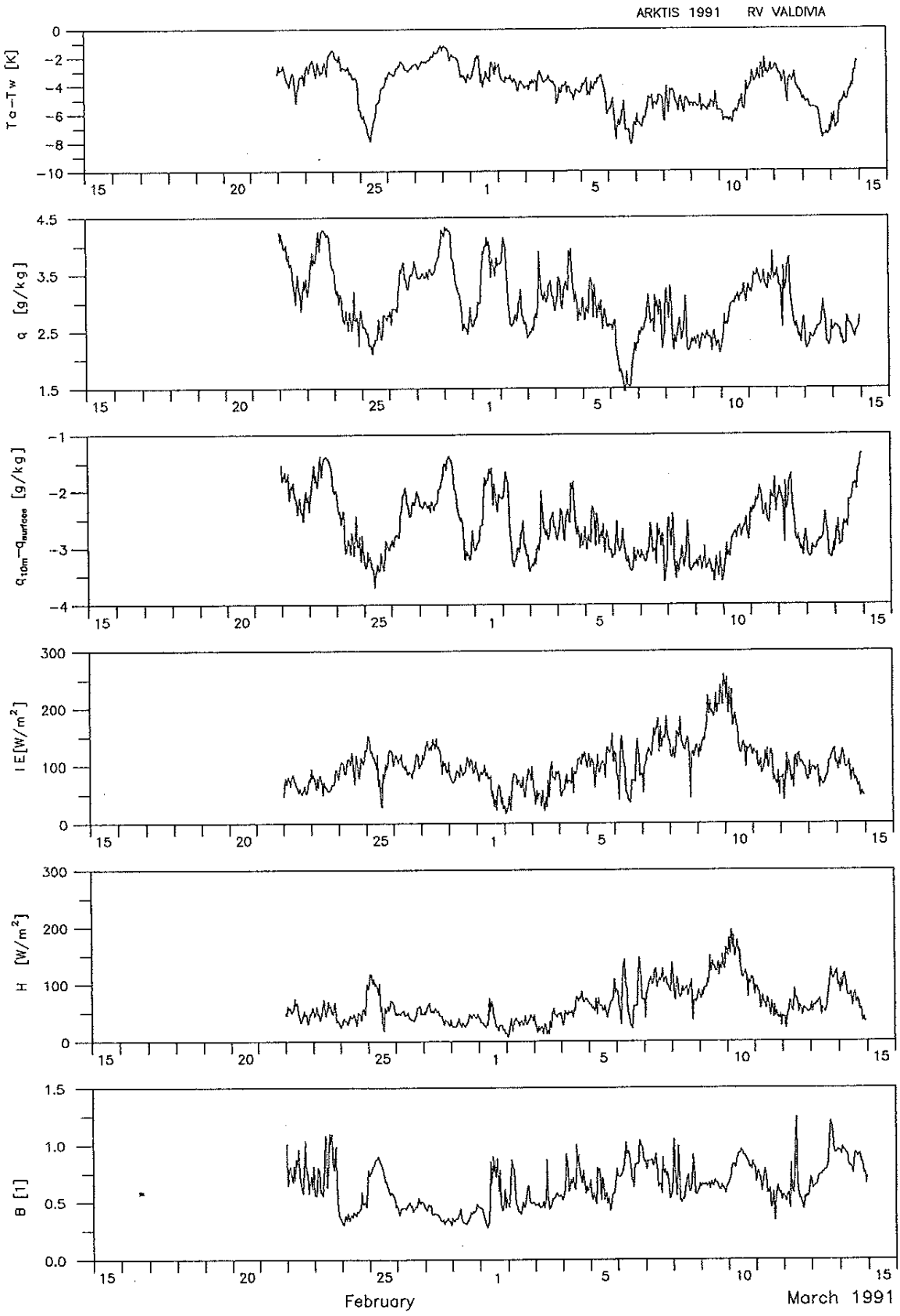

Figure 2.5b: Hourly values of T_a - T_w, specific humidity q_a, q_a - 0.98 q_s (T_w) (q_s is saturation specific humidity) sensible heat flux H, latent heat flux E and Bowen ratio B = H/E. All values are reduced to 10 m height.

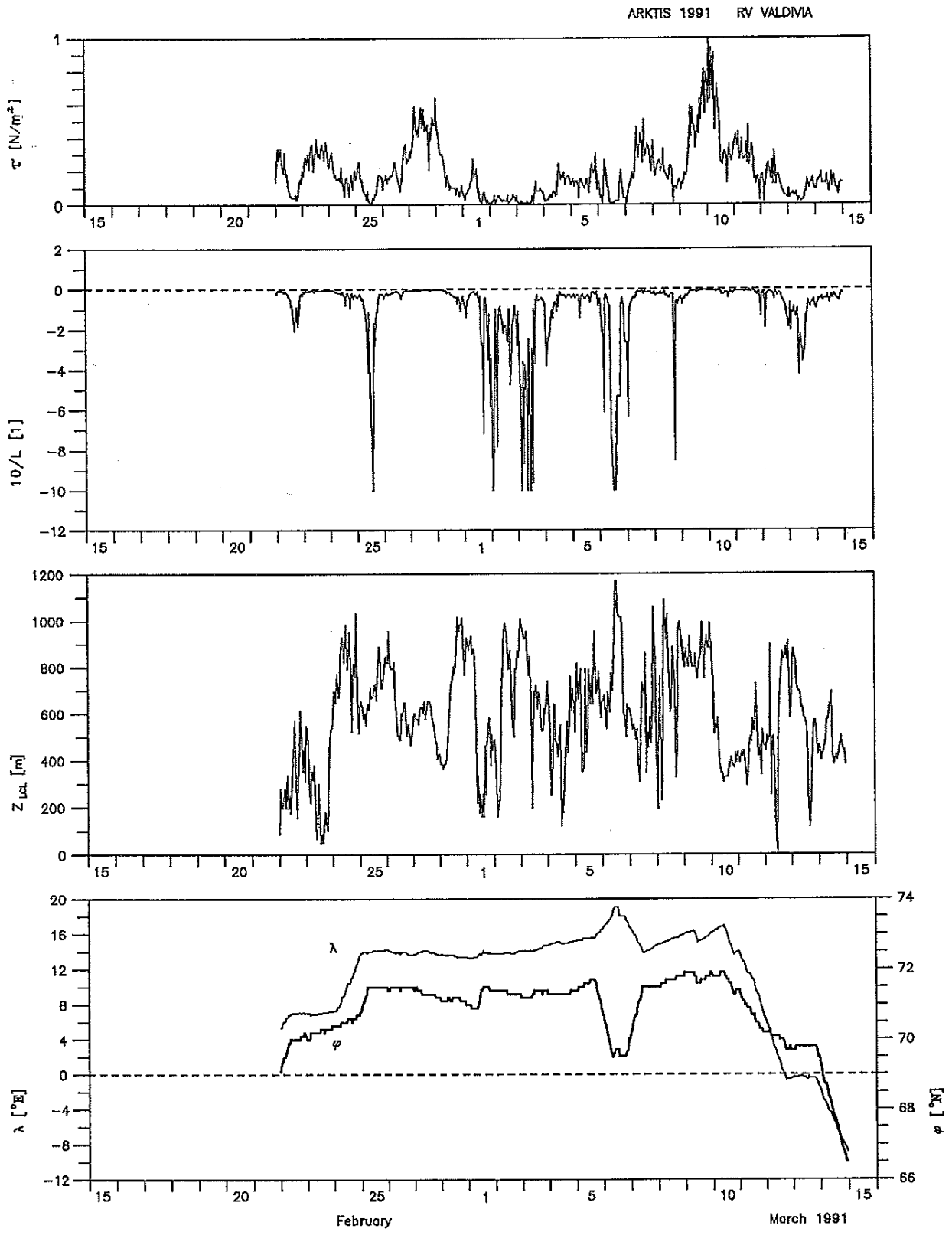

Figure 2.5c: Hourly values of momentum fluex τ, Monin-Obukhov stability z/L with z = 10 m, lifting condensation level z_{LCL} and latitude ρ and longitude λ.

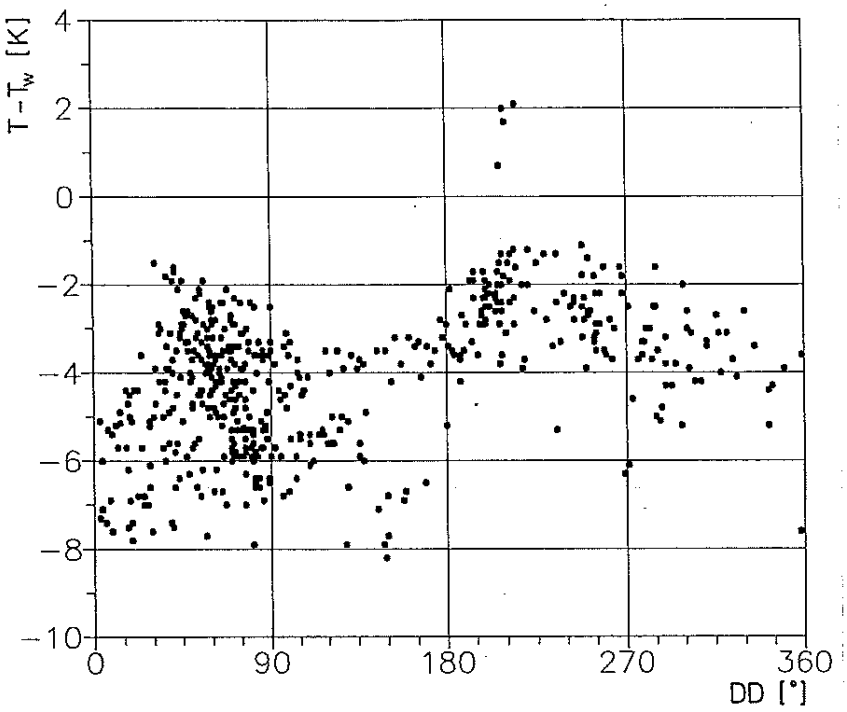

Figure 2.6a: Correlation between air-sea temperature difference, T - T_w and wind direction DD at VALDIVIA.

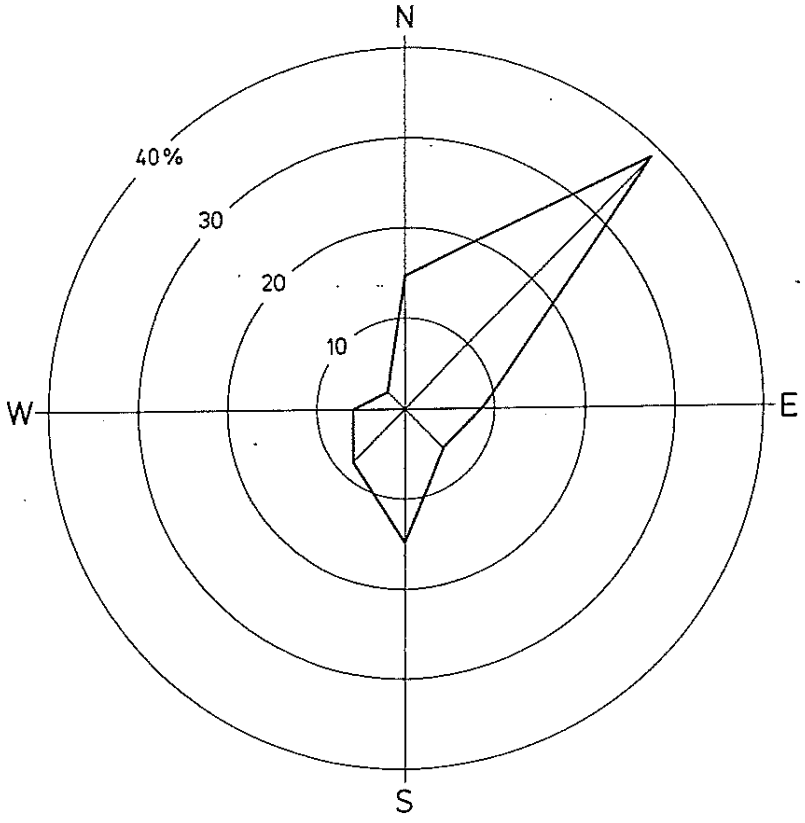

Figure 2.6b: Frequency distribution of wind direction at VALDIVIA.

2.3. *Phenomenological obeservations*

(G. Kruspe, Max-Planck-Institut für Meteorologie, Hamburg)

Phenomenological observations according to WMO reports were made every full hour. The whole measuring period comprises about 500 WMO-reports (Figures 2.7 - 2.10). They are of crucial importance for relating the quantitative parameters to characteristic meteorological phenomena (clouds, precipitation, etc.). The hourly cloud observations (cloud type, coverage, Figure 2.8 - 2.10) are restricted to daylight conditions from 07 UT until 19 UT, whereas the weather conditions (WW, Figure 2.7), especially events of hydrometeors, are also observed during hours of darkness. The WMO-codes for hydrometeors are 50-59 for drizzle, 60-69 for rain, 70-79 for solid hydrometeors, 89-90 for showers of various hydrometeors. The code numbers 14-16 and 20-27 refer to hydrometeor events during the last hour and around the station but at the observation time, respectively. About 32% of the WW-observations refer to hydrometeors, mostly as snow (group 70, 43%). Showers (group 80) during conditions of cellular convection made up about 25% of the observed hydrometeors. There were only 6 days without hydrometeor events, namely during the anticyclonic synoptic situations on 24 February, 26-28 February, 06 March and 09 March. The daily frequency of hourly reported hydrometeors varied between 2 and 22. On three days (22 February, 7 and 11 March), more then 14 reports of hydrometeors were made. On further 11 days the daily frequency of hydrometeor reports was between 7 and 14. If comparing these observations with the time-height cross-section of temperature in Figure 2.12a, we find that the long periods with hydrometeor events coincide with low-tropospheric warming up to 2 km and mid-tropospheric cooling (23 February, 01, 03, 05, 07, 11 and 14 March). Some longer events were also observed under opposite vertical thermal stratifications (02, 04, 08 and 09 March).

The total cloud cover N (Figures 2.8 and 2.10) was in 64% of the time more than five octas. The coverage of low clouds N_h exeeded five octas in 45% of the time. A large contribution to these numbers is from the persistent period of stratocumulus (C_L = 5) during prevailing anticyclonic weather conditions over Northern Scandinavia, which led to southerly wind components from 28 February until 03 March. Regarding the type of low level cloud (Figures 2.9 and 2.10), stratocumulus was the most frequent low-level cloud type during the experiment. Convective clouds are frequently observed under codes C_L = 1 (Cu hum), C_L = 2 (Cu con), C_L = 3 (Cb calv), C_L = 8 (Sc and Cu), and C_L = 9 (Cb cap). Clouds forming open cells are typically of type C_L = 2, 3, 9 and clouds within cloud streets are typically of type C_L = 1.

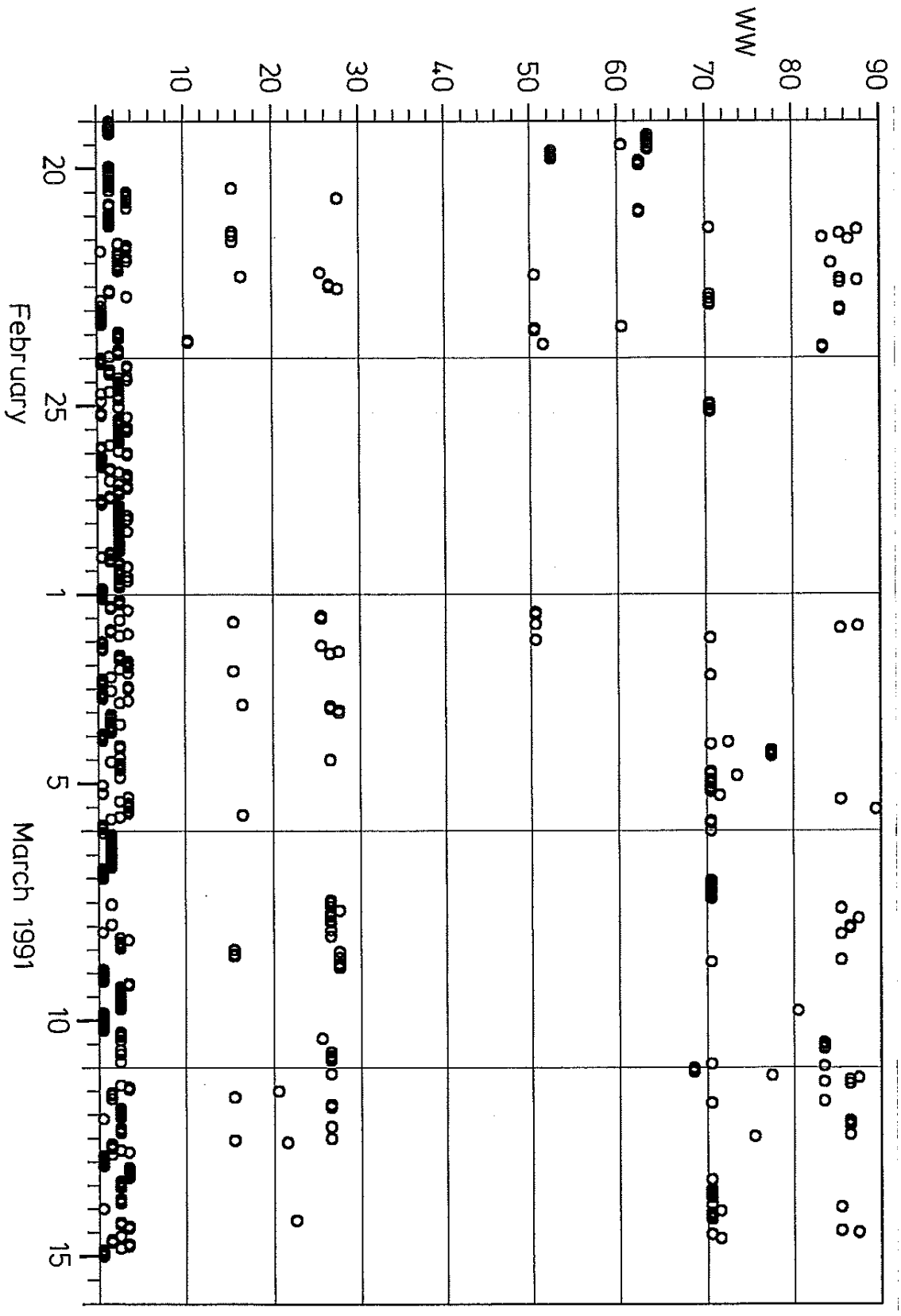

Figure 2.7: Time series of weather situation WW according to WMO code.

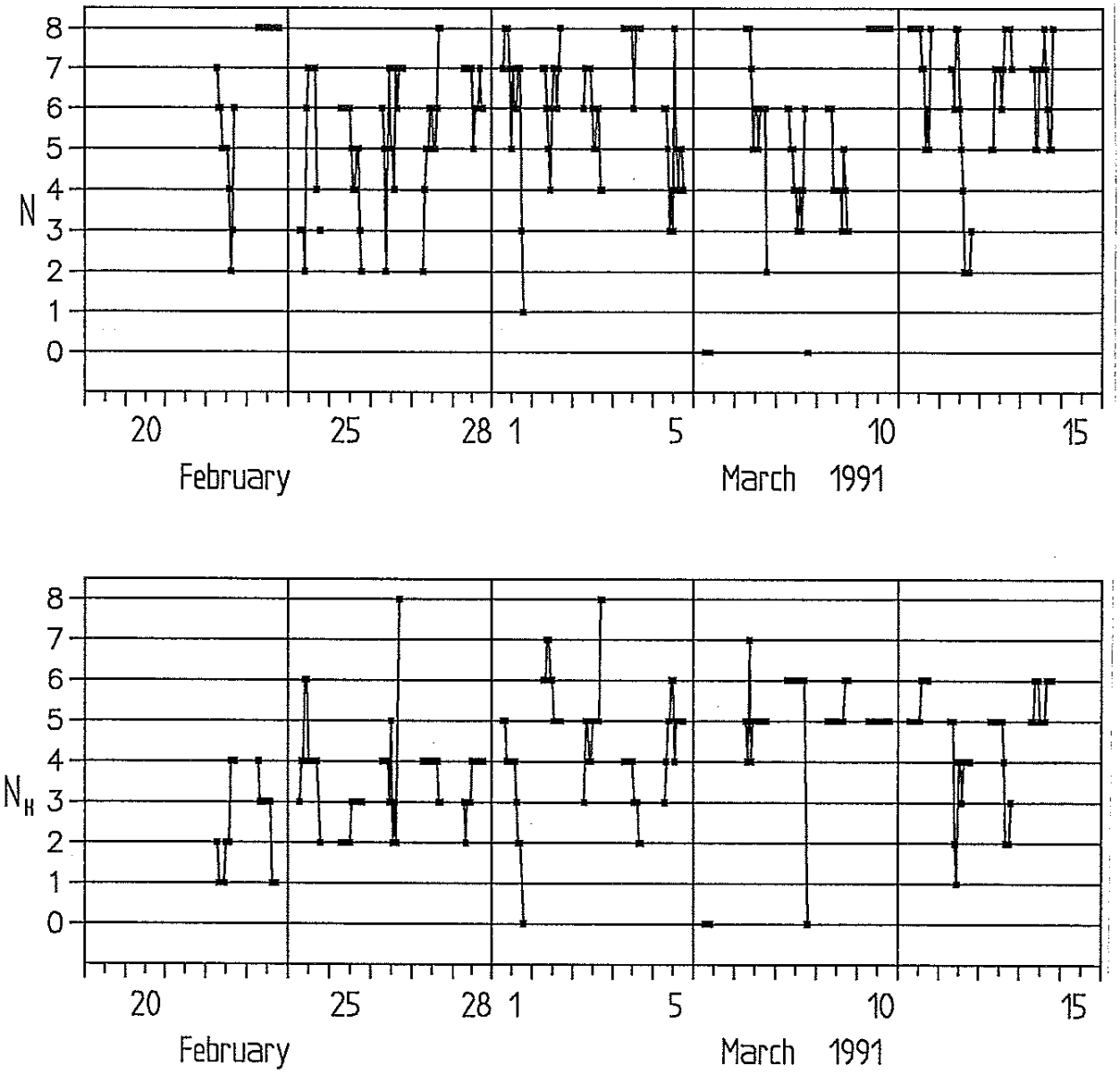

Figure 2.8: Time series of total cloud cover N and low-level cloud cover N_h (in octas) at VALDIVIA.

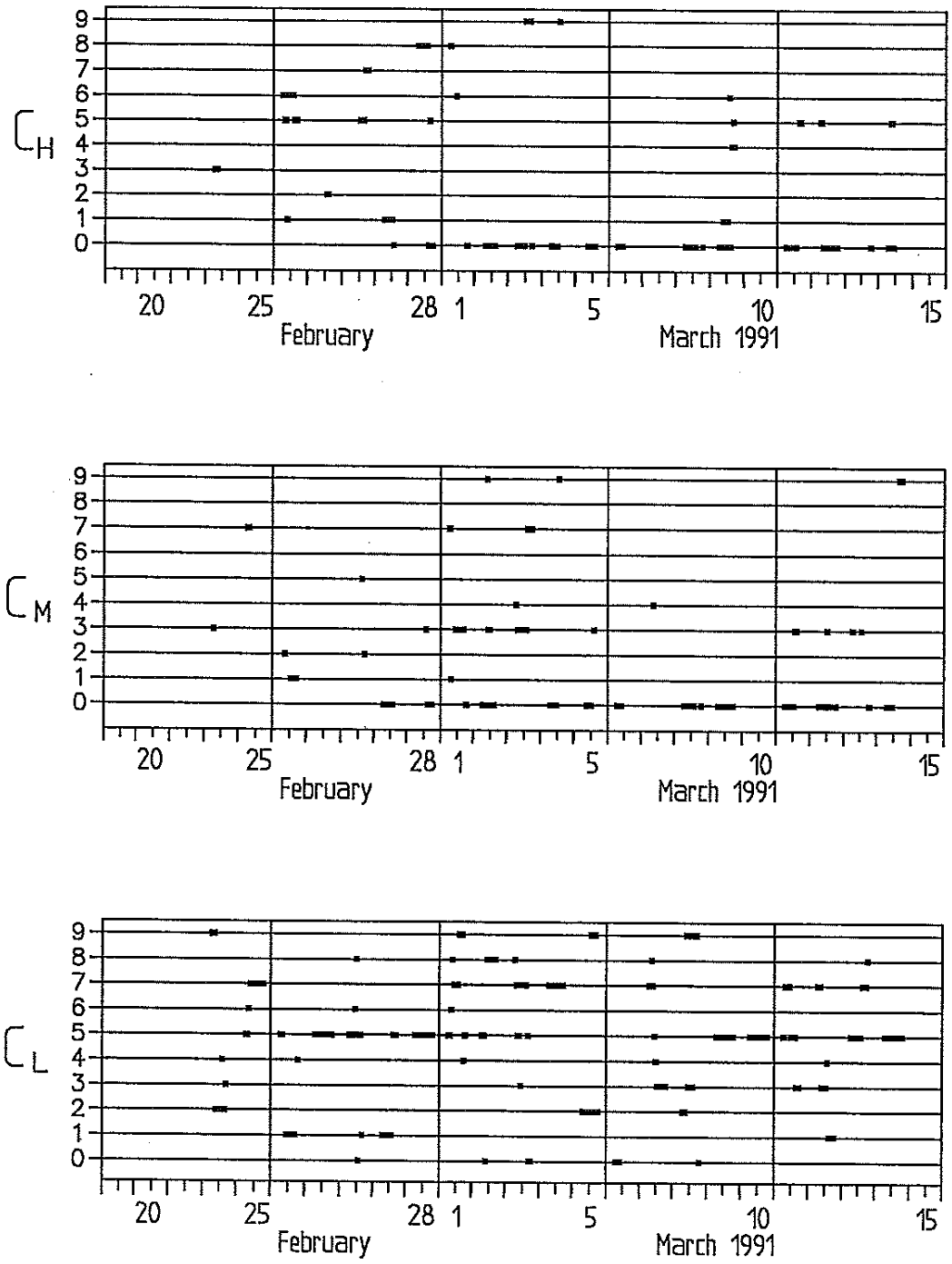

Figure 2.9: Time series of low-level cloud type C_L, mid-level cloud type C_M and high-level cloud type C_H according to WMO code.

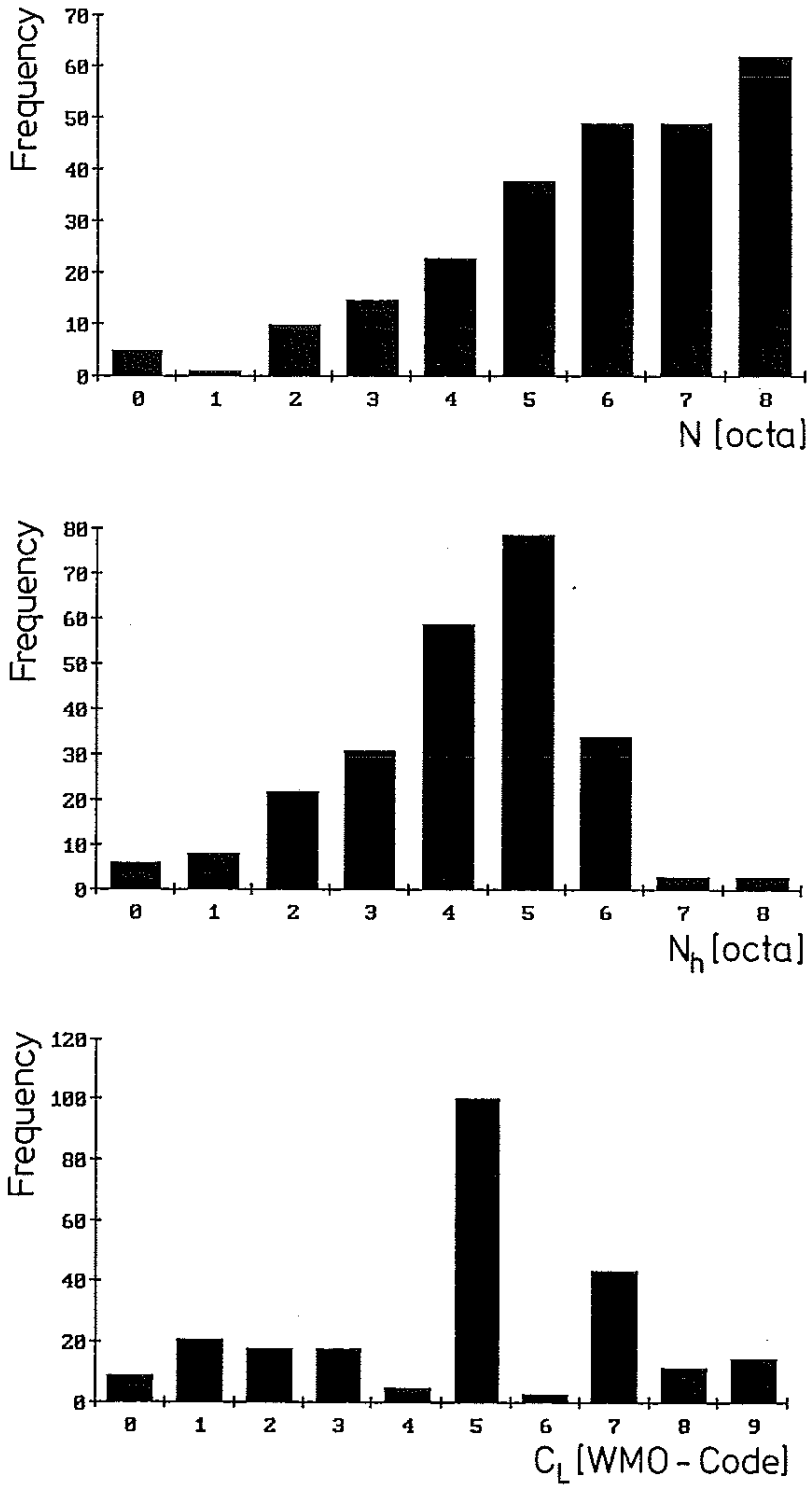

Figure 2.10: Frequency distribution of total cloud cover N, low-level cloud cover N_h and low-level cloud type C_L according to WMO code. Only for 07-19 UT observations.

2.4. *Aerological measurements*

(G. Kruspe, Max-Planck-Institut für Meteorologie, Hamburg)

2.4.1. *Equipment*

The upper air system used as Vaisala Micro Cora system with OMEGA wind finding. The Vaisala RS80/15N readiosonde was carried by 100 g balloons which were filled with 0.6 m^3 helium to provide a mean ascent rate of 240 m/min. The mean burst height of the balloons was about 14 km and was reached after 58 minutes. The accuracies of the thermodynamic parameters measured by the radiosonde are lited in Table 2.4.

Table 2.4: Radiosonde data quality according to Vaisala News 92/1981.

Parameter	Measurements Principle	> 600 hPa	600-300 hPa	300-160 hPa
Pressure	Aneroid Capsule	± 1.2	± 1.0	± 0.6
Temperature	Dielectric ceramic material	± 0.3	± 0.3	± 0.3
Relative Humidity	Humicap polymer thinfilm	- 0.4 ± 6.4	- 2.7 ± 4.4	- 3.0 ± 11.0

Concerning the RMS accuracy of the wind components, a value of about 1 m/s can be assumed due to the good receiving conditions of the OMEGA signals transmitted from the stations Norway, Liberia, Japan and Hawaii during the experiment. A major handicap of the OMEGA wind finding technique in the Micro Cora system is the lack of reliable wind data within the lowest several hundred meters, which are crucial for boundary layer studies. For wind calculations, phase/time curve fitting was adjusted to 2 minutes.

2.4.2. *Results*

a. *Remarks on the aerological data set*

From 22 February 00 UT until 14 March 24 UT a total of 125 soundings were launched successfully at four hours intervals. Launch time, position and burst heights are given in Table 2.1. The burst heights of the balloons mostly exceeded the heights of the tropopause level by several kilometers, as can be seen in Figure 2.11. The aerological data set provides a continuous coverage of tropospheric temperature, humidity, and horizontal wind. In the first step of the aerological data processing Vaisala's editing software is used to eliminate noise from the data and to check whether vertical gradients of the various parameters are within acceptable limits. In addition, obviously bad data are

removed by hand. For the determination of mean time-height cross sections the aerological data were smoothed in the following way. First they were interpolated to 50 m height intervals and then vertically smoothed with a Hanning taper. By time interpolation of neighbouring soundings, time series with hourly steps were created for each particular height. These data were smoothed by running cosine taper over 4 hours on either side of the particular time and then sampled in steps of 4 hours.

b. Time height cross-sections of mean fields in the troposphere

Various thermodynamic and dynamic quantities of the aerological data set are presented as time-height cross-sections (Figure 2.12a-g). The dominant synoptic features (passages of lows, highs, fronts etc.) and their characteristic thermodynamic and dynamic effects in the troposphere and lower stratosphere are clearly reflected in the figures (see for comparison the weather maps in Appendix B). Regions of strong baroclinicity, as indicated by the strong inclination of the temperature isolines T, are present on 26/27 February and 9/10 March (Figure 2.12a). These regions are also strongly correlated with variations of the tropopause height (increasing tropopause corresponds to tropospheric warming and low stratospheric cooling and vice versa). The most remarkable event is observed on 26/27 February in connection with an eastwards travelling trough system. Ahead of it intensive warm air advection occurs up to 9 km height, coupled with an increase of the tropopause height by 3 km. Behind this system a principal change of the synoptic regime was initiated with a nearly continuous tropospheric cooling until 8 March. The time variations of specific humidity q in the troposphere (Figure 2.12b) are about parallel to those of temperature. They show in a very impressive manner the change between moist/warm oceanic and cold/dry arctic air masses. Periods of local cloud formation are well documented by the contour plot of relative humidity RH in Figure 2.12c, where regions of relative humidities greater 85% are shaded. Near the tropopause level between 8 and 12 km, core like wind structures of the polar jet are well displayed in the cross-section of wind speed FF in Figure 2.12d. These pattern correspond to regions of strong baroclinicity. According to Figures 2.12e and f which show the zonal (u) and meridional wind component (v), respectively, the baroclinicity was mainly directed in east-west direction, whereas the wind core situation from 9/10 predominantly originates from meridionally alligned baroclinicity. Periods of cold air advection occurred on 24/25 February, 1 March, 6-8 March and 11-13 March. During most of these episodes the coldest air in the boundary layer is observed several hours later than in the upper troposphere. It appears that the destabilization of the troposphere is initiated from above and supported by a

permanent heating from the sea surface. When the coldest air in the boundary layer and the largest thermal air-sea instability is reached, the upper layer seem already to be stabilized due to sinking processes. This may be the reason that the largest boundary layer depth and consequently the deepest convection not necessarily coincide with times of the lowest air temperatures near the surface. During phases of cold air advection the boundary layer is between 1 and 3 km deep. This can be seen in the cross-section of the equivalent potential temperature Θ_e (Figure 2.12g) which is a conservative quantity with respect to moist adiabatic processes without precipitation.

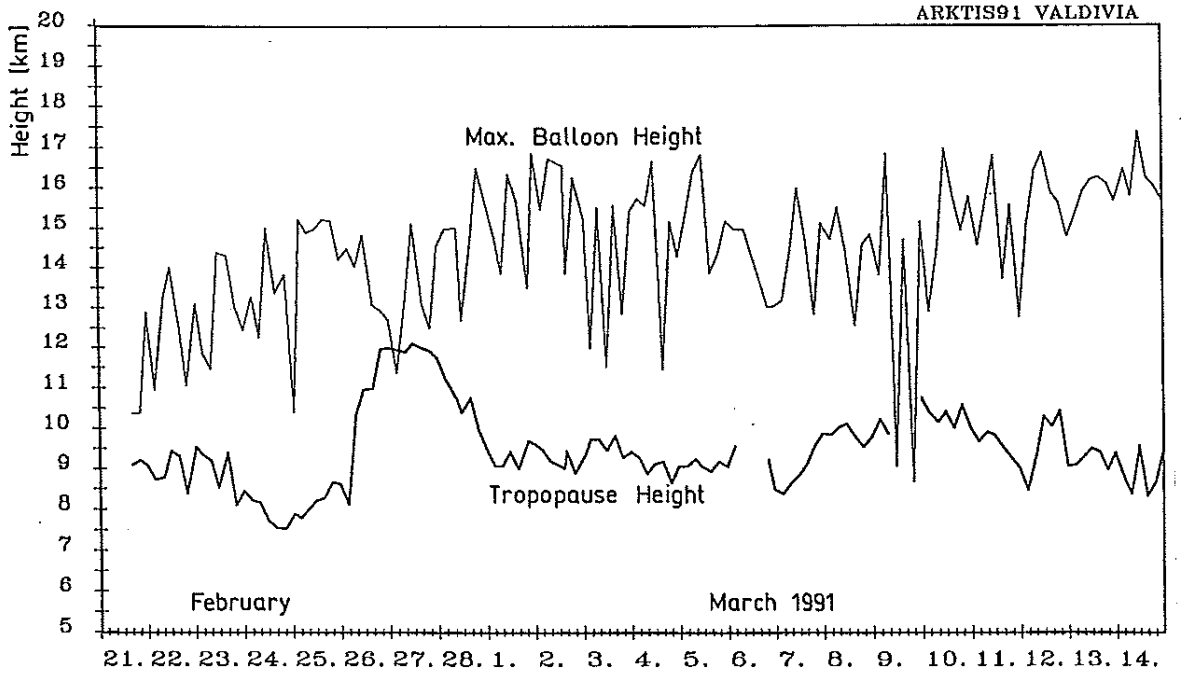

Figure 2.11: Time series of tropopause level and maximum radiosonde height at VALDIVIA during ARKTIS '91.

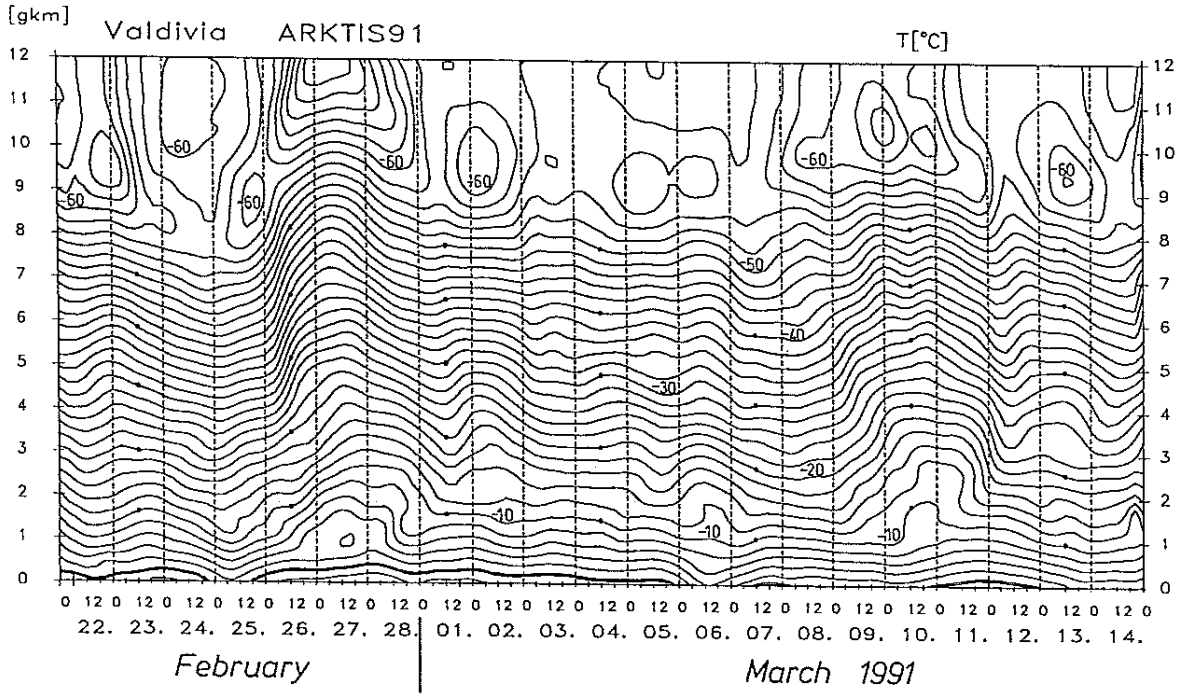

Figure 2.12a: Time height cross-section of temperature (°C) at VALDIVIA. Thick line: 0°C. Temperature interval 2 K. Thick points mark 10 K temperature intervals.

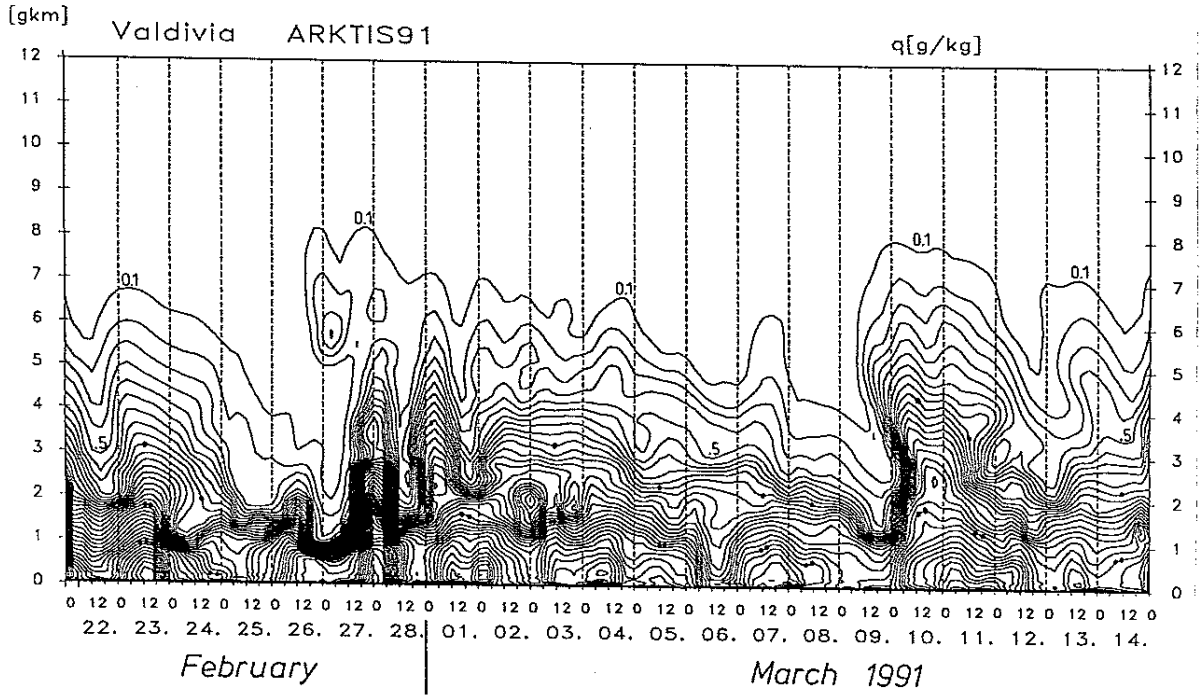

Figure 2.12b: Time height cross-section of specific humidity q. Interval: 0.1 g/kg. One, two or three thick dots mark the 1, 2 and 3 g/kg isolines, respectively.

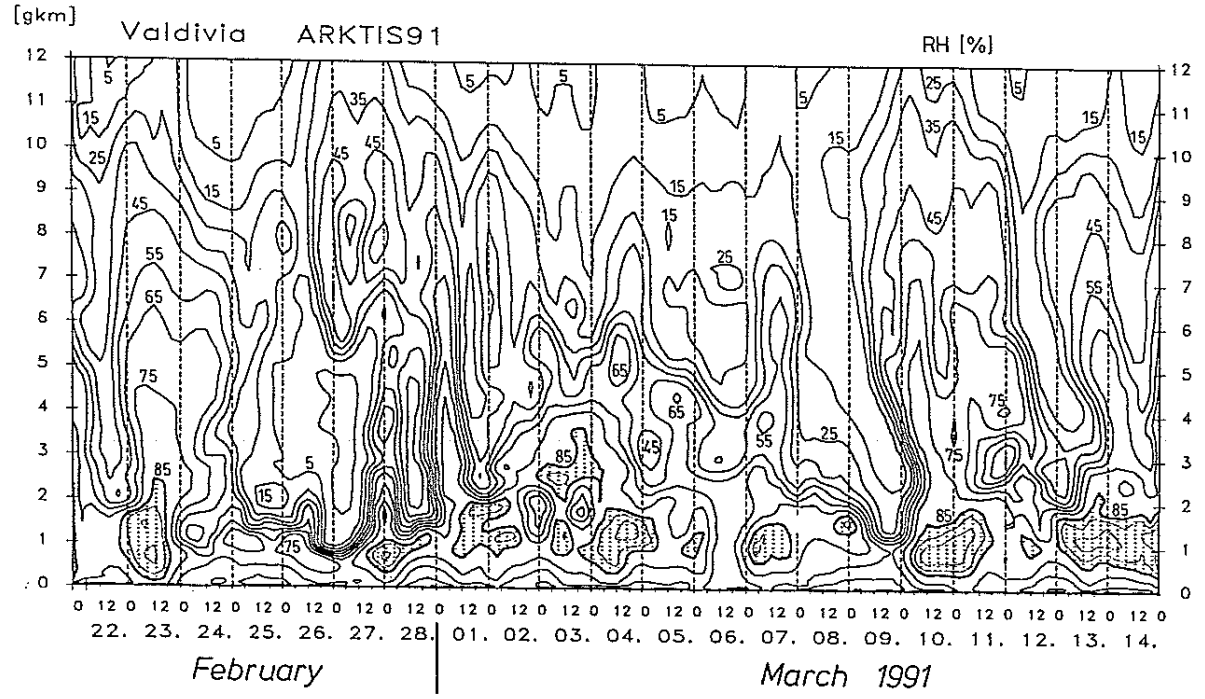

Figure 2.12c: Time height cross-section of relative humidity RH. Interval: 10%. Areas with RH > 85% are dashed.

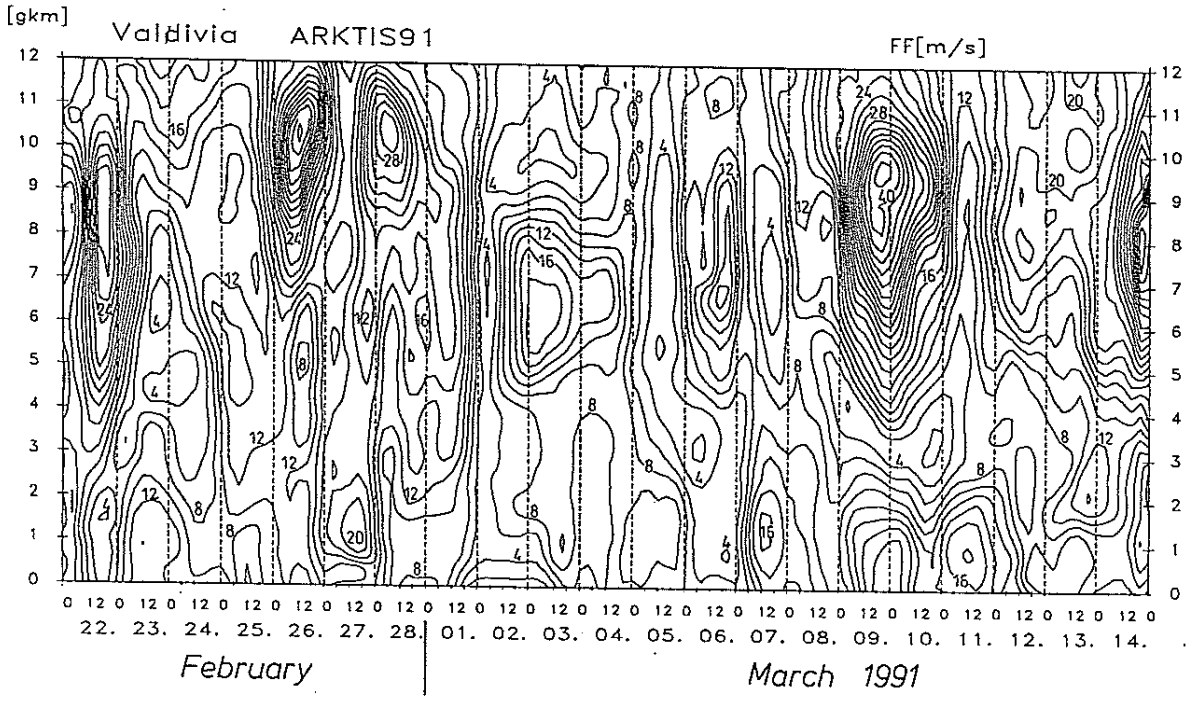

Figure 2.12d: Time height cross-section of wind speed FF. Interval: 2 m/s.

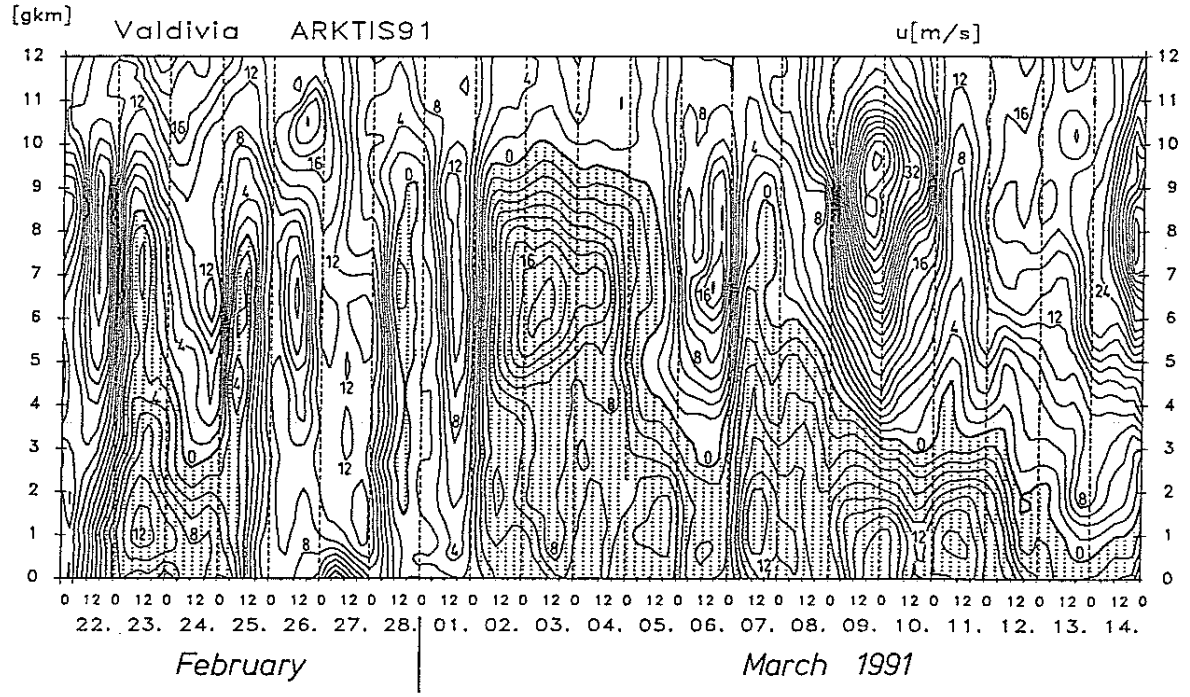

Figure 2.12e: Time height cross-section of zonal wind component u. Interval: 2 m/s. Areas with easterly wind (u < 0) are dashed.

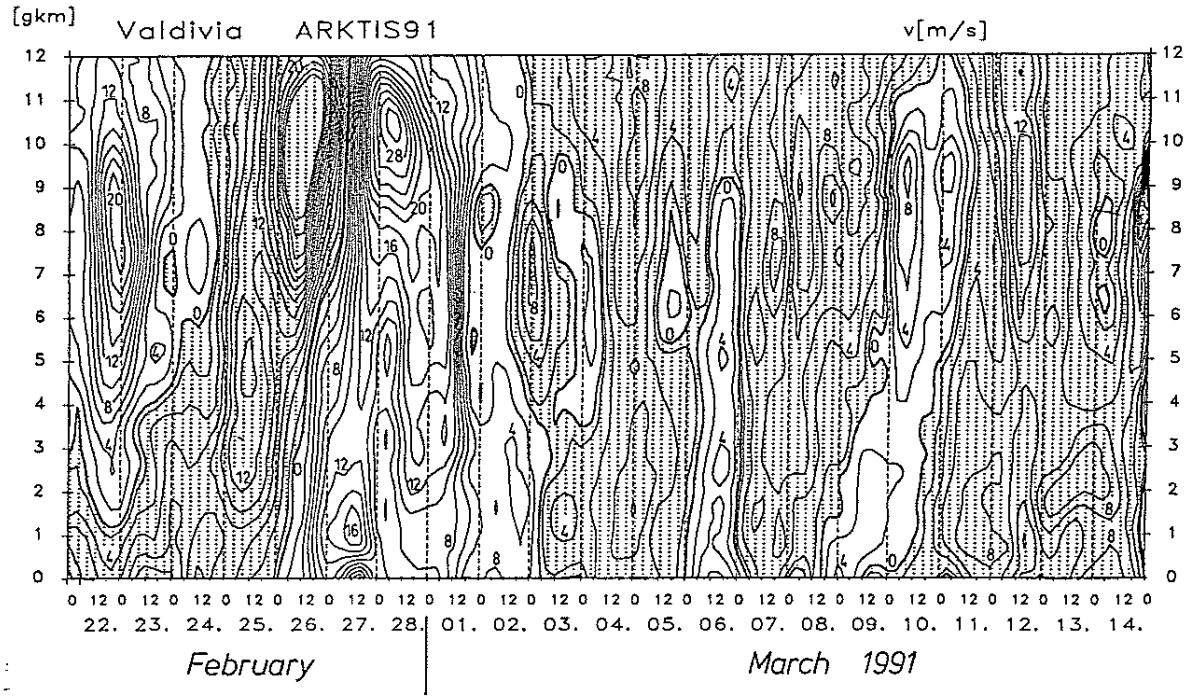

Figure 2.12f: Time height cross-section of meriodional wind component v. Interval: 2 m/s. Areas with northerly winds (v < 0) are dashed.

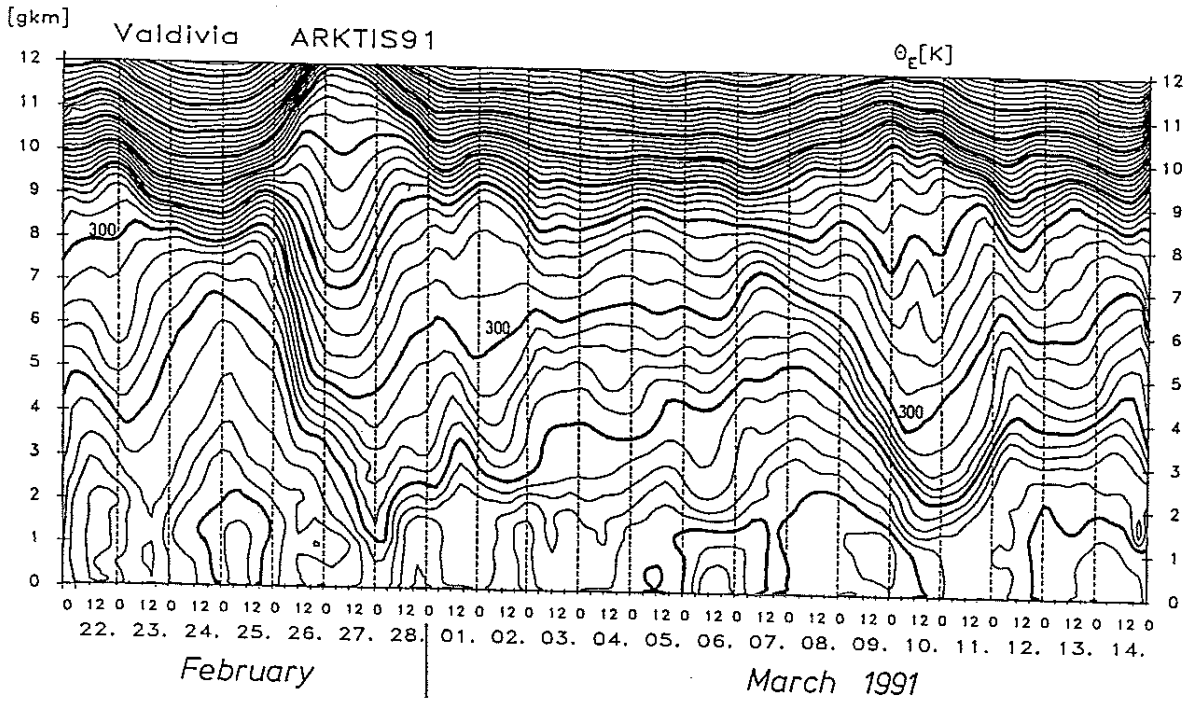

Figure 2.12g: Time height cross-section of equivalent potential temperature Θ_e. Interval: 2 K.

2.5. *Sea surface skin-temperature measurements*

(Peter Schlüssel, Meteorologisches Institut, Universität Hamburg)

2.5.1. *Experimental set-up*

Sea surface skin-temperature measurements were taken radiometrically with a KT4 radiometer equipped with a 10-12 µm bandpass filter. The radiometer was mounted on the port side of the bridge deck viewing the surface leaving radiation at a nadir angle of 50°. An on-line calibration of the radiometer was performed every other minute by a reference bath moved into the field of view of the KT4, and a one minute sample of the calibration source was taken. This reference bath was continuously renewed with sea water from the bottom of the tub which caused strong upwelling in the bucket guearanteeing the destruction of the skin layer and avoiding temperature gradients within the reference tub. A well calibrated PT-100 resistance thermometer monitored the temperature in the reference bath.

A linear relationship between radiometer counts and reference temperature was established at the end of the cruise by using all calibration measurements during the cruise. An offset for the actual measurement of the oceanic skin temperature was taken from the mean of two adjacent calibration cycles.

The radiometer measurements were recorded as 10 s means together with readings of the PT-100 reference temperature and the position of the bucket carying the reference bath.

The surface skin measurements were set up on 24 February 1991, 1545 UT, and were taken unti 16 March 1991, 1000 UT. Due to a malfunction of the water pump supplying the sea water to the calibration bath the calibration was interrupted from 5 March 1991, 1200 UT through 8 March 1991, 1345 UT and from 10 March 1991, 0715 UT through 11 March 1991, 1404 UT. During these periods no useful skin measurements could be obtained. Short periodical gaps in the time series were caused by maintainance work.

2.5.2. *Data processing and measurement examples*

From all KT 4 measurements only those were kept which were not affected by the moving water bucket at the beginning and at the end of each calibration cycle. The retained 10 s means were averaged to build means over 40 to 50 s, being representative of the one minute ocean view or calibration cycle, respectively. Measurement spikes were removed if they deviated more tha 0.15 K from

the mean of a one minute cycle. Additionally, we rejected those data outside the range 0 through 650 counts. Subsequently, the reference temperatures were fit to the radiometer counts of a subset being equally distributed between 0 and 650 counts. Having obtained a regression line we rejected outliers which deviated more than two standard deviations from the best fit and repeated the regression with the remaining samples. The final slope between temperature and radiometer counts obtained was $m = \Delta T/\Delta c = 0.0101$, valid for the temperature domain between 2.0 and 8.5°C which occurred during this cruise.

The adjacent calibration cycles before and after an ocean view of the radiometer define the actual offset of the regressio line. The rejection of many outliers was necessary due to the strong impact of the ship's radio traffic received by the data logger. A total of 20% of all measurements were eliminated by the error checks.

As an example a two days time series of the bulks-skin temperatue differences ΔT with respect to the bulk water temperature measured at a depth of 5.5 m is shown in Figure. 2.13a The distribution of all bulk versus skin measurements, shown in Figure 2.13b reveals a mode between 0.1 and 0.2 K with a wide scatter between -0.8 K (war surface layer) and 1.4 K (very cool skin).

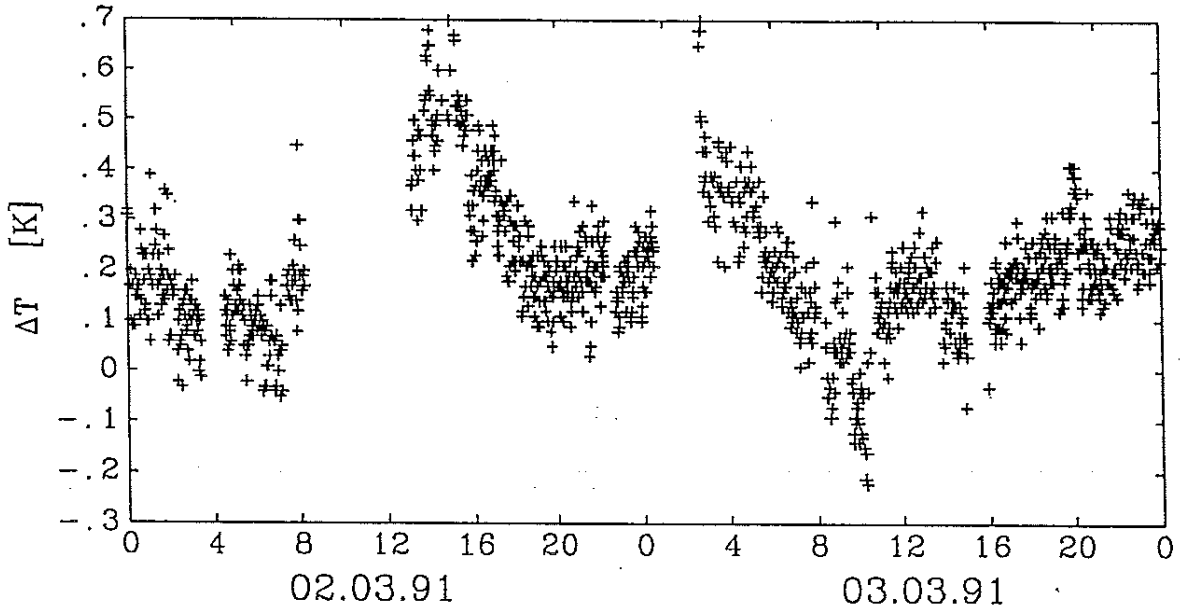

Figure 2.13a: Two days time series of bulk versus skin temperature difference.

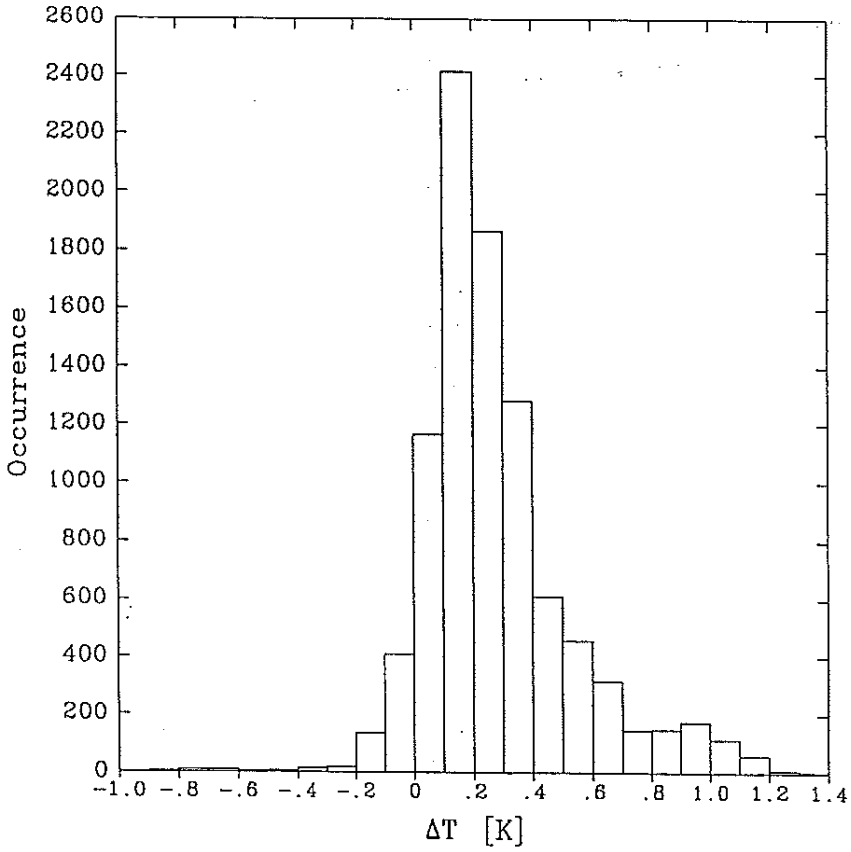

Figure 2.13b: Distribution of all one minute mean bulk versus skin temperature differences measured during ARKTIS '91.

2.6. *Oceanic profiling of temperature and salinity*

(G. Kruspe, Max-Planck-Institut für Meteorologie, Hamburg)

2.6.1. *Experimental set up*

The probe used was a so-called Kieler Multisonde (KMS) of the Institut für Meereskunde of the University of Hamburg. This probe contains sensors for pressure (Piezo-electric device), temperature (PT100), and conductivity (electrode analyzer). The data were transmitted to the ship by a single cable lead. Salinity, density and potential temperature were determined applying the UNESCO standard parameter sets. In addition, bulk sea water samples were taken several times the week and stored in bottles for later chemical analysis and calibration. The calibration by the Bundesanstalt für Seeschiffahrt und Hydrographie (BSH) in Hamburg yielded a difference of the salinity near the surface between KMS and the water probes of about +0.07%. The oceanographic data set comprises 120 up and down profiles. Most of them reach to 500 m depth (see Table 2.1). Times of data loss are: 22 February 23 UT, 28 February 23 UT, 4 March 19 UT, 9 March 11 and15 UT. The profiling routine was interrupted on 6 March from 03 until 19 UT during the cruise to Tromsø. The last profile was taken on 13 March at 23 UT.

2.6.2. *Results*

a. Coupling between oceanic and atmospheric boundary layer

Air and water temperatures are shown in Figure 2.14, covering the vertical interval between -300 m depth and 500 m height. The combined time-height cross-section is plotted in 0.1K steps for the ocean, and 1K steps for the atmosphere. The position of the ship must be taken in consideration when discussing the variations in the ocean because of the local character of the thermal structure in the ocean. From the hydrographic point of view, VALDIVIA operated from 25 February to 10 March within the warm and salty Norwegian Atlantic current (see Appendix E). On the coastal side of the current which is crossed during the cruise to Tromsø (5-7 March) the measurements reveal a cool and sweet ocean layer of 5°C and 32.6‰ salinity especially within the upper 15 m. Other front-like structures which are not associated with changes in location are due to mixing processes caused by strong winds.

With respect to the atmosphere, the temperature isolines express the transient events of different air mass advection.

b. The evolution of the oceanic mixed layer during strong winds

Figure 2.15 shows the evolution of potential temperature and salinity stratification during an instationary period with increasing winds (26-28 February). The middle and lower part of the Figure displays 13 successive profiles (time step 4 hours) marked by the sounding numbers 31-43. The corresponding times are given in the upper abscissa. Dashes indicate the 6°C and 35 ‰ values. The bottom of the upper isothermal layer is marked by a line showing the time evolution of the mixed layer depth. The upper part of the Figure shows time-series of the generation of turbulent kinetic energy E_t as derived from the bulk approximation τ du/dz and the evaporation flux E. Both quantities are mainly responsible for mixing processes at the sea surface. The increase of both quantities is clearly correlated with the deepening of the mixed layer from about 150 m at the beginning of the period down to about 300 m at the end.

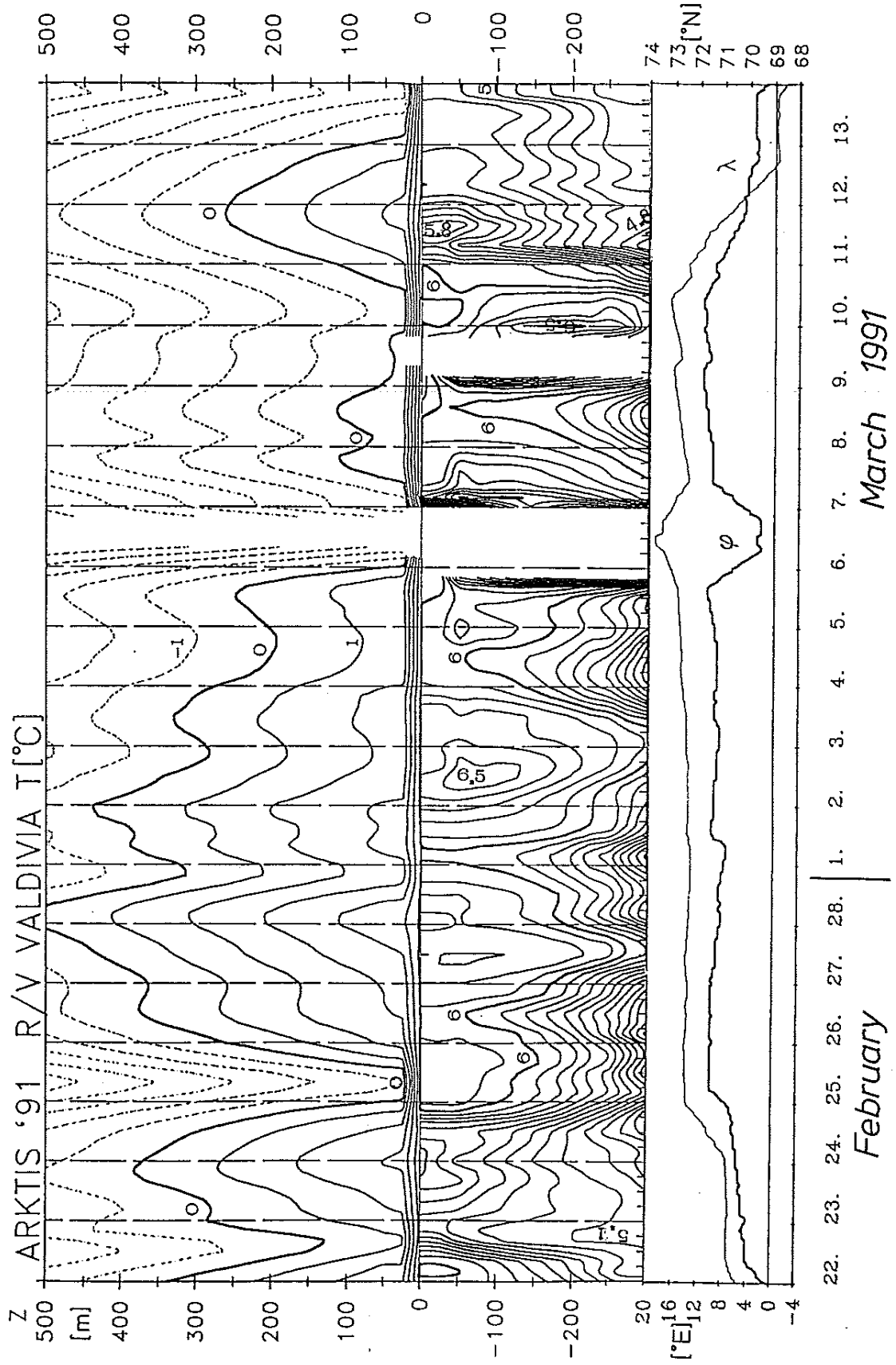

Figure 2.14: Time height/depth cross-section of temperature T from radiosondes and Kieler Multisonde. Interval: 1 K for atmosphere and 0.1 K for ocean. Position (ρ, λ) of VALDIVIA is given below.

ARKTIS'91 RV VALDIVIA

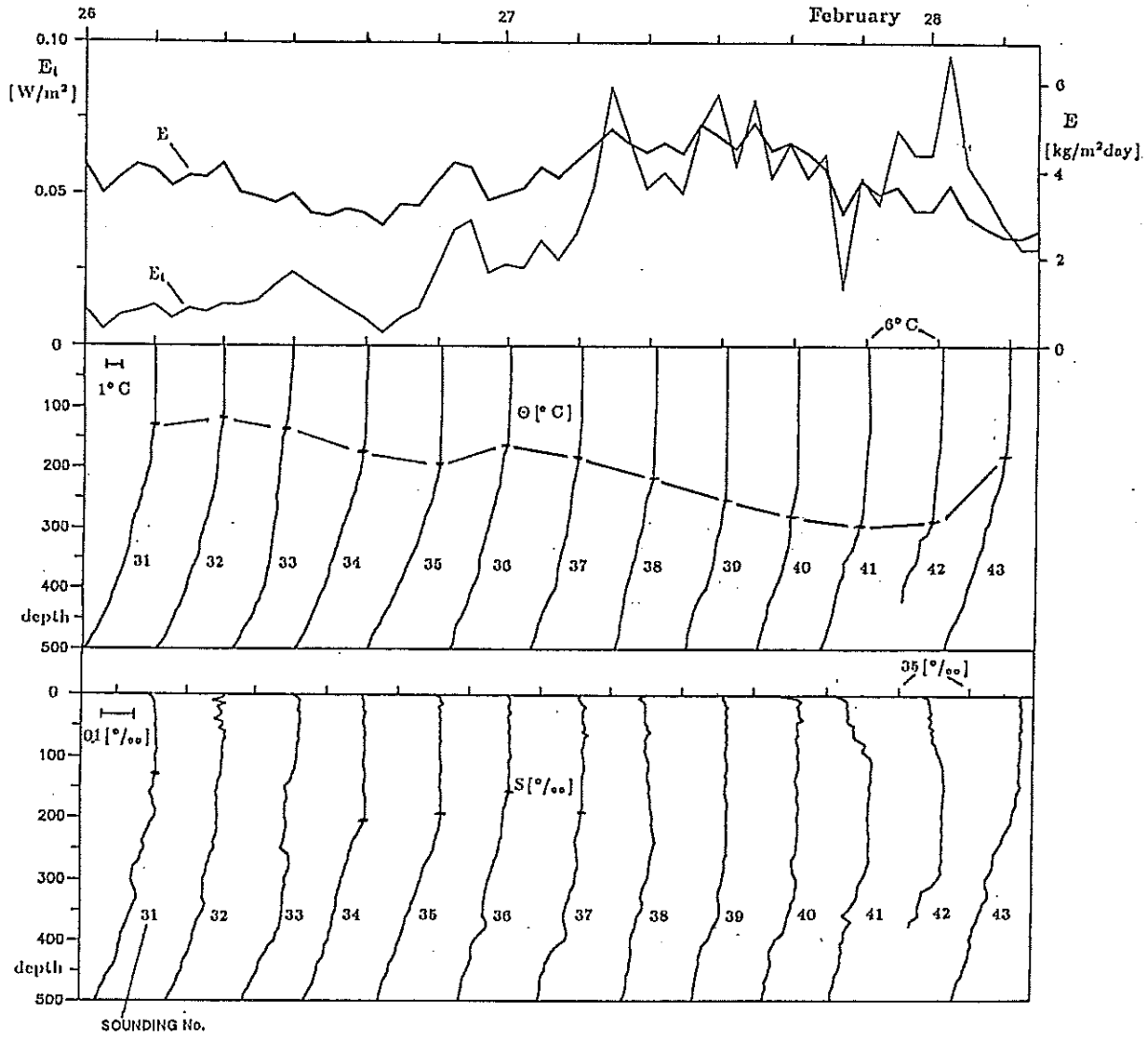

Figure 2.15: Deepening of mixed layer during the period 26-28 February. The upper part shows turbulent kinetic energy generation E_t at the surface and evaporation flux E. The middle part shows four-hourly profiles of potential temperature Θ (dashed line marks mixed layer depth). Numbers refer to sounding numbers. Dashes at abszissa mark the 6°C-value for each sounding. The lower part shows profiles of salinity S. Dashes at abszissa mark the 35‰-value for each sounding.

3. *Measurements on Bear Island*

(G. Kruspe, Max-Planck-Institut für Meteorologie, Hamburg
B. Brümmer, Meteorologisches Institut der Universität Hamburg)

3.1. *General remarks*

The Norwegian Weather Service, Det Norske Meteorlogiske Institutt, runs a weather station at the northern coast of the island (Figure. 3.1). At this station surface observations are taken every three hours and radiosondes are launched at 00 and 12 UT on a routine basis. The Norwegian Weather Service kindly agreed to support the experiment by providing these data as well as to launch two additional radiosondes at 06 and 18 UT. As on board the VALDIVIA, a Vaisala MicroCora system is used for the aerological measurements of pressure, temperature, relative humidity, wind speed and direction. After the experiment, surface observations and radiosonde data were sent in form of tables or on discettes to the Meteorological Institute of the University of Hamburg.

We gratefully acknowledge the support by the Norwegian Weather Service and particularly want to thank Prof. Dr. A. Eliassen and Dr. M. Lystad in Oslo, Dr. K. Wilhelmson in Tromsø and last not least the weather crew on Bear Island for their co-operation and help.

3.2. *Surface Observations*

As mentioned above, surface data were available every three hours. Bear Island and VALDIVIA are lying on the same trajectory during northeasterly flow with a fetch of about 420 km, which allows the study of air mass transformation along the path over the open water. Surface data of pressure p, air and water temperature T_a and T_w, relative humidity RH, wind speed FF and wind direction DD measured at Bear Island during the period 15 February until 15 March 1991 are presented in Figure 3.2. A comparison of the surface data at Bear Island with those at VALDIVIA are shown in Figure 3.3 and 3.4.

The different character of the ship and island station is obvious. The temperature difference between the two stations varies between 14K and about 1.5K, if VALDIVIA's Tromsø break (6 March) is neglected. The mean difference is >7K during off-ice winds from N or NE, whereas values of about 2K were observed during advection of Atlantic air masses from SW.

In the mean, the surface water at VALDIVIA was about 8K warmer than at Bear Island. The histograms of the air/sea temperature differences of the two stations in Figure 3.4 reveal higher convective instability over the open sea than over the ice station. The dominant peaks for T_a - T_w are situated at about -3.5K at VALDIVIA and at about - 0.5K at Bear Island.

The wind directions (Figure 3.3) do not differ remarkably between the two stations during the period from 23 February until the end of the campaign. With respect to wind speed, we find in most cases significantly higher wind speeds over the sea than over the island, in the mean the difference is about 5 m/s.

3.3. Aerological measurements

As mentioned above, radiosondes were launched every 6 hours. The data were submitted from Det Norske Meteorologiske Institutt in form of standard levels and marked points for the thermodynamic quantities p, T, RH and height and the wind values FF, DD and height separately. In order to calculate mean time-height cross-sections the data were handled in the same way as described in section 2.4.2a for R/V VALDIVIA. The results are presented in Figures 3.5a-g.

Most marked variations in the cross-sections are similar to those observed at VALDIVIA, such as the cold air event on 24/25 February, the extreme warm period around 27/28 February and the following slow but continuous cooling until 8 March. However, there are some events which are different. For example, the occlusion of 10/11 March reaches VALDIVIA with warm air but does not reach Bear Island. And also the very strong cold air outbreak on 13 March connected with a depression developing E/SE of Spitsbergen is only present in the data of Bear Island. The latter event was the stongest cold air outbreak during the field experiment ARKTIS 1991 and lasted for several days.

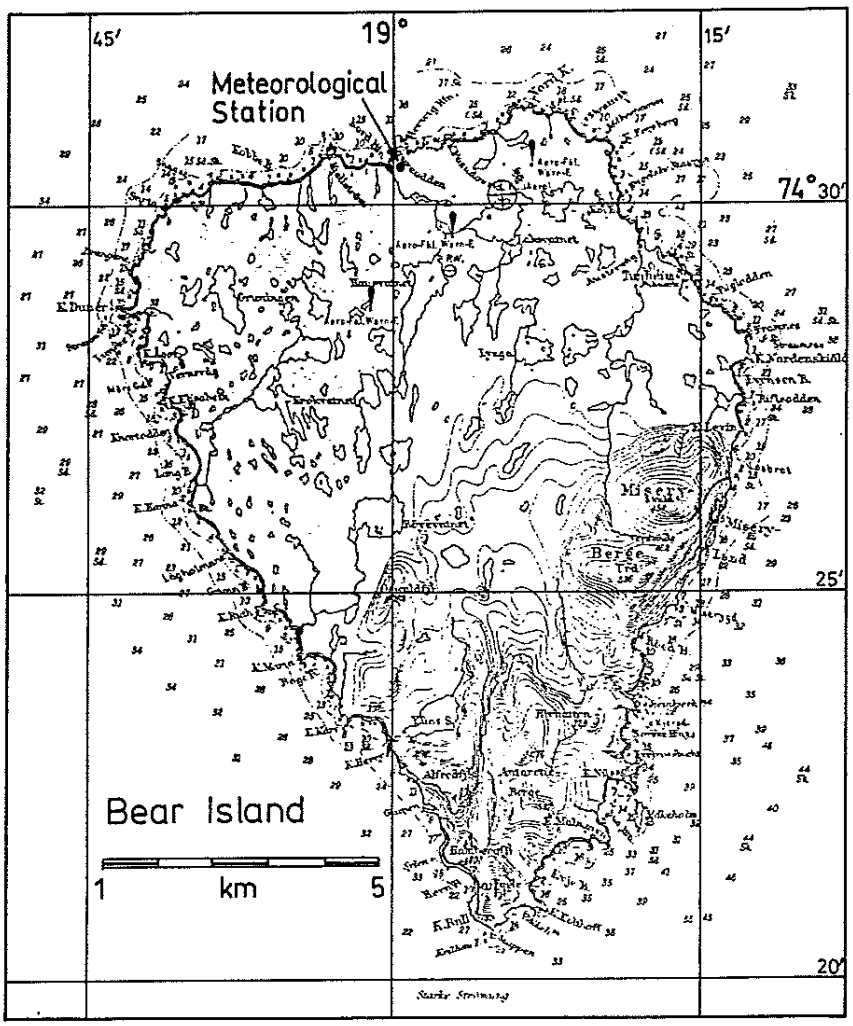

Figure 3.1: Map of Bear Island with meteorological station of Det Norske Meteorologiske Institutt at the northern coast.

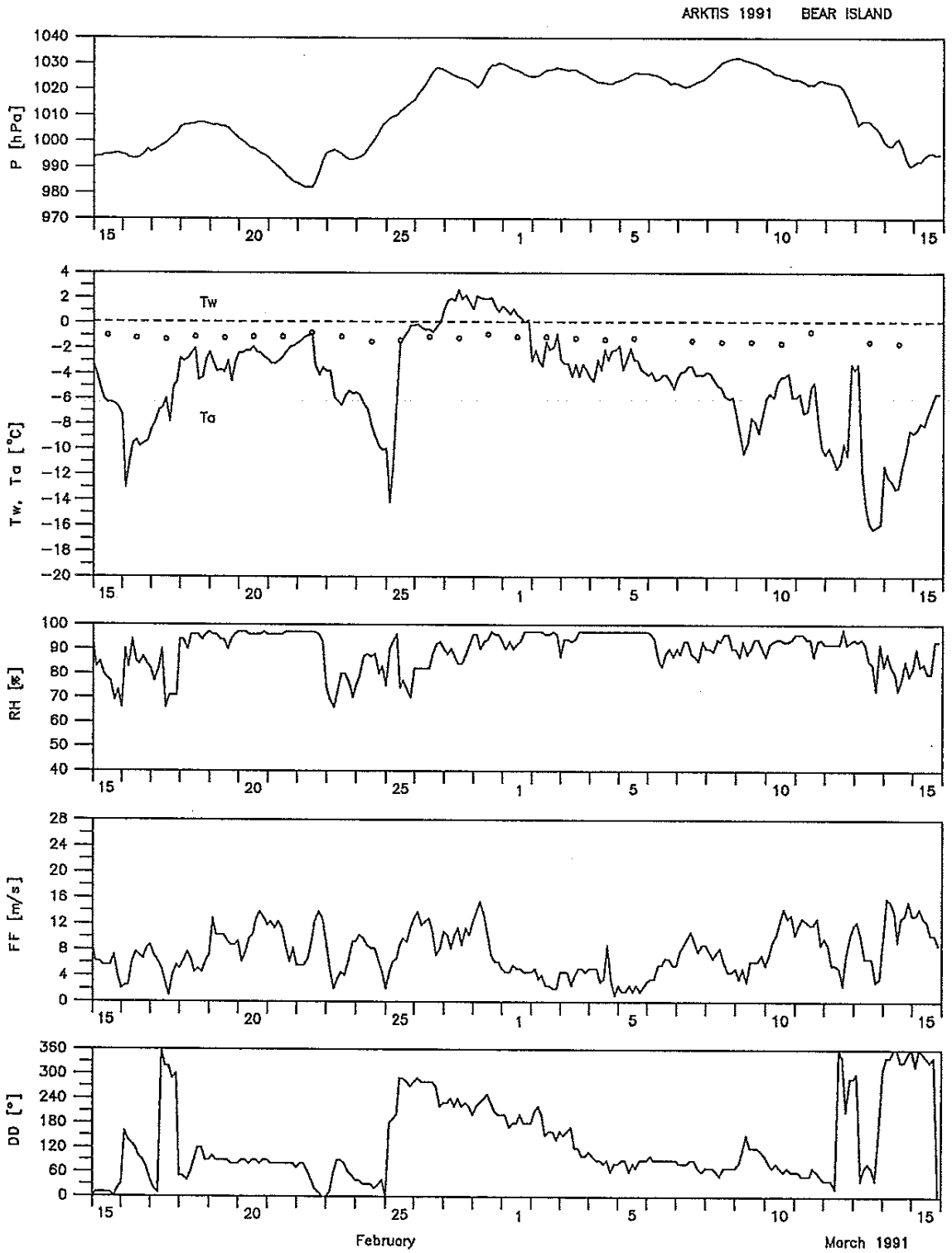

Figure 3.2: Time series of three-hourly surface observations of pressure p, air temperature T_a, water temperature T_w, relative humidity RH, wind speed FF and wind direction DD at Bear Island during the period 15 February until 15 March 1991.

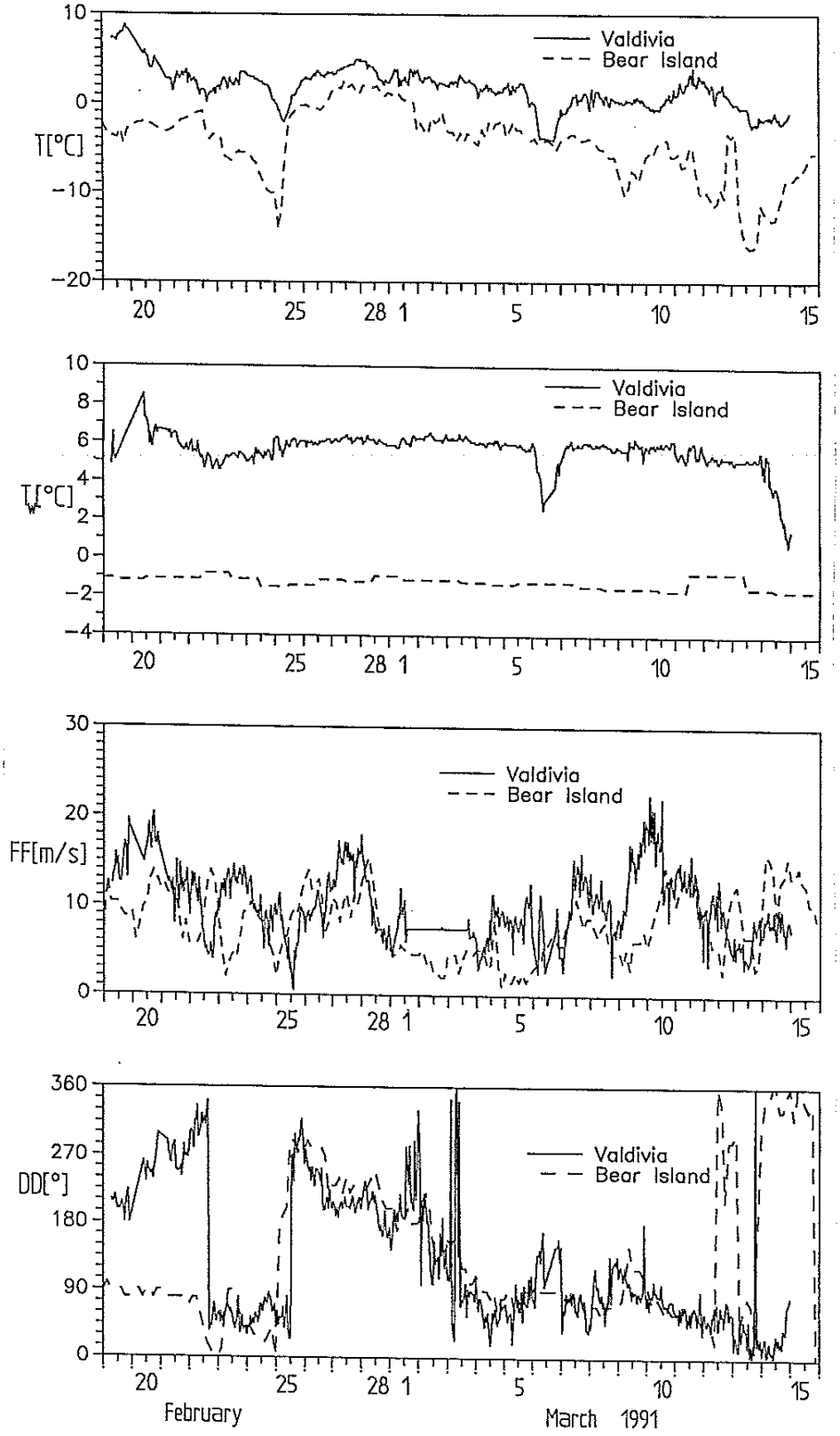

Figure 3.3: Comparison of surface data of air temperature T, water temperature T_w, and wind direction DD at Bear Island and VALDIVIA. Observations are three-hourly at Bear Island and one-hourly at VALDIVIA.

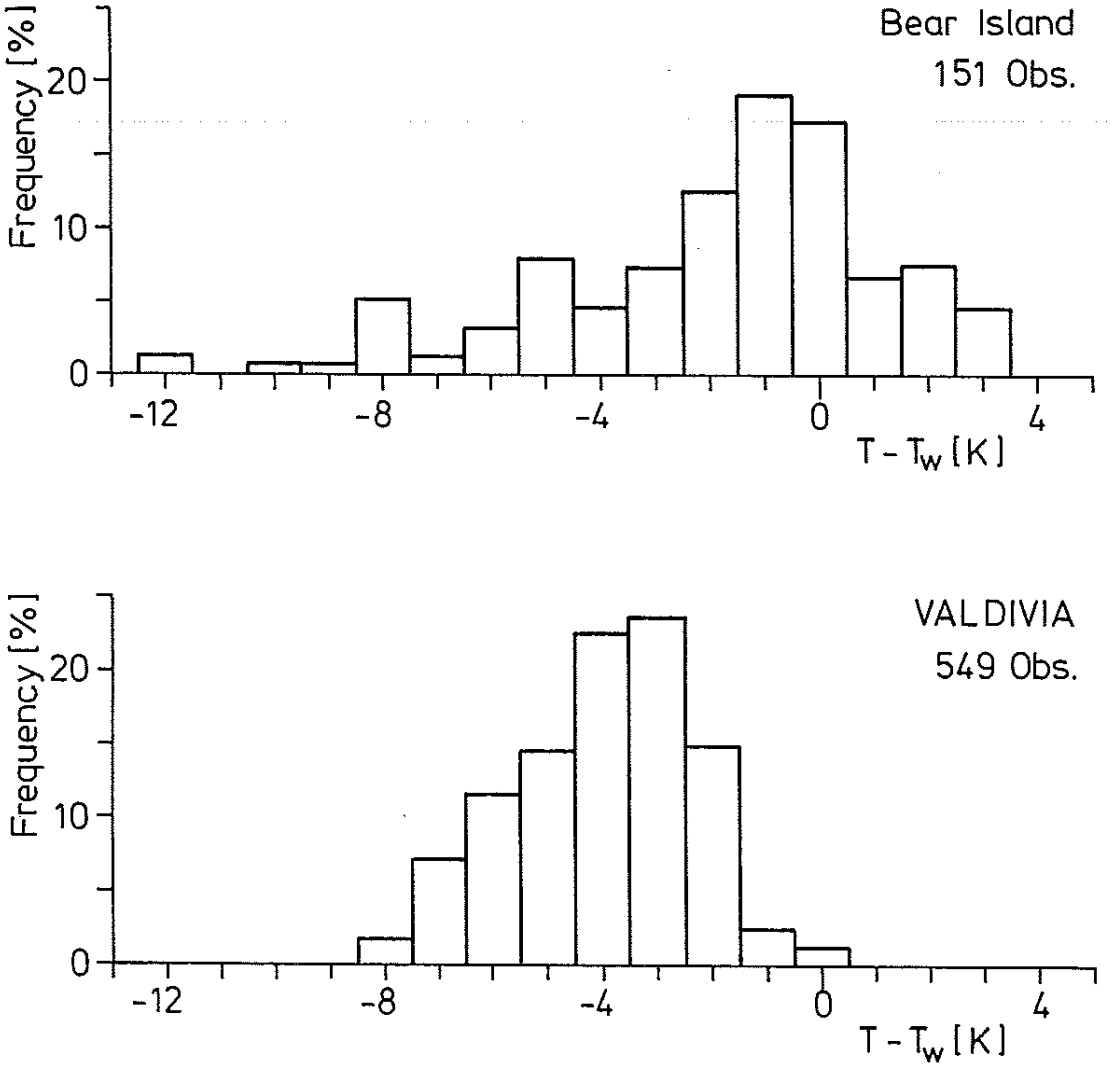

Figure 3.4: Frequency distribution of air-sea temperature difference T - T_w, at Bear Island (above) and VALDIVIA (below).

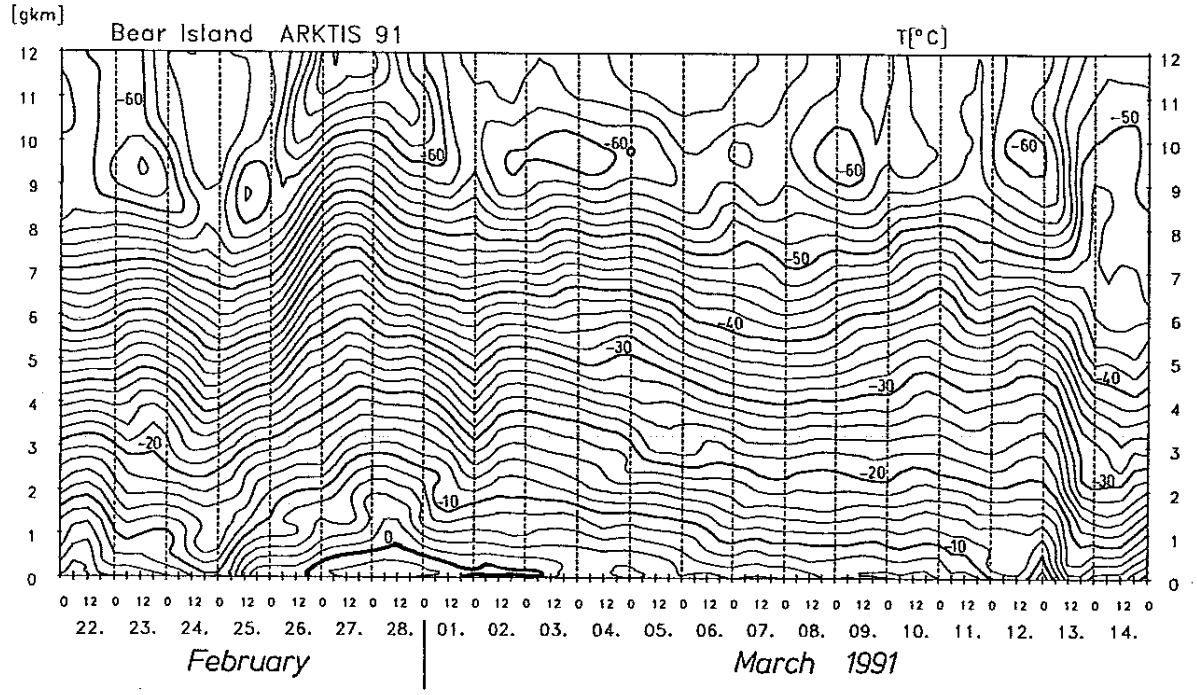

Figure 3.5a: Time-height cross-section of temperature T at Bear Island. Temperature interval: 2K.

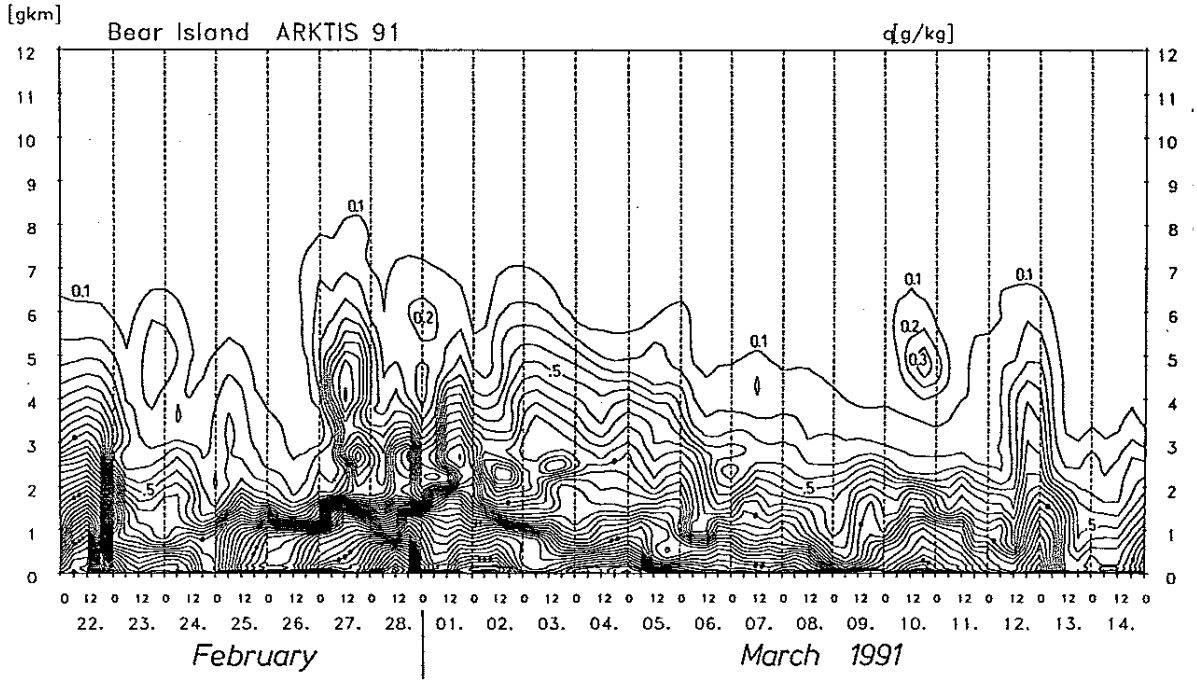

Figure 3.5b: Time-height cross-section of specific humidity q. Interval: 0.1 g/kg. One, two or three dots mark the 1, 2 and 3 g/kg isolines, respectively.

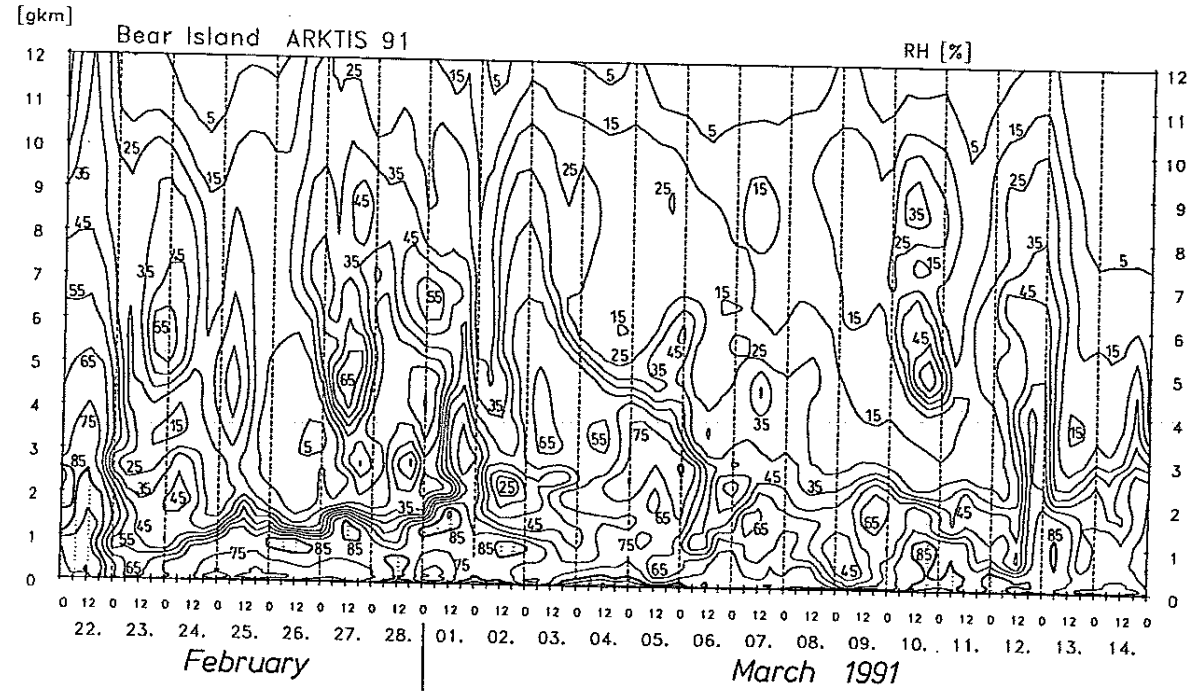

Figure 3.5c: Time-height cross-section of relative humidity RH. Interval: 10%. Areas with RH > 85% are dashed.

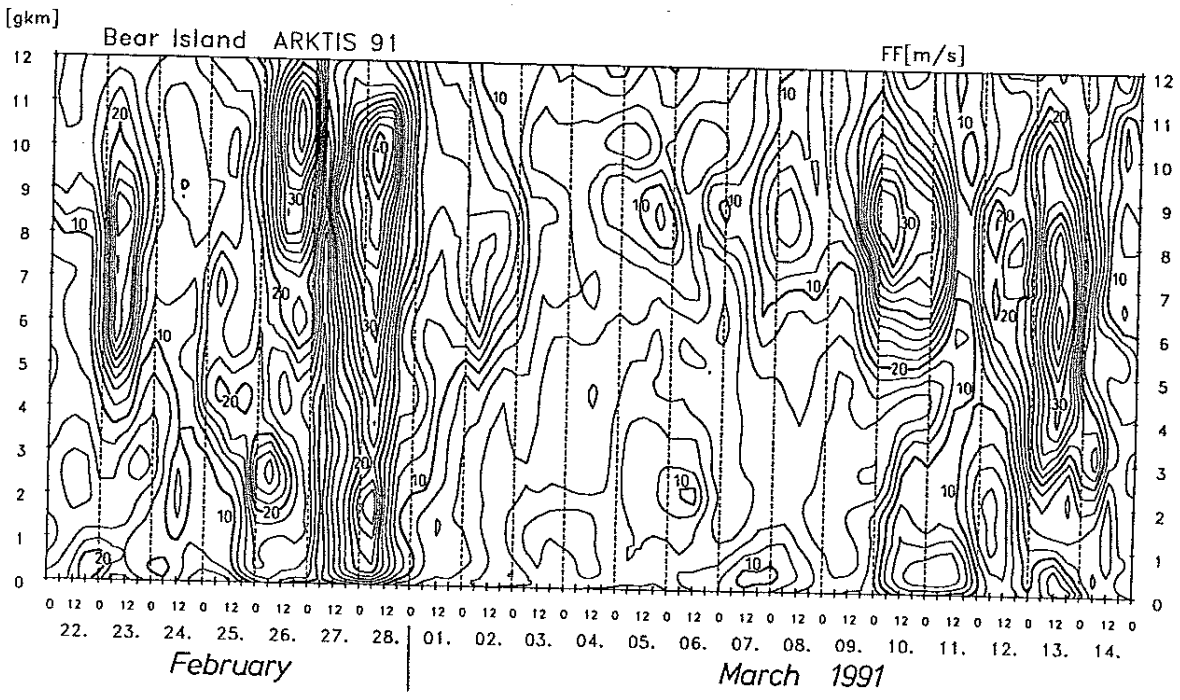

Figure 3.5d: Time-height cross-section of wind speed FF. Interval: 2 m/s.

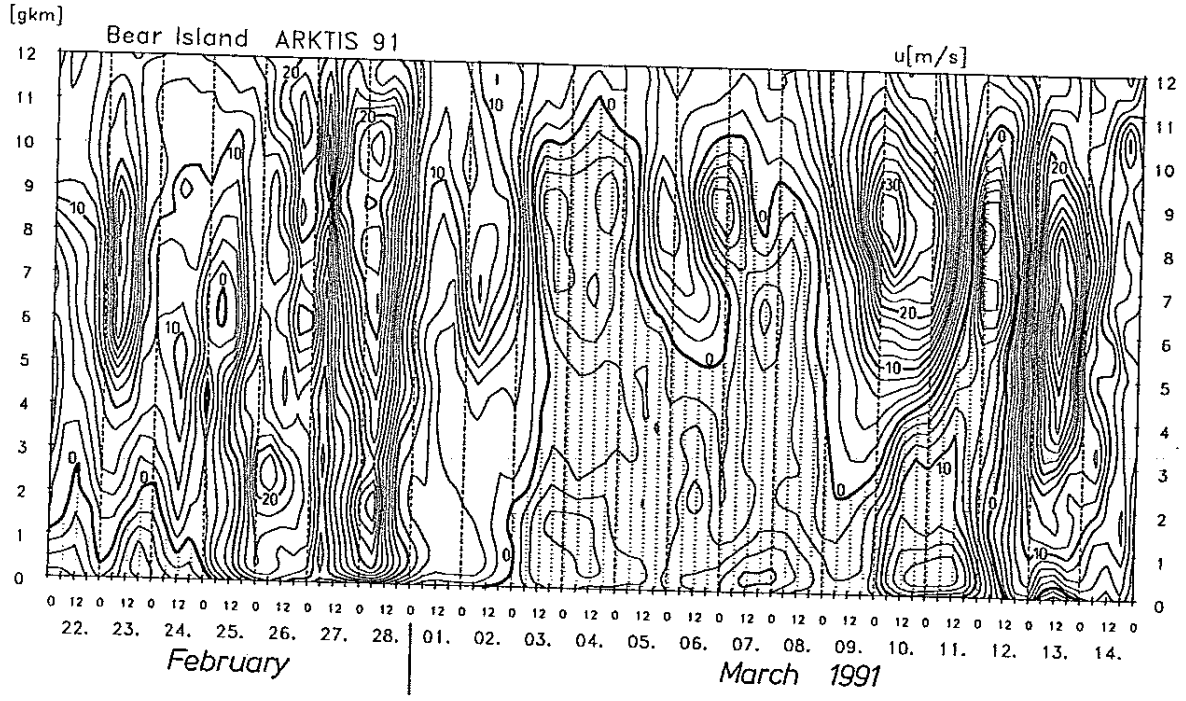

Figure 3.5e: Time-height cross-section of zonal wind component u. Interval: 2 m/s. Areas with easterly winds (u < 0) are dashed.

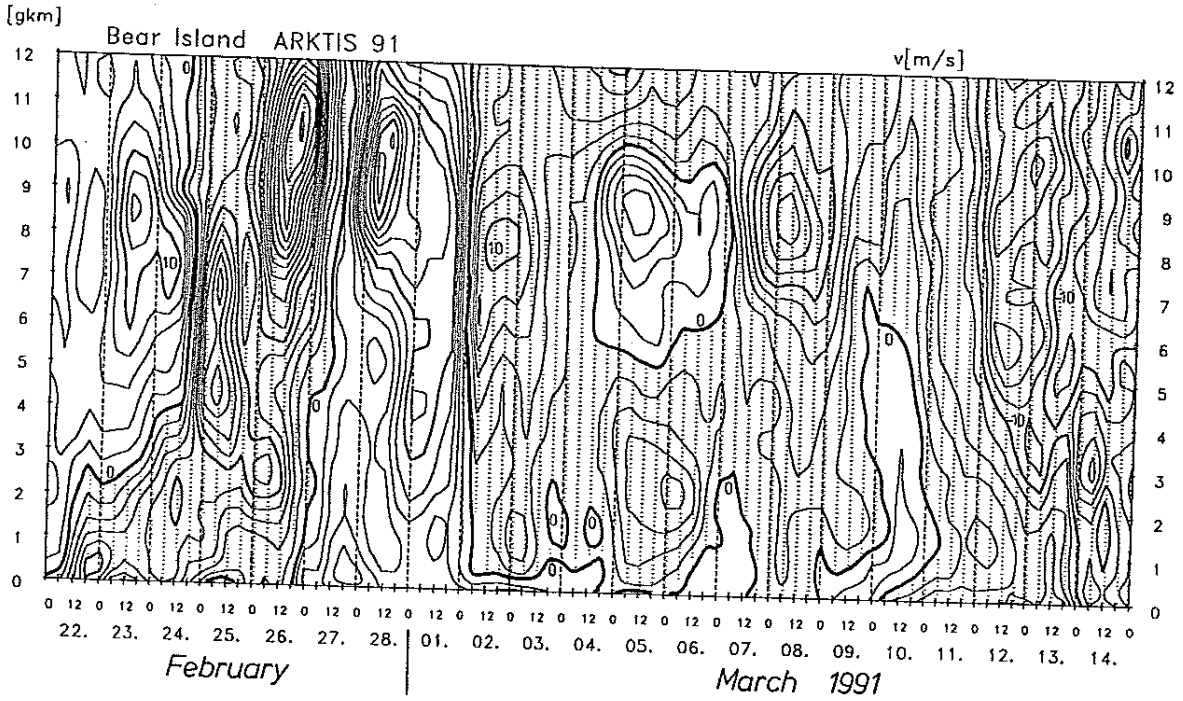

Figure 3.5f: Time-height cross-section of meridional wind component v. Interval: 2 m/s. Areas with northerly winds (v < 0) are dashed.

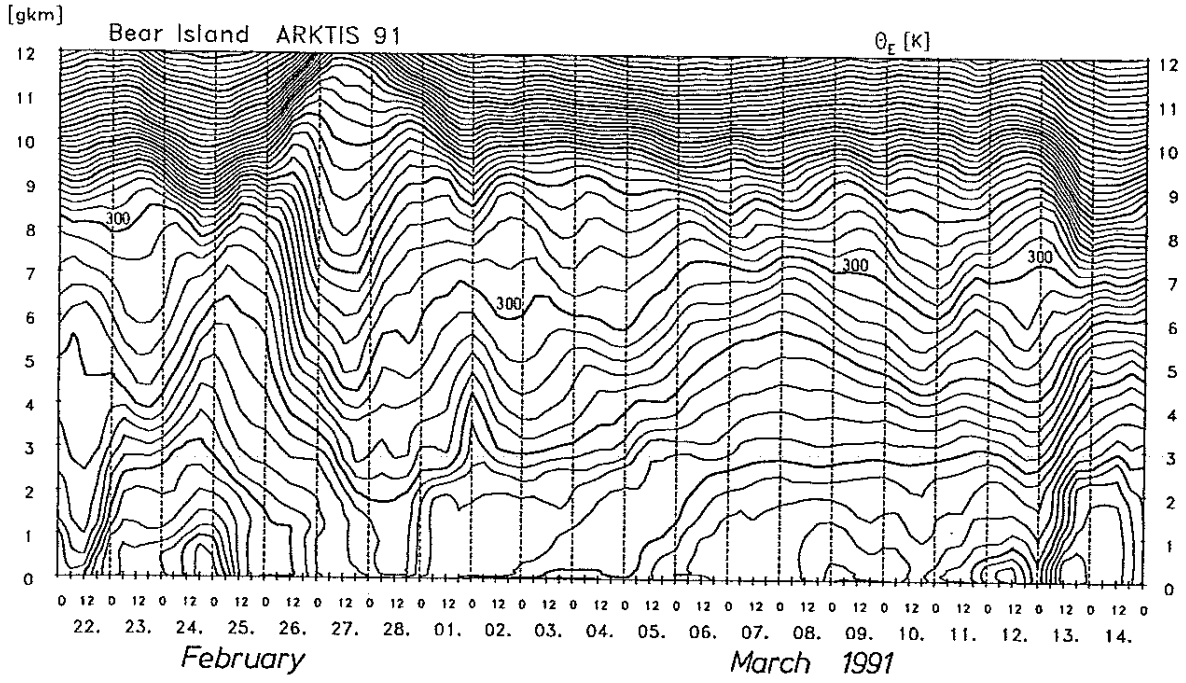

Figure 3.5g: Time-height cross-section of equivalent potential temperature Θ_e. Interval: 2 K.

4. *Measurements at Land Station Andenes*

(B. Rump, Meteorologisches Institut der Universität Hamburg)

4.1. Introduction

The ARKTIS 1991 operation center was established on Andøya, the northernmost of the Vesterålen Islands (Figure 4.1). The Andøya Rocket Range served as scientists lodging. It is situated next to Andenes in the north of the Island and about 5 km away from the airfield, where the two aircraft were stationed. For continuous weather observations a special surface station of the Max-Planck-Institute of Meteorology, Hamburg, was built-up on the airfield to measure standard meteorological data and radiation data. They were used for planning aircraft missions as well as for intercomparison with aircraft measurements at take-off and landing.

Besides that, routine surface observations of the Norske Meteorologiske Institutt were also taken at the airfield and were placed to our disposal after the expedition.

4.2 Measurements at the Automatic Surface Station

The automatic station for continuous observations of the relevant meteorological surface data and for radiation measurements was placed on a plain terrain at the end of a runway. The station was built-up on 20 February during a snow storm and was dismantelt on 12 March. Data collection started on 21 February at 12 UT and was stopped on 12 March at 1030 UT.

Mean values over 10 seconds were taken only the first 3 days, then means over one minute were preferred and stored on PC discs. Measurements were interrupted only twice, on 22 February from 0300 to 1030 UT due to power breakdown and on 6 March from 1550 to 1646 UT, where only radiation measurements are available.

The station was equipped with a pressure Digiquartz, a cup anemometer and a wind vane, a heated aspiration psychrometer and a dew-point mirror to obtain the meteorological surface quantities. Shortwave radiation was determined with an up- and downward looking Kipp & Zonen radiation measuring instrument. For the total radiation a Lange radiation measuring instrument was used (see Figures 4.2 and 4.3).

Two examples of the sampled data that were also used for flight mission plannings are shown in Figures 4.4 and 4.5. In both cases small lows passed the island during daytime which caused wind changes from southern directions in front of the low to northern afterwards. At the same time wind velocity increased while humidity decreased. Temperature variations were only small. The passing low was joined with rain on 24 February, with snow on 11 March. Radiation registrations show great short wave radiation variability on 24 February due to the partly cloud covered sky with stratocumulus. On 11 March the great albedo caused by snow cover and the small shortwave fluxes due to total cloud cover led to small values of radiation balance.

For comparison with the sea station VALDIVIA hourly surface data, averaged over 10 minutes around the full hour, were calculated. Figure 4.6 shows the relevant meteorological data and radiation data for the whole measuring period.

4.3. Routine Surface Observations

The daily synoptic observations were taken by the Norske Meteorologiske Institutt at Andenes airfield tower. They are available for the time period from 15 February to 15 March, but four observations per day, only. Besides measurements of the standard meteorological data like temperature, pressure, humidity and wind, precipitation and snow heights were recorded. Moreover the data set contains informations about cloud cover and weather phenomena, which will be useful for the interpretation of local weather conditions. The proximity to the location of the automatic station makes it possible to use them for intercomparison.

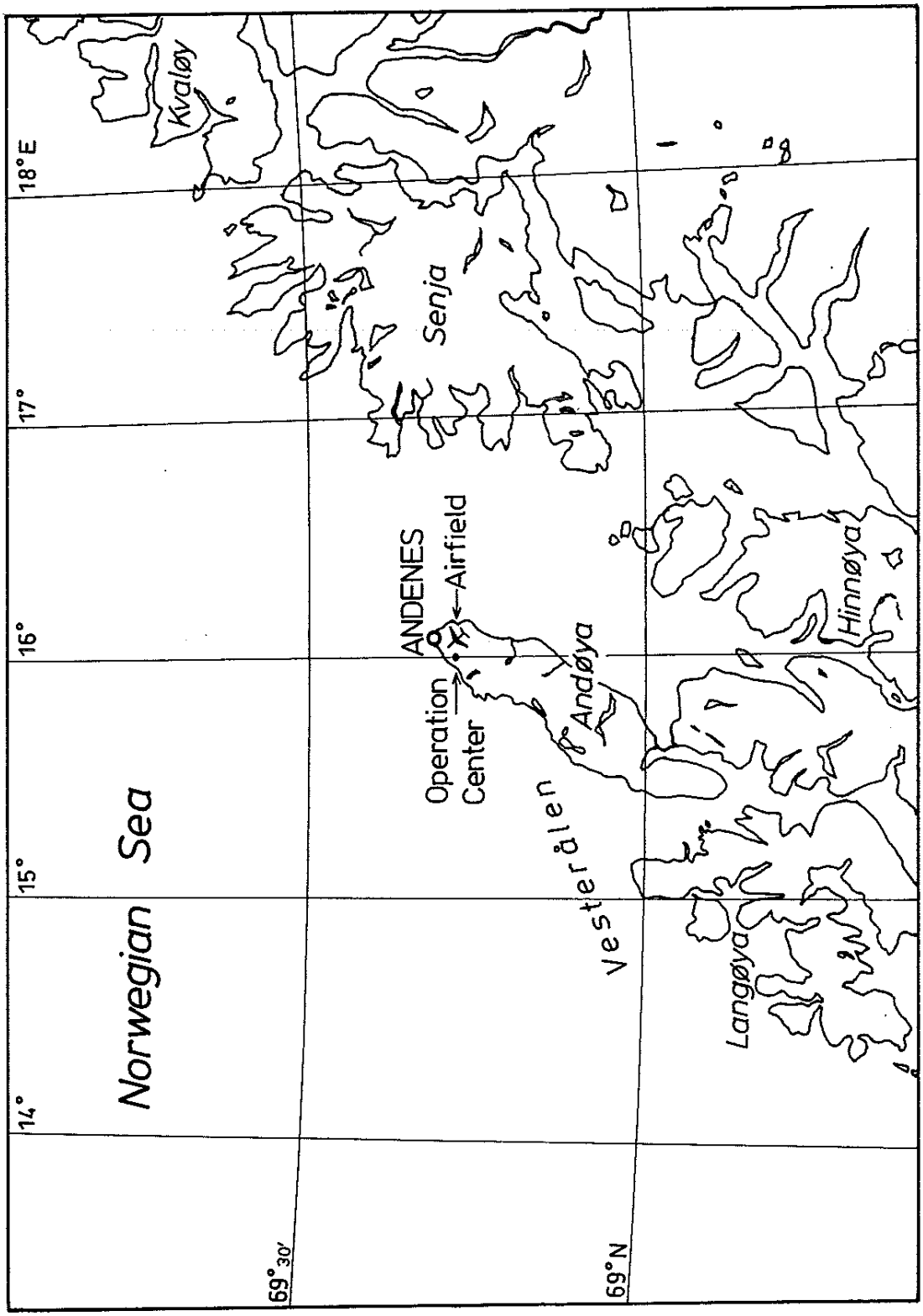

Figure 4.1: Geographical location of station Andenes with airfield and ARKTIS '91 operation center at the Andøya Rocket Range on the Vesterålen island Andøya.

Figure 4.2: The automatic station for meteorological surface data mounted at the airfield Andenes.

Figure 4.3: The automatic radiation station mounted at the airfield Andenes.

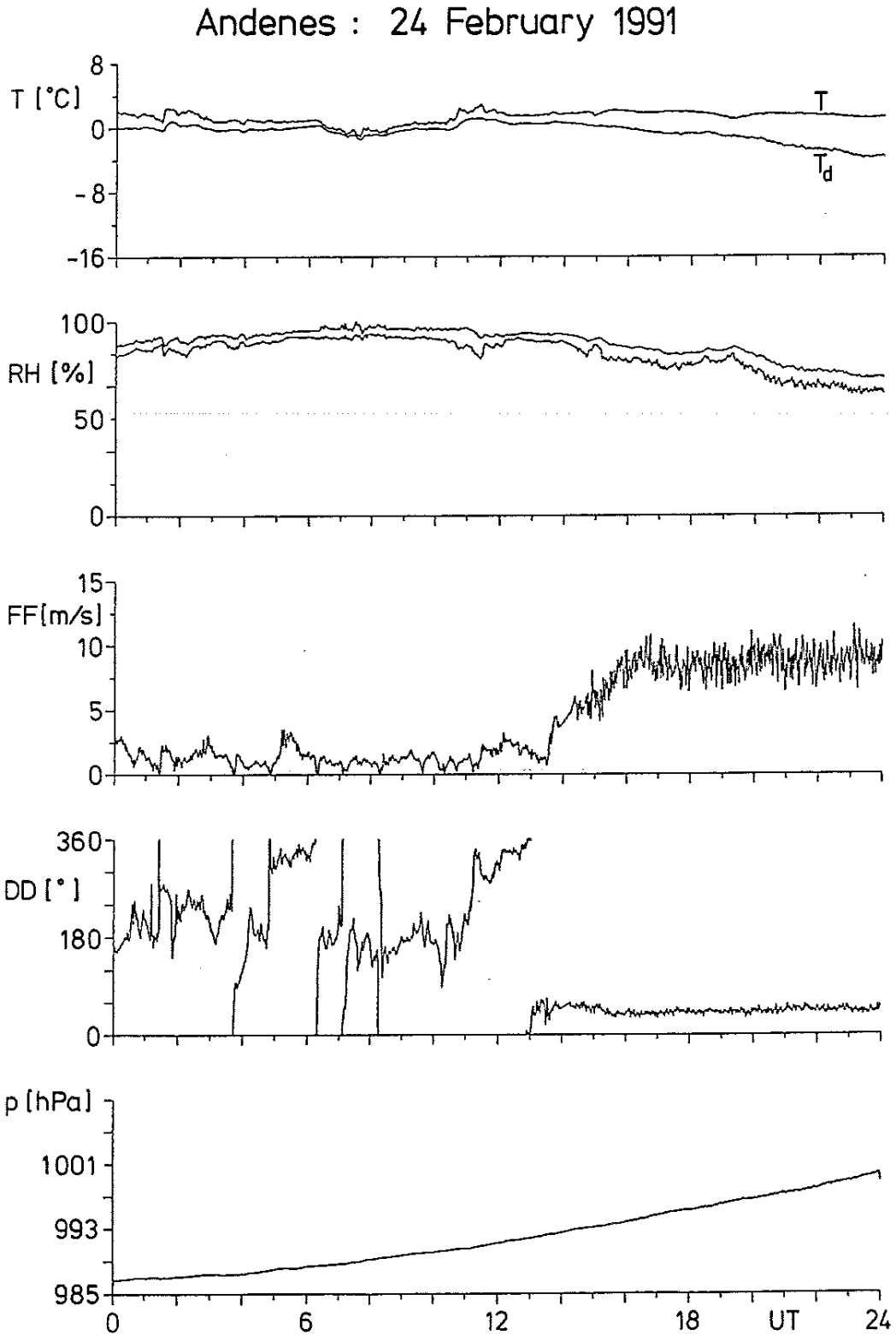

Figure 4.4a: Time series of 1-minute averages of temperature T, dew-point T_d, relative humidity RH, wind speed FF, wind direction DD, and pressure p at station level (≈ 5 m above NN) measured on 24 February 1991 at Andenes.

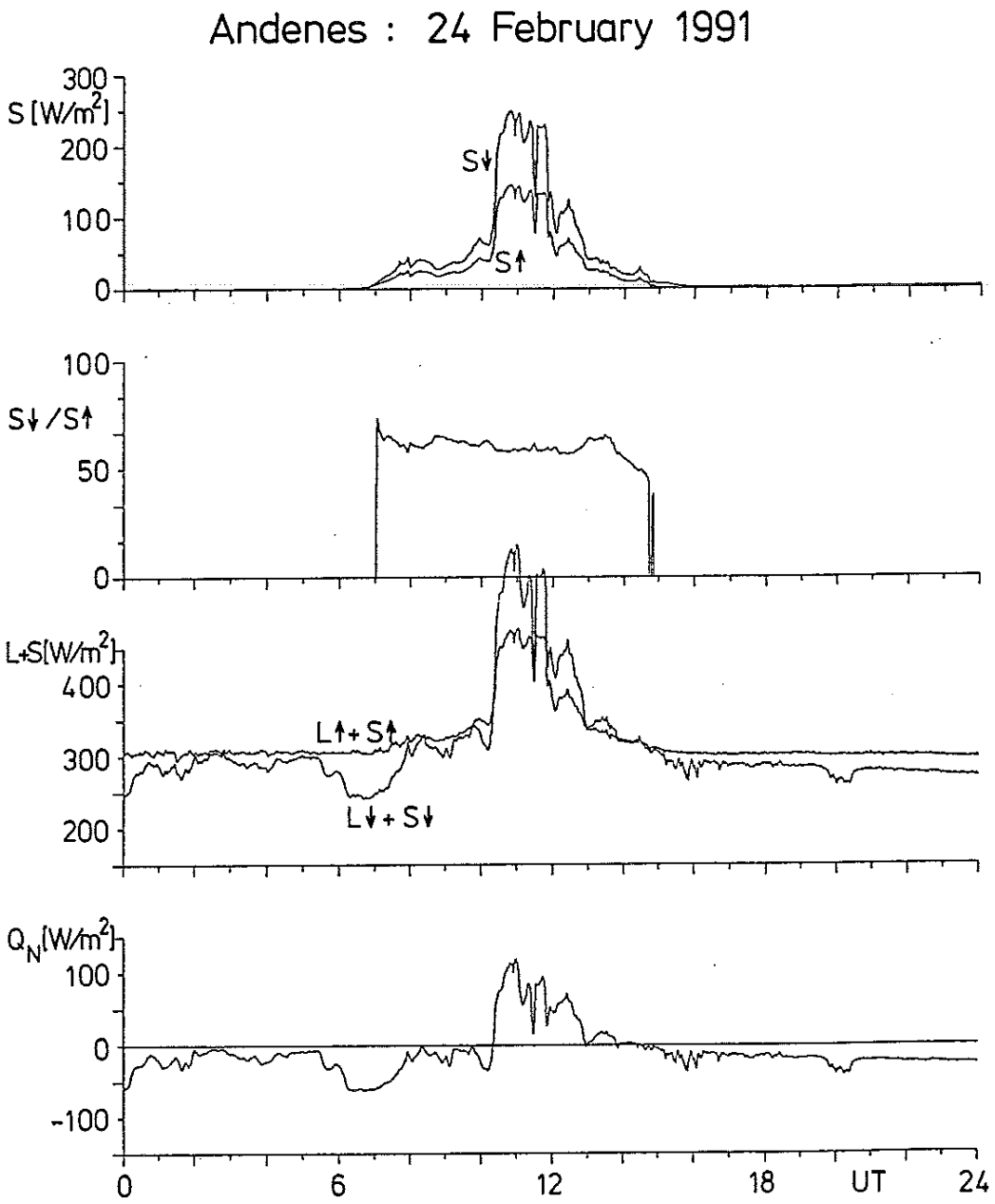

Figure 4.4b: Time series of 1-minute averages of the radiation data measured on 24 February 1991 at Andenes: shortwave radiation from above and below, S↓ and S↑, albedo S↑ / S↓, total radiation from above and below, S↓ + L↓ and S↑ + L↑, and radiation balance, S↓ + L↓ - S↑ - L↑.

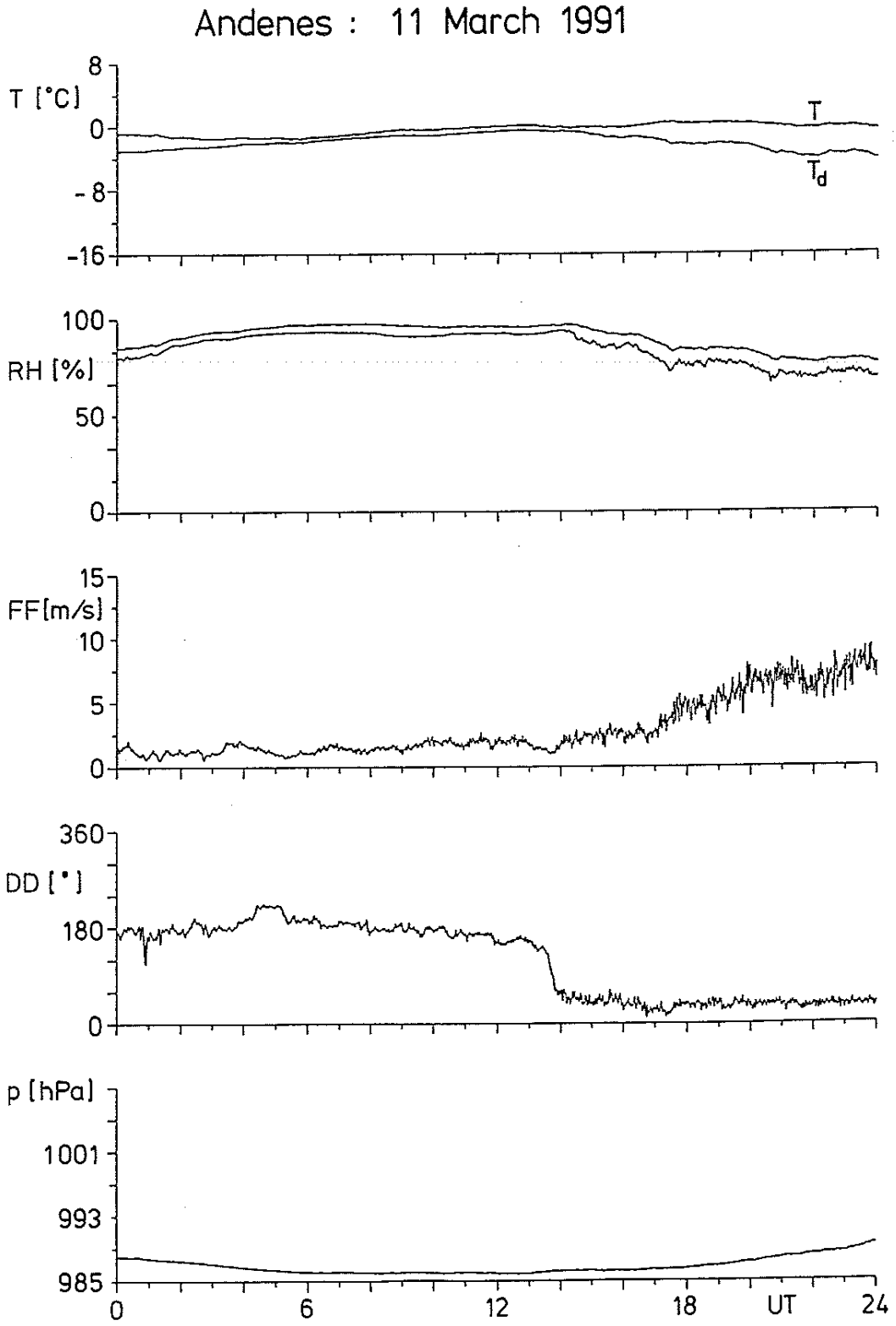

Figure 4.5a: As Figure 4.4a, but for 11 March 1991.

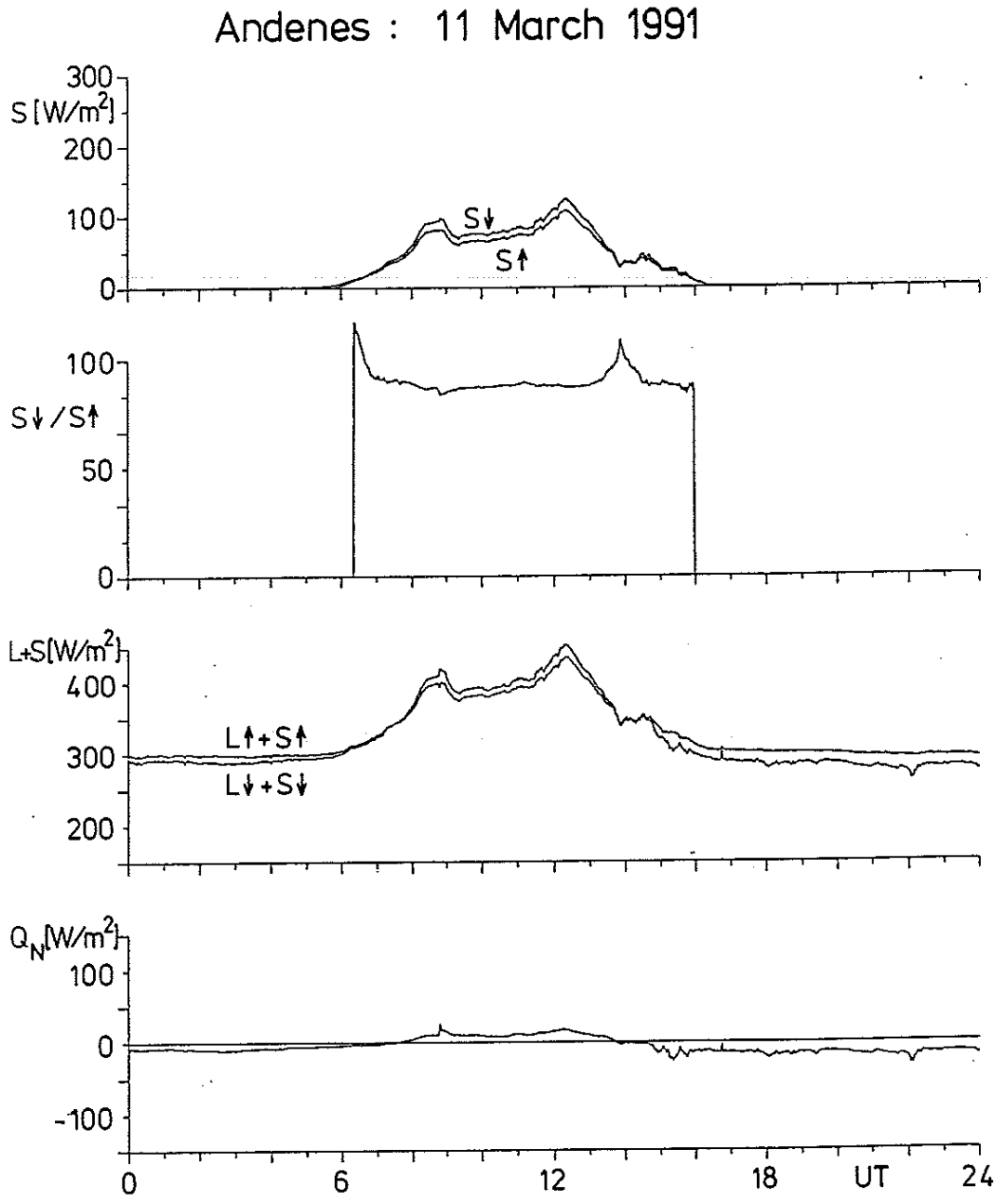

Figure 4.5b: As Figure 4.4b, but for 11 March 1991.

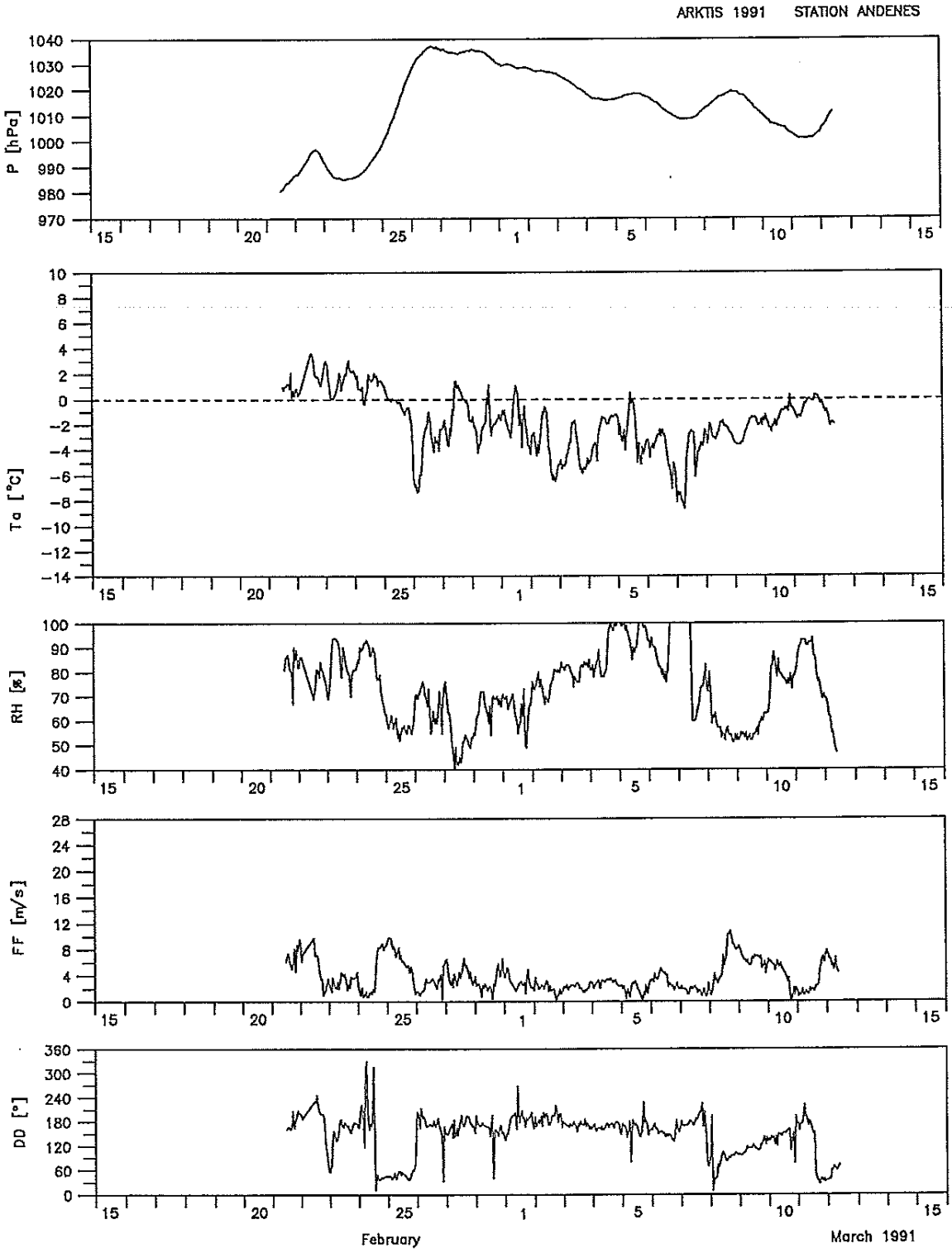

Figure 4.6a: Hourly 10-minutes averages of temperature T, dew-point Td, relative humidity RH, wind speed FF, wind direction DD, and pressure p at station level at the automatic station Andenes.

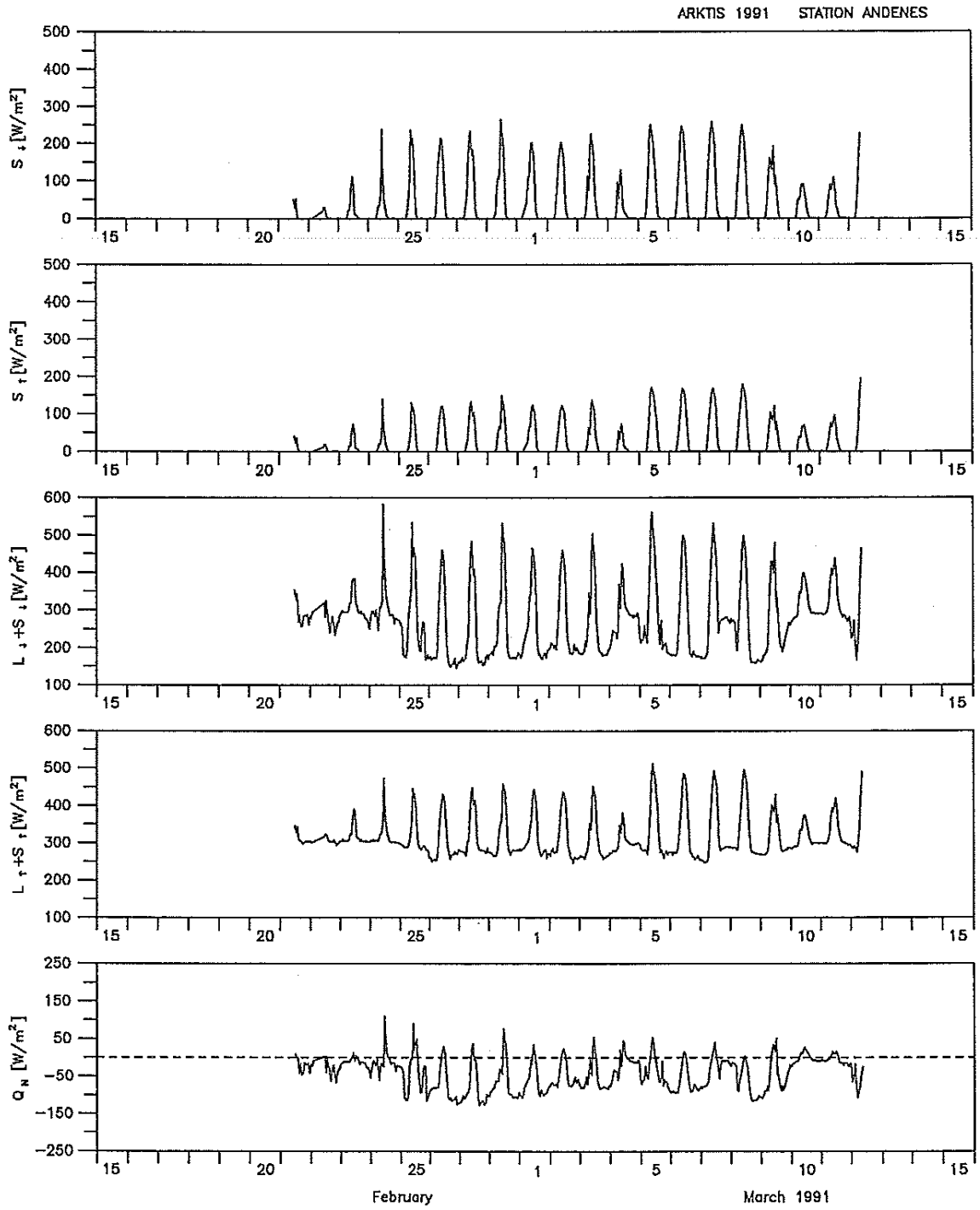

Figure 4.6b: Hourly 10-minutes averages of shortwave radiation from above and below, S↓ and S↑, total radiation from above and below, S↓ + L↓ and S↑ + L↑, and radiation balance, Q_N = S↓ + L↓ - S↑ - L↑.

5. *Aircraft measurements*

5.1. *General remarks*

(B. Brümmer, Meteorologisches Institut der Universität Hamburg)

Two aircraft participated in the field experiment ARKTIS 1991: a FALCON-20 of the Deutsche Versuchsanstalt für Luft- und Raumfahrt (DLR) at Oberpfaffenhofen (Munich) and a DORNIER-128 (DO-128) of the Technical University at Braunschweig. Details about the specifications and instrumentations of the two aircraft follow in Section 5.2.

Both aircraft operated from the Norwegian military airfield Andenes which is situated on the island Andöya at about 69° 18' N and 16° 06' E (see Figure 4.1). A separate hangar was available for each aircraft - a fact which is absolutely necessary under the local climatic conditions. The airfield was operated for 24 hours on all days although flight missions were only performed during daylight hours. The meteorological flight briefing for pilots and scientists was made by the staff of the local airfield weather station. Their engaged support is particularly mentioned. The cooperation with the airfield staff (technicans, aircraft controlers, etc.) during the campaign was unbureaucratic and effective. We thank the head of the Andenes airfield for allowing us to use the airfield and its facilities. In this context we appreciate the help of Major K. Alvheim who was the contact person between our group and the airfield administration.

The operation center of the ARKTIS 1991 experiment as well as all participants involved in the aircraft operations were accommodated near Andenes at the Andøya Rocket Range belonging to the Norwegian Space Center. There, the experimentators found excellent conditions for office rooms and for board and lodging in two nearby buildings. Furthermore, the Rocket Range is an excellent place for steering and conducting field experiments, because of the good communication infra-structure. We thank Mr. K. Adolfsen, the head of the Rocket Range, that we could use this facilities and we are also grateful to him and his staff for their help during the preparation and realization phase of the experiment.

Planning meetings in the operation center took place twice per day, one in the morning to decide on the aircraft activities of the current day and the other in the late afternoon to plan tentatively the activities of the following day. In cases

of not clearly foreseeable weather developments additional planning meetings were fitted in between.

As decision background for planning the aircraft missions three sources of information were taken into account. First, quick-look satellite images of NOAA 9, 10 and 11 received at Tromsø Satellite Station were transmitted via data link to Andøya Rocket Range. Details about the subsequent on-line and off-line processing and pictorial presentation of the satellite data are given in Section 6. Second, weather maps - analyses and prognoses - of the German and Norwegian Weather Service were used. The charts were transmitted via telefax from Hamburg, Oslo, Tromsø or Andenes airport to the operation center. The central weather office in Oslo also supplied the latest ice and water temperature charts. As third information, the latest weather data (surface observations and radiosonde ascent) measured at research vessel VALDIVIA within the observational area were taken into account. These data were transmitted as telex via Rogaland Radio to the operation center.

The weather conditions, either on Andenes airfield or outside in the operational area, were always within the limits of the international flight rules, so that each flight mission could be executed as planned. Only in a few cases with very heavy snow showers down to the sea surface, the aircraft had to fly round these showers. Other air traffic in the observational area was little so that the flight missions could be placed where the weather conditions appeared to be best.

The scientific ojective of ARKTIS 1991 was the investigation of cold air outbreaks from the Arctic ice over the adjacent open water of the Nord Polar Sea or the Barents Sea. The particular task of the aircraft was to document the downstream development of boundary layer structure and cloud coverage and the change of cloud patterns. The downstream modifications typically take place over several hundred kilometers, so that they cannot be measured by one aircraft only due to the limited endurance of the two aircraft. Therefore, the experimental strategy was to split the tasks of the two aircraft according to their specifications: the DO-128 operated within an area of not more than 300 km distance from Andenes airfield and the FALCON-20 operated nearer to the ice edge between 300 and 500 km distance from the airfield.

Flight patterns within the experimental area consisted of vertical profile soundings between 90 m and 3000 m (DO-128) or up to 9000 m (FALCON) and several horizontal traverses in the subcloud and cloud layer. Horizontal flights at 90 m

height were made during each mission in order to measure the lower boundary conditions, i.e. the turbulent fluxes of temperature, humidity and momentum as well as the sea surface temperature by use of a radiation thermometer.

In order to use the available flight time optimally, the transit flights between Andenes and the operational area were flown at low levels (mostly 90 m) by DO-128 and at high levels (between 4 and 9 km) by FALCON. The measurements during transit will also be useful for scientific evaluation. The high level transit with the FALCON gave a good overview about the weather situation and the possibility to find the best place for the aircraft operations in the boundary layer.

The members of the aircraft groups and the operation center are listed below:
Meteorologisches Institut der Universität Hamburg: H.-H. Brecht, B. Brümmer, A. Manschke, Th. Martin, G. Müller, A. Rhodin, B. Rump.
Max-Planck-Institut für Meteorologie, Hamburg: S. Bakan.
Deutsche Forschungsanstalt für Luft- und Raumfahrt (DLR), Oberpfaffenhofen: H.G. Christner, F. Eisenhut, H. Fimpel, H. Horst, H. Keller, W. Meier, R. Rahn, J. Stingl, D. Zander.
Institut für Flugführung der Technischen Universität Braunschweig: D. Brunner, R. Hankers, A. Knüppel , L. Seiler, H. Schulz.
All this place, I want to thank all participants - pilots, technicians, operators and scientists - for their engaged contribution to the success of the field campaign.

5.2. The aircraft and their meteorological instrumentations

(B. Brümmer, Meteorologisches Institut der Universität Hamburg)

5.2.1. FALCON-20

The FALCON-20 is a two engine jet aircraft with a wing span of about 15 m and a length of about 17 m (Figures 5.1 and 5.2). It can operate up to 41000 feet. The typical flight speed at low levels during operations in the boundary layer is about 100 m/s and at high levels during transit about 250 m/s. The endurance at low levels is about 3 hours. For operations over water - as in our case - the flight crew consists of 3 persons, so that at most 4 persons can be on board additionally for the scientific programme.

The FALCON-20 is equipped with two temperature sensors, three humidity sensors, sensors for static and dynamic pressure and an instrument system to measure the three-dimensional wind vector in connection with an inertial reference system. Furthermore, it has a radio altimeter, a surface temperature infrared radiometer, upward and downward facing pyranometers for the shortwave radiation fluxes and upward and downward facing pyrgeometers for longwave radiation fluxes. In addition, it was equipped with a liquid water content sensor and two instruments to measure size distributions of small particles (cloud droplets) and large particles (snow, ice), respectively. A forward facing video camera is fixed at the cockpit window and records the experimental conditions during the entire flight mission.

All sensors on board the FALCON, their accuracies, sampling frequencies and specifications are summarized in Table 5.1. Figure 5.2. shows where the individual sensors are installed. Apart from the relative wind which is measured at a 1.8 m long carbon fibre boom in the undisturbed air stream ahead of the aircraft and apart from the particle measuring probes which are installed in separate tubes below the aircraft, all other parameters are measured at the body of the plane. A detailed description of the FALCON instrumentation is given by Fimpel (1987).

The signals of the meteorological and aircraft related sensors were recorded in digital form on cassettes. Parallel to this, a preliminary data processing takes place on board the FALCON during the flight, so that the aircraft scientist can obtain on-line information about a selected number of parameters (including the three-dimensional wind vector). These on-line products in the form of tables or plots are printed on paper and are also displayed on screens. Details on the on-board data acquisition system are reported by Wilcke and Gehricke (1988).

In order to inspect interesting meteorological events with a higher resolution, to obtain a general view of the entire flight or to look at other parameters not displayed by the on-line system, a quick-look processing was made immediately after the flight at the operation center in Andenes. The complete processing of all data channels with the highest time resolution will be made later at Oberpfaffenhofen and Hamburg.

References

Fimpel, H.P. (1987): The DLR meteorological research aircraft FALCON -E: Instrumentation and examples of measured data. Preprint: Proceedings of the sixth symposium on meteorological observations and instrumentation. Am. Met. Soc. January 12-16. 1987, New Orleans, LA.

Wilcke, G., and Gehricke, A. (1988): On-board data axquisition system of the FALCON-E aircraft, a new approach. International telemetering conference, Las Vegas, October 17-20, 1988.

Figure 5.1: The FALCON-20 of the DLR.

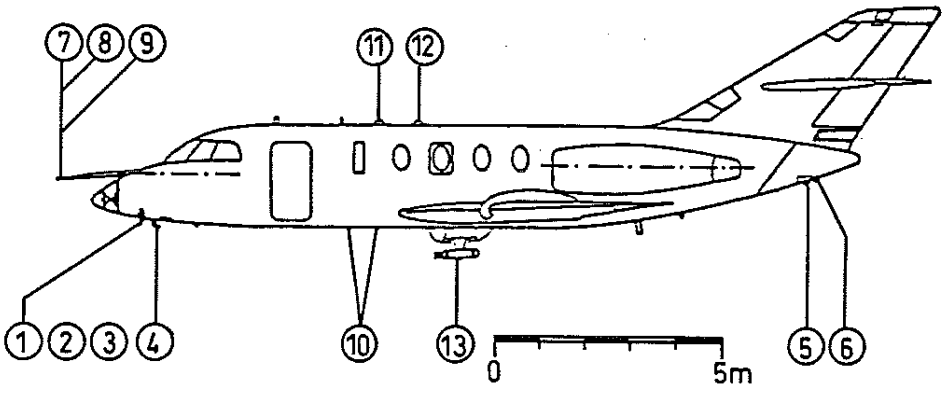

Figure 5.2: Side view of FALCON and location of instruments: (1) temperature, (2) humidity, (3) Johnson-Williams LWC, (4) outlet of humidity tube, (5) pyrgeometer downward, (6) Pyreonometer downward, (7) static pressure, (8) impact pressure, (9) flow angle sensor, (10) photo windows, (11) pyranometer upward, (12) pyrgeometer upward, (13) droplet spectrometer and CSIRO-King LWC.

Table 5.1: Parameters measured on board the FALCON-20.

Parameter	Absolute accuracy	Resolution	Sampling Frequency Hz	Sampling Distance m *)	Primary Instrument, Type, Manufacturer
Wind					
u, v	± 5.0 m/s	± 0.02 ms^{-1}	100	1	Flow Angle Sensor, (5-Hole-Probe) (Rousemount 858 J)
w	0.8 m/s				
Temperature					
T	± 0.3 K	± 0.006K	100	1	Open-wire Total Air Temperature Probe, PT 100 (Rousemount 102 BM/BV)
T	± 0.3 K	± 0.006K	10	10	Total Air Temperature Probe, PT 500 (Rousemount 102 AU2AG)
Humidity					
ρ_w	± 0.7 g m^{-3}	0.002 mg^{-3}	100	1	Lyman-α-Humidometer (El. Res. Crop. BLR)
RH	± 5%	± 0.007%	10	10	Humicap (Vaisala HMP 11)
T_D	± 0.5K	± 0.007K	10	10	Dewpoint Probe (General Eastern 1011B)
Cloud Droplet Spectrum	± .17 % of total No.	± 1	10	10	FSSP-100 (Range 2-32 µm)
(2 probes)	**)	± 1	10	10	OAP-2D2-C (Range 25-800 µm)
Radiation					
E_s (up and down)	± 4 Wm^{-2}	± 0.1 Wm^{-2}	10	10	Pyranometer (Epply PSP)
E_i (up and down)	± 10 Wm^{-2}	± 0.2 Wm^{-2}	10	10	Pygreometer (Epply PIR)
Surface temperature	± 0.5K	± 0.006K	10	10	Infrared Radiometer (Barnes PRT-6)
Pressure					
P_s	± 1 mb	± 0.07 mb	100	1	Pitot-static Probe (Rousemount)
Position	***)				
Lat., Long	(~800 m/h)	± 0.6"	10	10	Inertial Platform (Honeywell V6 177)

In addition: Forward facing video camera

*) Assumed air speed 100 ms^{-1}
**) Not yet known
***) Depends on flight time

5.2.2. DO-128

The DO-128 is a twin turboprop-engine powered STOL aircraft with a wing span of 15.55 m, a length of 11.71 m, and a height of 3.90 m (Figure 5.3). Operations are possible up to 10000 feet without oxygen masks and up to 20000 feet with oxygen masks. Typical flight speeds in the boundary layer lie between 120 and 150 knots. The endurance at low levels is about 4.5 hours. During the flight missions 4 persons were on board the DO-128: two pilots, a data operator and the aircraft scientist.

Figure 5.3: The DO-128 of the Technical University of Braunschweig.

The DO-128 was equipped with a temperature sensor, a humidity sensor, sensors for static and dynamic pressure and an instrument system to measure the three-dimensional wind vector in connection with an inertial reference system. Furthermore, it had a radio altimeter, a surface temperature infrared radiometer and an instrument to measure size distribution of particles (snow and ice crystals). Particularly interesting meteorological phenomena were recorded with a hand-held video camera by the pilots. A summary of the instruments and their specifications is given in Table 5.2.

Table 5.2: Parameters measured on board the DO-128.

Parameter	Absolute Accuracy	Resolution	Sampling Frequency	Remarks	Type of Sensor
Wind					
Direction	± 2°	± 0.1°	25	in horizontal flight	computed
Speed	± 0.5 m/s	± 0.08 m/s	25	at wind speed of 10 m/s	computed
Vertical Wind	± 0.2 m/s	± 0.01 m/s	25	in horizotal flight	computed
Air Data					
Static Pressure	± 0.3 hPa	± 0.01 hPa	25		ROSEMOUNT static pressure
Barom. Alt.	± 2.4 m	± 0.1 m	25	standard atmosphere	computed
True Airspeed	± 0.5 m/s	± 0.08 m/s	25		ROSEMOUNT 1221F2VL diff. pressure
Aircraft Data					
True Heading	± 0.4°	± 0.1°	25		HONEYWELL Lasernav YG1761B
Radio Altitude	3 ft	20 cm	25		SPERRY AA-300 Radio Altimeter
Temperatures					
Static Temp.	±0.5 K	± 0.025 K	25		ROSEMOUNT 102EJ1BB Total Temp. delced
KT4 - Temp.	?	± 0.025 K	254		
Humidity					
Rel. Humidity	5 %	± 0.025 K	25		AERODATA AD-FS 88 Humidity sensor
Cloud Droplets and Ice Crystals	-----	-----	-----	See details in Section 5.4.3	Optical Array Grey Probe (Range 10-600 µm) Particle Measuring Systems

The relative wind is measured by a 5-hole probe at a special noseboom to avoid flow distortions by the airplane. The particle measuring probe was mounted below the left wing outside the influence zone of the propeller. The temperature and humidity sensors are located at the front part of the aircraft body.

Extensive computer power for on-line signal processing (including the calculation of the three-dimensional wind vector) is provided by a PDP 11/73 and a Motorola WME bus processor. Data are recorded on 64 channels with 50 or 25 Hz sampling rate on a streamer tape recorder for off-line evaluation. A detailed description of the aircraft, the instrumentation and the on-board data acquisition system is given by Hankers (1989).

As for FALCON, a quick-look processing of selected data from the DO-128 was made immediately after the flight at the operation center. The complete processing of all data with full time resolution will be made later at Braunschweig and Hamburg.

References

Hankers, R. (1989): The equipment of a research aircraft with emphasis on meteorological experiments. Society of flight test engineers; 20th Annual Symposium Proceedings 1989, Reno, Nevada.

5.3. The flight missions

(B. Brümmer, Meteorologisches Institut der Universität Hamburg)

In total, nine missions were flown. Eight of them were joint missions of FALCON-20 and DO-128 in situations of cold air outbreaks from the Arctic ice or in situations of cold air advection from other directions. One mission, the FALCON flight on 28 February 1991, had a different scientific objective: to study the conditions under which contrails develop and dissolve. This mission is described in Section 5.4.4.

An intercomparison of the FALCON-20 and DO-128 instruments was made on 13 March 1991 at the beginning of the regular flight mission on that day. Results from this intercomparison and information about other "indirect" intercomparisons between both aircraft, when their take-offs were separated by only a few minutes, are given in Section 7.

A brief summary of the aircraft missions is listed in Table 5.3

Table 5.3: Summary of the flight missions during ARKTIS 1991 (F = FALCON-20, D = DO-128).

Date	Flight Time (UT)	Flight Patterns (P = Profile, L = Legs)	Comments
22 February	F 1100 - 1352 D 1036 - 1408	3 P, 4 L 8 P, 5 L	Open cells modulated by meso-scale cloud bands to the west of Andenes.
24 February	F 1230 - 1519 D 1208 - 1543	5 P, 6 L 6 P, 4 L	Cold air outbreak SW of Bear Island with small Sc cells.
25 February	F 0908 - 1150 D 0855 - 1224	4 P, 3 L 4 P, 3 L	Cold air outbreak under high pressure conditions with closed cells.
28 February	F 1130 - 1230	2 P, 2 L	Contrail mission.
04 March	F 0942 - 1205 D 0928 - 1301	5 P, 3 L 5 P, 4 L	Mesoscale low. Open and closed cells.
07 March	F 0958 - 1307 D 0953 - 1334	4 P, 9 L 7 P, 3 L	Small open cells.
08 March	F 0950 - 1338 D 0951 - 1326	3 P, 5 L 4 P, 3 L	Large open cells.
12 March	F 0907 - 1138 D 0859 - 1234	3 P, 3 L 2 P, 4 L	Open cells and cloud streets.
13 March	F 1309 - 1531 D 1310 - 1351	3 P, 3 L 2 P, 2 L	Intercomparison. Intensive cellular convection around cold front.

A detailed description of each flight mission follows in the flight catalogue below. The areas, where the missions were flown, are shown in Appendix C.

Flight Catalogue:

(compiled by G. Müller, Meteorologisches Institut der Universität Hamburg)

Date: 22 February 1991 DO-128: T/O 1036 UT T/D 1408 UT FALCON: T/O 1100 UT T/D 1352 UT Flight No: ARKTIS 9/F1778 Mission: Convective oceanic PBL with open cells.

Synoptic situation: Low pressure zone (980 hPa) S of Bear Island moves NE-ward and weakens. The observational area is situated in moderate NW/SW-flow.

Coordinates of flight patterns: A: 6900 N 1000 E, B: 6950 N 950 E, C: 6900 N 1200 E, D: 6935 N 1200 E
X: 7000 N 300 E, Y: 7000 N 500 E, Z: 6955 N 920 E, VALDIVIA: 7000 N 700 E

Time (UT)	Patterns and Heights		Remarks (Weather etc.)
DO-128			
1036	Start at Andenes		
1055 - 1132	Run at 300', Andenes-A,	Hdg. 260°	5-6/8 Cu and showers.
1133 - 1143	Profile 300' - 8000' towards A		4-6/8 Cu, base 1800' - 2000', top 2000'. Few isolated tops are higher.
1143 - 1154	Profile 8000' - 300' at A		4-6/8 Cu, top 3200' - 4500'.
1155 - 1214	Run at 300', A - B,	Hdg. 355°	3-4/8 Cu below 3/8 As. Northward more intense convection than southward. 1203 - 1205: Crossing a shower out of a Cb with cloudbase at sea-level.
1214 - 1222	Profile 300' - 6000' at B		Clouds: Base 1900', top 5500' - 6000'.
1222 - 1231	Rectangle at 6800'		Flying a rectangular pattern in order to check the wind measurements.
1231 - 1237	Profile 7000' - 2000' at B		6/8 Cu, base 2000', top 6100'. The sounding crosses a shower.
1237 - 1252	Run at 2200', B-A,	Hdg. 175°	Near B: 4/8 Cu (base 2000') below 4/8 Ac. Near A: 6/8 Cu. Flying near cloud base, before 1242 below clouds, after 1242 inside clouds.
1255 - 1301	Profile 50' - 5500' at A		4/8 Cu, base 2500', top 4700'.
1301 - 1310	Profile 5500' - 300' at C		3/8 Cu, top 4900'.
1311 - 1330	Run at 300', C-D,	Hdg. 0°	Near C: 3/8 Cu. Near D: 5-6/8 Cu. Flying near cloud base below clouds.
1330 - 1338	Profile 300' - 7000' at D		2-3/8 Cu/As, base 2500', top 6300'. Some isolated tops are higher than 7000'.
1338 - 1348	Profile 7000' - 300' near D		3/8 Cu/As, top 6300' - 7000'.
1349 - 1400	Run at 300', D - Andenes		2-4/8 Cu.
1407	Landing at Andenes		
FALCON			
1100	Start at Andenes		
1100 - 1116	Profile 300' - 28000' at Andenes		Cu/Cu con, base 2000', top 7500' (most) - 11000' (max.). Open cells are visible.
1116 - 1143	Run at 28000', Andenes - X,	Hdg. 280°	Flight above open cells and cloud bands. The centers of the open cells are partially filled with thin As-layers.
1143 - 1201	Profile 28000' - 300' at X		Descent into the cloudfree center of an open cell. Base of the cell margin 1600' (most) - 1000' (min), top of the cell margin 7000' (most) - 10000' (max). Turbulences at 4500'. After 1148 entering the cloud of cell margin.
1204 - 1215	Run at 300', X - Y,	Hdg. 100°	The run crosses 2 cloudfree cell centers and 2 cloud bands of cell margins. 2-6/8 Cu/Cu con.
1215 - 1219	Profile 300' - 8000' at Y		Ascent through clouds of a cell margin, base 1500', top 3800'. Few isolated tops 6000' - 6500'.
1222 - 1226	Profile 8000' - 2000' at Y		Descent through Cu con.
1227 - 1238	Run at 2000', Y - X,	Hdg. 280°	Run near cloud base. Two cloud bands of cell margins are crossed. Estimated cell diameter: 30 km.
1239 - 1303	Run at 300', X - VALDIVIA	Hdg. 115°	Snow showers at margins of open cells. Overflying VALDIVIA while snow shower at 1302.
1303 - 1315	Run at 300', VALDIVIA - Z	Hdg. 110°	1306: Leaving snow shower and flying inside open cell near cell margin. 1309-1311: Crossing cell margin. 2-3/8 Cu.
1315 - 1327	Profile 300' - 19000' at Z		Ascent inside cloudfree center of an open cell. Top 4500'-6500'. From 17000' observed total cloud cover: 3-6/8 Cu, Cu con.
1329 - 1337	Profile 19000' - 5000' near D		Cloud top 8000' (max). No clouds are crossed.
1337 - 1343	Run at 5000', Z - Andenes,	Hdg. 100°	Flight near highest cloud tops.
1343 - 1352	Profile 5000' - ground at Andenes		
1352	Landing at Andenes		

Commentary:

The experimental area was characterized by open cells and mesoscale cloud bands. The cloud bases ranged from 1200' to 2000' and the tops from 4500' to 11000'. The vertical extension of convection decreased from east towards west. The intensity of convection decreased with time while the pressure increased behind the removing low. The satellite picture showed open cells which were modulated by mesoscale cloud bands. These bands with horizontal distances of about 100 km were organized in spirals which run together at the center of the low. West of VALDIVIA and near the coast snow showers were observed.
The operation area of the DO-128 was characterized by moderate SW-winds without any marked wind veering. The FALCON recorded NW-winds and a wind veering from 250° to 350° between 600 m and 1200 m. The air-sea temperature difference measured by the VALDIVIA was 3K. The temperature profiles did not indicate any marked inversions.

Date: 24 February 1991 DO-128: T/O 1208 UT T/D 1543 UT FALCON: T/O 1230 UT T/D 1519 UT Flight No: ARKTIS 10/F1779 Mission: Marine convective PBL during cold air outbreak.

Synoptic situation: Cold air outbreak with strong NE-flow between a high pressure zone over Greenland and a depression over the Barents Sea and the west coast of the northern part of Norway influences the experimental areas.

Coordinates of flight patterns: A: 7030 N 1300 E, B: 7100 N 1150 E, C: 7115 N 1030 E, D: 7025 N 1045 E
W: 7330 N 1700 E, X: 7345 N 1530 E, Y: 7245 N 1530 E, Z: 7300 N 1430 E

Time (UT)	Patterns and Heights		Remarks (Weather etc.)
DO-128			
1208	Start at Andenes		
1208 - 1250	Run at 300', Andenes-A,	Hdg. 330°	First: 8/8 St. 1216: 4/8 Cu below 2/8 Ac. 1228-1231: Snow/rain shower. After 1231: Cloud cover decreases to 1/8 Cu. The clouds are now organized in bands parallel to wind direction.
1250 - 1257	Profile 300' - 6000' at A		2/8 Cu, base 3000', top 4000'.
1257 - 1302	Run at 6000', A - B,	Hdg. 330°	Flight above 2/8 Cu.
1302 - 1313	Profile 6000' - 50' at B		4/8 Cu, base 3700', top 5000'.
1313 - 1325	Run at 300', B - C,	Hdg. 310°	0-1/8 Cu below thin St.
1325 - 1338	Profile 300' - 11000' at C		Cu, base 3800', top 11000'. The weather radar indicates a shower.
1339 - 1350	Profile 11000' - 3000' at C		1/8 Cu, base 4000'.
1350 - 1352	Profile 3000' - 4500' towards B		Cloud base 4000'.
1352 - 1403	Run at 4500', C - B,	Hdg. 110°	Flight at 500' above cloud base, later near cloud base.
1403 - 1406	Profile 4500' - 300' at B		
1406 - 1421	Run at 300', B - D,	Hdg. 210°	0 -1/8 Cu. VALDIVIA in sight.
1421 - 1426	Profile 300' - 5000' at D		2/8 Cu, top 5000' (max).
1426 - 1439	Rectangle at 5000'		Flight of a rectangular pattern in order to check the wind measurements.
1439 - 1443	Profile 5000' - 50' at D		Cloud base 4500'.
1444 - 1539	Run at 300', D - Andenes,	Hdg. 110°	Cloud cover increases from 1/8 Cu to 8/8 Cu. Cloud bands parallel to wind direction. The weather radar indicates shower.
1543			Landing at Andenes.
FALCON			
1230	Start at Andenes		
1230 - 1248	Profile, ground-28000' towards W		8/8 As, base 1800', top 5000'. Cu shreds below As layer with base 800'. The profile ends above 5-6/8 Cu.
1248 - 1302	Run at 28000', Towards W,	Hdg. 0°	First: Flight above Ci. Since 1257: Flight above Cu in cloud street formation.
1303 - 1319	Profile, 28000' - 300', towards W		Turbulence at 12000'. 7/8 Sc, base 2000', top 3800'.
1319 - 1323	Run at 300', towards W,	Hdg. 0°	The diffuse cloud base is partially touching the ground.
1324 - 1331	Run at 300', W - X,	Hdg. 300°	Heavy turbulences. 7/8 Sc and a lot of snow showers.
1331 - 1336	Profile, 300' - 7000', at X		8/8 Sc, base 1700', top 5900' ± 200'. This cloud layer may be composed out of a Cu layer with top at 4800' below an As layer with top at 5800'.
1340 - 1350	Run at 2000', X - W,	Hdg. 110°	Flight below diffuse cloud base. The ground remains visible. Snow showers are recognizable.
1352 - 1402	Run at 300', W - Y,	Hdg. 200°	First: Flight in snow shower, heavy turbulences. Since 1355: Flight below 7/8 Sc, clear view towards ground.
1403 - 1409	Run at 300', Y - Z,	Hdg. 310°	Cells with diameter of about 2500 m - 3000 m. Near Z 7/8 Sc with snow showers.
1409 - 1414	Profile, 300' - 8000', at Z		Cu/Sc, base 2000' - 2500', top 5400' (most) - 6500' (max). As layer above Cu/Sc layer. Top of As layer is not reached at 8000'.
1418 - 1428	Run at 2000', Z - Y,	Hdg. 110°	Flight below 6-7/8 Cu/Sc near cloud base. Near Y: 5-6/8 Cu/Sc. No clouds above the Cu/Sc layer.
1430 - 1442	Profile, 300' - 21000' at Y		6/8 Cu/Sc, base 2500', top 5500'.
1444 - 1453	Run at 21000', Y-Andenes,	Hdg. 170°	Flight in thin Cs. At lower level 4-5/8 Cu.
1453 - 1502	Profile, 21000'-3000' towards Andenes		5/8 Cu/Sc, base 2500' - 3000', top 6000'. From 5000' to 3000' flight in clouds.
1502 - 1507	Run at 3000' towards Andenes,	Hdg. 170°	Flight inside clouds near top.
1519	Landing at Andenes		

Commentary:

The NE-flow of cold air caused an air-sea temperature difference of 10K at the northern part of the FALCON area. The Bear Island, the VALDIVIA and parts of the measure areas of the DO-128 and FALCON were located at the same trajectory. This mission should be viewed in context with the one of the next day: The mission of 24 February took place before the maximum of the cold air outbreak, the mission of the following day took place after this maximum.
The operational areas of the two aircrafts were characterized by different cloud situations:
DO-128: While the transit between Andenes and B the cloud cover decreased from 4/8 Cu to 1/8 Cu. The cloud bases ranged from 3000' to 3700' and the tops from 4000' to 5000'. At point C the cloud situation was characterized by heavy convection activity with showers. Here the top of a compact Cu-field rised to 11000'.
FALCON: 5-7/8 Sc/Cu and shower activity was observed at the entire measure area. The bases of clouds ranged from 1800' to 3000' and the top heights increased westward from 3800' to 5500'. At the western part a second cloud layer of As was found above the Sc/Cu-layer.

Date: 25 February 1991 DO-128: T/O 0855 UT T/D 1224 UT FALCON: T/O 0907 UT T/D 1150 UT Flight No: ARKTIS 11/F1780 Mission: Convective marine PBL during cold air outbreak.

Synoptic situation: High pressure area over Greenland and NE of Iceland. Low pressure area over Novaja Semlja and the west coast of Norway. A NE-flow from the ice edge transports cold air into the coastal region of the northern part of Norway. The northern part of the measure area near Bear Island is already influenced by a SW-flow north of a ridge of the high.

Coordinates of flight patterns: A: 7130 N 1730 E, B: 7100 N 1900 E
W: 7400 N 2100 E, X: 7200 N 1900 E, Y: 7110 N 2040 E, Z: 7100 N 2200 E

Time (UT)	Patterns and Heights		Remarks (Weather etc.)
DO-128			
0855	Start at Andenes		
0856 - 0947	Run at 300', Andenes towards A,	Hdg. 20°	Cloud cover increases from 5/8 Sc/Cu to 7/8 Sc/Cu. Slight showers.
0947 - 0956	Profile, 300' - 7000' towards A		6-7/8 Sc/Cu, base 3000', top 5000'.
0956 - 1006	Profile, 7000' - 50' at A		6-7/8 Sc, base 3400', top 4600'. Cloud tops look uniform.
1011 - 1027	Run at 300', A - B,	Hdg. 130	6-7/8 Sc at A. 5/8 Sc at B.
1028 - 1034	Profile, 300' - 6000' at B		Slight snow fall. Cloud base 3500', top 4500'.
1038 - 1102	Run at 3500', B - A,	Hdg. 330°	Flight just below cloud base. Since 1055: Flight inside of clouds near cloud base.
1104 - 1120	Run at 2000', A - B,	Hdg. 130°	7/8 Sc. 1104-1105: Flight inside of snow shower. Since 1110: 8/8 Sc/St.
1125 - 1131	Profile, 300' - 6000' at B		7/8 Sc, base 3600', top 5000'.
1131 - 1141	2 rectangles		Flight of 2 rectangular flight patterns in order to check the wind measurements.
1141 - 1153	Profile, 600' - 300' near B towards Andenes		Cloud base 3800', top 5200'.
1153 - 1217	Run at 300', B - Andenes,	Hdg. 210°	Cloud cover decreases to 3-4/8 Sc/Cu.
1224	Landing at Andenes		
FALCON			
0907	Start at Andenes		
0907 - 0926	Profile, ground-29000' at Andenes		2-6/8 Cu/Sc, base 3500', top 5500' - 5700'. Open and closed cells are discernible. The tops look uniform.
0926 - 0953	Run at 29000', Andenes - X,	Hdg. 20°	Field of 7/8 Sc with parallel cloudfree stripes with distances of 10-20 km. Since 0941: Cloud streets of 3/8 Cu. Since 0950: Sc-field with mesoscale band structures oriented in wind direction.
0953 - 1013	Profile, 29000 - 300', at W		2 or 3 cloud layers: 7/8 Sc, base 5700', top 7800'. At 7000' in clouds. 5-6/8 Cu, base 1500' - 1700', top 3500' - 4700'. At 300' the wind direction is SW. The air-sea temperature difference is about 10K.
1013 - 1020	Profile, 300' - 15000' at W		Ascent during heading change.
1020 - 1041	Run at 15000', W - X,	Hdg. 200°	Transit for reason to leave the region of SW-flow.
1041 - 1051	Profile, 15000' - 300' at Y		7-8/8 Sc, base 1900', top 5200' (max). Entering cloud at 4700'. Structures of closed cells are discernible. A lot of snow showers are visible.
1053 - 1059	Run at 300', Y - Z,	Hdg. 110°	Regions with 6-7/8 Sc and snow showers and regions with 4/8 Sc without snow shower. Air-sea temperature difference of about 11K.
1101 - 1107	Run at 2000', Z - Y,	Hdg. 290°	Flight below cloud base. The run starts and ends in snow shower. This might be a run from cell edge to cell edge.
1110 - 1115	Run at 4200', Y - Z,	Hdg. 110°	Run in clouds. At 1111 short inside cloud gap.
1117 - 1121	Run at 5200', Z-Andenes,	Hdg. 250°	Flight at cloud top level. Temporary below top in clouds. Temporary above clouds.
1121 - 1126	Profile, 5200' - 15000' towards Andenes		Above closed cells.
1126 - 1134	Run at 15000', towards Andenes,	Hdg. 250°	Above closed and open cells.
1134 - 1150	Profile, 15000'-ground at Andenes		4-6/8 Sc, top 5600', base 3200'.
1150	Landing at Andenes		

Commentary:

The operation area of the FALCON should be located near Bear Island. But at point W a SW-wind was found instead of the expected NE-wind. This SW-flow was caused by a high ridge which moved SE-ward and terminated the cold air outbreak near Bear Island and west of this region. For that reason it was decided to shift the operation area of the FALCON S-ward towards the region which was still influenced by cold air which was moved from the ice edge over the Barents Sea towards North-Norway.
The DO-128 and the FALCON found 4-7/8 Sc. The cloud base height ranged from 1900' to 3600', and the top height varied between 4500' and 5200'. The clouds seemed to be organized in closed cells. The air-sea temperature difference was about 10K. The low-level wind was around 10 m/s from 10° - 20°.

Date: 26 February 1991 DO-128: T/O 1053 UT T/D 1217 UT Mission: Flight for checking the measure instruments.
Flight No: ARKTIS 12

Synoptic situation: A high pressure zone over Scandinavia causes a moderate S-flow at the measure area.

Coordinates of flight patterns: A: 6918 N 1518 E

Time (UT)	Patterns and Heights	Remarks (Weather etc.)
DO-128		
1053	Start at Andenes	
1059	Touch down at runway	The aircraft touches the runway near the ground station to compare the aircraft measurements of temperature and moisture with the measurements of the ground station.
1100 - 1119	Profile, ground - 5800'at A	No clouds.
1119 - 1124	Profile, 5700' - 50', at A	No clouds.
1130 - 1156	3 rectangles at 3100' at A	Flying 3 rectangular patterns in order to check the wind measurements.
1217	Landing at Andenes	

Commentary:

The measure area was cloudfree. Each of the rectangular flight patterns consisted of 4 runs of 30 seconds. The reason for the rectangular flights was to compare the wind measurements under the assumption that the wind remains constant during the rectangular flight.

Date: 28 February 1991 FALCON: T/O 1130 UT T/D 1230 UT Mission: Contrail.
Flight No: F1781

Synoptic situation: On the east side of an intense high pressure system over northern Scandinavia warm air was transported into the experiment area with southerly winds, resulting in thin cirrus cloud coverage.

Coordinates of flight patterns: Y: 6910 N 1510 E, Z: 6955 N 1520 E

Time (UT)	Patterns and Heights		Remarks (Weather etc.)
FALCON			
1130	Start at Andenes		5/8 Ci.
1100 - 1144	Ascent to 25000',	Hdg. 270°	
1144 - 1152	Ascent to 30000'		Thin Ci above flight level.
1152 - 1157	At 30000'		Attempt to recognize, whether a contrail is produced by FALCON. Contrail very short and not permanent.
1157 - 1205	Ascent to 33000'		
1204 - 1208	Run at 33000', Y - Z ,	Hdg. 0°	1206: Sinking to 29000'. Contrail still very short and not permanent. Above occasional Ci.
1208	Left turn at Z at 29000'		
1210	Sinking to 25000',	Hdg. 170°	Still above Ci or As.
1214	At 20000'		Thin cloud layer passed. Heading into cloud free area.
1217	At 21000'		Mission cancelled.
1230	Landing at Andenes		

Commentary:

The mission plan was to produce a defined contrail by the FALCON and to make, subsequently, measurements within this contrail. As it was not possible to create such a permanent contrail, perhaps due to very dry conditions, there was hope to make at least some measurements within a Ci layer. This was neither possible with expenditure, due to layered and horizontally inhomogeneous Ci streaks.

Date: 04 March 1991

DO-128: T/O 0928 UT T/D 1301 UT
FALCON: T/O 0942 UT T/D 1205 UT
Flight No: ARKTIS 13/F1782

Mission: Soundings at a mesoscale eddy embedded in large scale anticyclonic conditions.

Synoptic situation: The satellite image shows a mesoscale eddy of diameter of about 200 km which is located at 70°N 11°E off the Norwegian coast. The weather charts does not give any hint of this phenomenon. At the weather charts this area is characterized by weak pressure gradients. The large scale synoptic situation is characterized by an extended but weak high pressure ridge over the Barents Sea and weak pressure gradients over Scandinavia.

Coordinates of flight patterns: VALDIVIA: 7125 N 1500 E, A: 7130 N 1800 E
Y: 7000 N 800 E, Z: 7130 N 1100 E

Time (UT)	Patterns and Heights		Remarks (Weather etc.)
DO-128 0928	Start at Andenes		
0928 - 0940	Profile, ground - 10000' at Andenes		1-2/8 Cu. Haze at 1800'. 1-2/8 Ci.
0940 - 0949	Profile, 10000' - 400' at Andenes		1/8 Cu. Tops and bases diffuse.
0950 - 1022	Run at 300', Andenes - VALDIVIA,	Hdg. 350°	Below 1-2/8 Cu. Since 0959: Below 6-7/8 Sc. Since 1011: 1/8 Cu below 8/8 As. Haze and sometimes snowfall.
1023 - 1034	Profile, 300' - 10000' towards VALDIVIA		As, base 3300' (diffuse), top 9500'. Ground remains visible until 5600'. Wind 5 m/s from N.
1034 - 1042	Profile, 10000' - 300' at VALDIVIA		As layer above 1-2/8 Cu. As, base 4300', top 6000'. 1-2/8 Cu, base 1500', top 3700'.
1042 - 1049	Run at 300' over VALDIVIA,	Hdg. 330°	The distance to VALDIVIA was 5 nm.
1049 - 1055	Run at 100' over VALDIVIA,	Hdg. 135°	
1100 - 1127	Run at 300', VALDIVIA - A,	Hdg. 80°	Flight below 1-2/8 Cu. 8/8 As/Sc layer above Cu layer. 1109 - 1113 flight below shower.
1140 - 1149	Profile, 300' - 8000' at A		8/8 Sc, base 1700' (diffuse), top 6300'.
1149 - 1200	Profile, 8000' - 400' at A		8/8 As, base 5000', top 6600'. 6/8 Cu, tops in As layer, base 1300' (diffuse). Precipitation below clouds. Wind at low level: FF 8 m/s, DD 220°.
1200 - 1251	Run at 300', A - Andenes,	Hdg. 200°	1210 - 1216: Slight snowfall and haze. Since 1222: 2/8 Cu below As tr. Since 1238: 1/8 Cu below 5/8 Ac.
1301	Landing at Andenes		
FALCON 0942	Start at Andenes		
0944 - 1030	Run at 300', Andenes - Y,	Hdg. 325°	2/8 Ac. Since 0952: 4-5/8 Cu without precipitation. T_L 0°C, T_w 6°C, FF 6 m/s, DD 180°. Since 0956: A lot of snow showers out of 4-8/8 Cu. Wind decreases from 5 m/s to 0 m/s, wind direction turns over SE to E. Since 1018: Better visibility. A few showers. T_L 1-2°C, T_w 6°C, FF 10 m/s, DD 40°. The run crosses an area of convergence.
1030 - 1034	Profile, 300' - 10000' at Y		Cu con with squall-line, base 1200', top 5000'. 8/8 As, base 2500', top 6500' - 7200' (max).
1036 - 1041	Profile 10000' - 300' at Y		Thin As layer at 9400'. Fibrous Cu con, top 6300'. At 5000' out of clouds. At 4200' in clouds. At 2800' out of clouds. Below 2800': 0-1/8 Cu fra, base 1000'.
1042 - 1101	Run at 300', Y - Z,	Hdg. 210°	NE-wind of 8 m/s. 1043 - 1045: Slight rain below 8/8 Cu/As. Since 1045: 3/8 Cu below As. Since 1050: 0-1/8 Cu fra.
1101 - 1105	Profile, 300' - 10000' at Z		2/8 Cu con, base 2600', top 3600', a few tops more than 6000'. Ascent not through clouds. The convection pattern resembles the one of the open cells of 22-02-91.
1106 - 1112	Profile, 10000' - 300' at Z		2/8 Cu con, base 2500', top 3600', a few tops more than 6000'. Descent not through clouds.
1112 - 1154	Run at 300', Z - Andenes,	Hdg. 85°	Flight below 2-5/8 Cu with slight snow showers. NE-wind of 5 m/s. Water temperature 5.7°C, air temperature 1.9°C. Since 1130: Flight below 8/8 Cu/Cu con with showers. Decreasing wind speed. Since 1142: Flight below 8/8 Cu/Sc and 8/8 As/Ac. SE-wind. Water temperature 6.7°C, air temperature 0.4°C.
1154 - 1158	Profile, 300' - 10000' towards Andenes		8/8 St, base 1600', top 4500' - 5000' (max). The cloud base is diffuse and the top is well defined.
1158 - 1205	Profile, 10000' - ground at Andenes		8/8 Sc/St, base 3000', top 6000'. Thin Cu fra below 3000'.
1205	Landing at Andenes		

Commentary:

DO-128: The DO-128 operated NE of the center of the mesoscale eddy. At the measure area there was a mostly closed As-layer with base heights ranging from 3300' to 5000' and top heights between 6000' and 9500'. Below this As-layer 1-2/8 Cu with base heights ranging from 1300' to 1500' was observed. At the west part of the operation area near the VALDIVIA there was an additional Ci layer. At the VALDIVIA there was a NE-wind which turned towards SW at point A.

FALCON: The runs between Andenes and Y i.e. Z crossed an area of convergence with S/SE-wind of about 5 m/s at the eastern part and N/NE-wind of about 10 m/s at the western part of these runs. Between the two areas of different wind regimes there was an area of weak winds. Probably the center of the mesoscale eddy was located SW of the measure area which would be consistent with the observed wind situation. At Y and Z the vertical soundings did not show any marked temperature inversion or wind veering. Here open cells were observed. Near Andenes there was a stratiform cloud cover below a weak inversion at 6000'. Here the wind profile showed a veering from S/SE below 2000' towards W/NW above 2000'. The air-sea temperature gradient of 3-5K is weaker at the west part of the mission area than near the coast because of the flow of cold air from the land and the higher water temperature. The further growing of the cloud top height was probably suppressed by the wind veering and the temperature inversion.

Date: 07 March 1991 DO-128: T/O 0953 UT T/D 1334 UT FALCON: T/O 0958 UT T/D 1307 UT Flight No: ARKTIS 14/F1783 Mission: Oceanic PBL with cloud streets changing into open cells.

Synoptic situation: A depression with center between Iceland and Faeroe Islands. An occluded front off the Norwegian coast moves slowly N-ward. The operation area of the FALCON is influenced by an E-flow. Weak winds are observed at the measure area of the DO-128.

Coordinates of flight patterns: A: 6850 N 1050 E, B: 6830 N 730 E
W: 7150 N 2100 E, X: 7220 N 2100 E, Y: 7220 N 1300 E, Z: 7150 N 1300 E

Time (UT)	Patterns and Heights		Remarks (Weather etc.)
DO-128 0953	Start at Andenes		
0953 - 1006	Profile, ground - 9000' at Andenes		0-1/8 Cu.
1006 - 1012	Run at 9000', Andenes - A,	Hdg. 240°	Above 0-1/8 Cu. 1006-1009: Heating of the cases of temperature- and moisture-sensors is switched off.
1012 - 1026	Profile, 9000' - 300' towards A		4/8 Cu, top 5000' - 5300' (max.), base 2500'.
1026 - 1033	Run at 300', Andenes - A,	Hdg. 240°	First 4/8 Cu, then 8/8 St. 1027 - 1030: Heating of the cases of temperature- and moisture-sensors is switched off.
1033 - 1044	Profile, 300' - 8000' at A		8/8 St, base 1400', top 6300'.
1044 - 1056	Profile, 8000' - 300' at A		4/8 Cu, base 2200', top 6300'. Descent without heating of temperature- and moisture-sensor cases.
1056 - 1102	Profile, 300' - 5000' at A		0-1/8 Cu, top 4000' (diffuse).
1102 - 1109	Profile, 5000' - 50' at A		Cloud base 2300', top 4000' (diffuse). Slight showers.
1109 - 1120	Profile, 50' - 8000' between A and B		Cloud base 2700', top 4600' - 5700' (max.).
1120 - 1129	Rectangle at 8000' between A and B		Flight of a rectangular flight pattern in order to check the wind measurements. Clouds: 2-4/8 Cu and St fra.
1129 - 1140	Profile, 8000' - 50' towards B		Cloud base 2400', top 6000' - 6500' (max.).
1140 - 1144	Run at 300', A - B,	Hdg. 240°	Turn towards Andenes at B.
1145 - 1330	Run at 300', B-Andenes,	Hdg. 60°	Since 1145: 2/8 Cu. Showers are visible. 1214 - 1215: Flight through shower of hail. Since 1215: 2/8 Cu. 1235: Flight through slight shower. Since 1240: 1/8 Cu below 6-7/8 Sc. 1250: Flight through slight shower. Since 1252: Ac-fields below 4/8 Cu. 1308: Flight through slight shower. 1312: 6/8 Cu. An extended precipitation area is visible N of the aircraft. Since 1323: 2/8 Cu.
1334	Landing at Andenes		
FALCON 0958	Start at Andenes		
0958 - 1008	Profile, ground - 20000' at Andenes		1/8 Cu fra at 2500'.
1008 - 1028	Run at 20000', Andenes - W	Hdg. 25°	Flight above Sc-field with Karman eddies.
1028 - 1039	Profile, 20000' - 300' at W		5/8 Cu/Sc, top 5400' (max.). Entering cloud at 4100'.
1039 - 1046	Run at 300', W - X,	Hdg. 350°	3-4/8 Cu/Sc organized in meandering cloud streets. T_L -0.9°C, T_w 5.3°C, FF 12 m/s, DD 100/110°.
1048 - 1056	Run at 2500', X - W,	Hdg. 180°	Flight just below base of 2-4/8 Cu. 1052 - 1054: Flight above cloud base inside of clouds. The cloud cover decreases S-ward.
1057 - 1101	Run at 3600', W - X,	Hdg. 0°	Flight in clouds. Cloudy sections are often interrupted by cloud gaps.
1103 - 1105	Profile, 300' - 5000' at X		4/8 Cu, base 2800', top 4000'.
1105 - 1126	Run at 5000', X - Y,	Hdg. 270°	Probably small open cells of 4-5/8 Cu. Cloud tops at the eastern part ot the run: 5000' - 6000'. Cloud tops at the western part of the run: 6000' - 7500'. Since 1117: the aircraft is temporarily in clouds.
1128 - 1133	Profile, 9000' - 300' at Y		4/8 Cu, base 2800' - 3000', top 6000' - 7500'. At 5000' inside of clouds for a short while. A snow shower ahead.
1133 - 1142	Run at 300', Y- Z,	Hdg. 180°	4/8 Cu organized in small open cells or meandering cloud streets. T_L 1°C, T_w 6°C, FF 11-14 m/s, DD 90°.
1145 - 1155	Run at 2650', Z - Y,	Hdg. 0°	Flight below cloud base. Height of cloud base 2800' - 3000'. There are some showers with lower bases. The cloud cover decreases N-ward.
1158 - 1208	Run at 4000', Y - Z,	Hdg. 180°	Flight inside cloud level. Open cells are crossed. During the first part of the run through lower part of clouds, later through upper part of clouds near top.
1210 - 1220	Run at 6000', Z - Y,	Hdg. 0°	Flight in clouds below top. Since 1213: Flight just above cloud top. Small open cells organized in band formation.
1222 - 1229	Run at 1500', Y - Z,	Hdg. 180°	Flight below clouds at midst of sub cloud layer.
1231 - 1237	Profile, 300' - 20000' at Z		Cloud base 3000', top 8000' (max.). Entering cloud at 4200', leaving cloud at 6800'. Intense precipitation.
1238 - 1250	Run at 20000', Z - Andenes,	Hdg. 155°	First above broken Sc, later above closed Sc.
1250 - 1307	Profile, 20000' - ground at Andenes		8/8 Sc, base 4400', top 5500'. 2-4/8 Cu below Sc layer, base 2000', top partially in Sc layer.
1307	Landing at Andenes		

Commentary:

DO-128: The DO-128 operated S of the FALCON at an area of weak winds. Near B and near the coast the cloud situation was characterized by convective clouds (2-4/8 Cu). Between these areas stratiform clouds predominated. The base heights varied from 1400' to 2700' and the top heights from 4600' to 6000'. There were showers at the measure area. Two run sections and one vertical sounding were flown without heating the case of temperature- und moisture-sensors.
FALCON: The FALCON operated in E-flow of about 13 m/s. This E-flow did not represent a real outbreak of cold air but it enabled the investigation of the development of an instable PBL during heating from below. The air-sea temperature difference was about 5 K. At the eastern part of the operational area the clouds were organized in street formation with base 2700' to 2800' and top 4000' to 5400' while small open cells predominated at the western part of the area. The height of cloud tops raised westward towards 6000' to 8000' at Y.

Date: 08 March 1991

DO-128: T/O 0951 UT T/D 1326 UT
FALCON: T/O 0950 UT T/D 1338 UT
Flight No: ARKTIS 15/F1784

Mission: Oceanic PBL with open cells in E-flow S of Bear Island.

Synoptic situation: High pressure area over Greenland and Novaja Semlja. Low pressure area over Iceland, northern part of Scandinavia and southern part of Barents Sea. Between these pressure systems an E/NE-flow moves cold air into the measure area. The satellite image shows the whole Barents Sea covered by open cells.

Coordinates of flight patterns: A: 7030 N 1520 E, B: 7130 N 1430 E
W: 7300 N 2100 E, X: 7400 N 1930 E, Y: 7220 N 1725 E, Z: 7250 N 1600 E

DO-128 0951	Start at Andenes		
0951 - 1025	Run at 300', Andenes - A,	Hdg. 355°	First cloudfree, then flight below 1-2/8 Sc/Cu. FF 15 m/s, DD 70°.
1025 - 1035	Profile, 300' - 9100' at A		3-4/8 Cu, base 3000', top 6100'. Snow shower ahead.
1036 - 1045	Profile, 9100' - 300' at A		The descent crosses a shower. Cloud top 6100' (diffuse), base 2000'. Heavy turbulences.
1046 - 1102	Run at 300', A - B,	Hdg. 345°	Flight below 3-4/8 Cu. 1049: Short shower with hail. Since 1057: Almost cloudfree.
1106 - 1134	Run at 3000', B - A,	Hdg. 165°	Run at level of cloud base. Flight below 3/8 Cu. The cloud bases are partially sharp marked but some bases touch the ground. 1114 - 1119: Flight crosses a shower.
1135 - 1201	Run at 4500', A - B,	Hdg. 345°	Run inside cloud layer. 4/8 Cu. 1140 - 1144: Flight crosses a shower with heavy turbulences; the aircraft ices up. Since 1144: Flight crosses center of open cell; 1/8 Cu hum. 1150 - 1156: Flight crosses shower.
1210 - 1224	Profile, 30' - 11000' at B		Ascent crosses shower. 3/8 Cu con, base 3000' (diffuse), top 6000' (most) - 8000' (max.). Some clouds have the appearance of typical Cu with sharp marked surfaces, some have fibrous surfaces like outflowing Cb's.
1224 - 1237	Profile, 11000' - 300' towards A		Descent crosses separated Sc-field with diameter of 3 km. Cloud top 7000' (diffuse), base 2500'. 1230: Aircraft enters cloud.
1237 - 1326	Run, A - Andenes,	Hdg. 150°	Below 3-4/8 Sc/Cu not as convective as N of point A. Cloud cover decreases. 1250: 1/8 Sc. Since 1330: Cloudfree conditions.
1326	Landing at Andenes		
FALCON 0950	Start at Andenes		
0950 - 1007	Profile, ground - 29000' at Andenes		Cloudfree conditions.
1007 - 1027	Run at 29000', Andenes - W,	Hdg. 25°	Flight above cloudfree area. Since 1014: Above well developed open cell of estimated diameter of about 30 km within thin As above the cell centers.
1030 - 1038	Profile, 29000' - 300' at W		Descent into cloudfree center of an open cell. As/Cu, base 2000', top 8000' - 10000' (most), some tops up to 11000'. The descent ends below cell edge in heavy snow shower.
1041 - 1054	Run at 300', W - X,	Hdg. 320°/ 330°	A few little heading changes to avoid heavy snow showers. Cloudfree areas with weak SE-wind alternate with snow showers with stronger NE-wind. The convective activity decreases near X. T_L - 1 to -2°C, T_w 5.5 to 6.0°C, FF 7 to 10 m/s, DD 50 to 70 °.
1054 - 1101	Profile, 300' - 10000' at X		Ascent with little heading change to avoid heavy snow shower. Cloud base 1500'. From 2300' to 3000' in cloud. N of point X the convection activity seems to be cut of, here 4-5/8 flat Cu hum.
1105 - 1120	Run at 2000', X- W,	Hdg. 140°/ 140°	Run near cloud base. Sometimes in clouds, simetimes below cloud base. Cloudfree areas alternate with showers.
1122 - 1140	Run at 300', W - Y,	Hdg. 220°/ 225°	1122 - 1128: Inside cell center below 0-1/8 Cu/Cu fra. 1128 - 1130: Below cell edge, 8/8 Cu con/Cb, slight shower. 1130 - 1140: Inside cell center, 0-1/8 Cu fra. The run ends just in front of the next cell edge.
1141 - 1151	Run at 300', Y- Z,	Hdg. 325°/ 340°	1141 - 1147: Inside cell center. 1147 - 1148: Below cell edge. 1148 - 1151: Inside cell center. T_L -1 to -0.5°C, T_w 5.5 to 6.5°C, FF 9 m/s, DD 90°.
1153 - 1154	Run at 2000', Z - Y,	Hdg. 150°	Run below cloud base. Run has to end earlier than planned because of lack of fuel.
1155 - 1203	Profile, 300' - 20000' between Y and Z		4/8 Cu con/Cb, base 2200' - 2400', top inside cell center 4500' - 5000', top at cell edge 8000' - 10000'. Heading change to avoid a shower. At 5000' short in clouds.

Time (UT)	Patterns and Heights	Remarks (Weather etc.)
1203 - 1223	Run at 20000', Z - Andenes, Hdg. 175°/ 180°	Flight above open cells. Since 1214: Above small open cells. Clouds are deformed probably because of wind veering. Since 1222: bove cloud streets.
1223 - 1238	Profile, 20000' - ground at Andenes	Descent starts above cloud streets and ends at cloudfree area.
1238	Landing at Andenes	Snow-drift in spite of cloudfree sky.

Commentary:

The satellite image show open cells over the Barents Sea and NW of N-Norway at an area which is influenced by a cold air outbreak. The DO-128 and the FALCON found similar conditions at their measure ares: Off the coast it was almost cloudfree probably because of lee-effects of the Norwegian mountains. N of the coastal region a zone of strong convection with open cells with diameter of about 30 km was found. Between these regions there was a transient zone with small open cells and cloud streets. The cell edges of the large open cells were formed of Cu con / Cb with base heights of about 2000' and maximal top heights of 10000'. Most of the centers of the open cells were covered by a layer of 1-2/8 Cu hum / Cu fra. There were a lot of snow showers with cloud bases touching the surface. Two of the vertical soundings of the DO-128 crossed snow showers. N of the two measure areas at point B, i.e. X only slight convection activity with flat Cu hum was observed. The border between the two areas of different degrees of convective activity was surprisingly marked and a zone of gradual transient was not recognizable.

The vertical soundings of the two aircrafts did not show any temperature inversion or wind veering. The air-sea temperature difference was about 5-6K. The FALCON registrated an E/NE-wind of about 10 m/s while the DO-128 found a stronger wind of about 15 m/s out of E/NE.

Date: 12 March 1991

DO-128: T/O 0859 UT T/D 1234 UT
FALCON: T/O 0907 UT T/D 1138 UT
Flight No: ARKTIS 16/F1785

Mission: Convective oceanic PBL with open cells and cloud streets.

Synoptic situation: The operational area is influenced by an E/NE-flow of about 10 m/s between a low E of Finland and a high NE of Greenland and Spitsbergen. The northern and the southern parts of the operational area are separated by a line of convergence. N of this line cloud streets predominate, S of it are open cells.

Coordinates of flight patterns: A: 7045 N 1200 E, B: 6950 N 1440 E
Y: 7300 N 1400 E, Z: 7215 N 1530 E

Time (UT)	Patterns and Heights	Remarks (Weather etc.)
DO-128 0859	Start at Andenes	
0859 - 0954	Run at 300', Andenes A, Hdg. 320°	First: Cloudfree conditions. Since 0914: 0-2/8 Cu hum. Since 0929: 3-4/8 Cu hum. Since 0931: Intense convection activity, 5-6/8 Cu/Cb. 0936 - 0937: Below edge of an open cell in snow shower. 0937 - 0947: Inside center of the open cell, 0-1/8 Cu hum. 0947 - 0953: Below cell edge in snow shower.
0954 - 1006	Profile, 300' - 9300' at A	Ascent at center of open cell. Cloud base of cell edge 2500'. The bases of showers are lower. Top of 5-6/8 Cu/Cb at cell edge 8300'. The cell center is covered by flat 2-3/8 Cu hum. 1002: A cloud top is crossed. Some of the clouds of the cell edge have sharply marked surfaces, others have diffuse surfaces like St neb.
1014 - 1051	Run at 2500', A - B, Hdg. 110°	Run at level of cloud bases. 1014 - 1020: Below cell edge temporarily in snow shower. Cloud bases of showers touch the surface. 1020 - 1029: Inside cell center. Flat layer of 2/8 Cu hum with base 2500'. 1029 - 1033: Below cell edge in shower. The aircraft ices up. 1037 - 1043: The flight crosses an area of moderate convection activity with slight showers and 3/8 Cu. Since 1043: Flight below 0-1/8 Cu hum.
1054 - 1130	Run at 5000', B - A, Hdg. 320°	Run inside of cloud layer. 1054 - 1104: 0-1/8 Cu hum, base 3000' - 4000', top 4000' - 5000'. 1104 - 1117: Zone of moderate but permanently increasing convective activity. 4/8 Cu, top 4500' (min) - 6000' (max). 1117 - 1118: Cell edge crossed. 1118 - 1125: Inside cell center. 1125 - 1130: In clouds of cell edge, snow, aircraft ices up.
1133 - 1208	Run at 7000', A - B, Hdg. 110°	1133 - 1138: Most time in clouds of cell edge. The pilot announces strong electrostatic charge. Cloud top 6000' - 8000'. 1138 - 1149: Inside cell center near cell edge. The cell has moved SW-ward since last run. 1149 - 1152: Inside clouds of cell edge. 1157: Open cell left ahead. Since 1200: The aircraft is now above cloud top. The convection activity decreases. 4/8 Cu, top 6000'. Cells are not discernable. Since 1204: Above 1/8 Cu hum with estimted top of about 4000'.
1208 - 1217	Profile, 7000' - 45'at B	0-1/8 Cu hum, base 2500', top 3000'.
1218 - 1234	Run at 300', B - Andenes, Hdg. 120°	Cloudfree conditions. Very well visibility.
1234	Landing at Andenes	

Time (UT)	Patterns and Heights		Remarks (Weather etc.)
FALCON 0907	Start at Andenes		
0907 - 0917	Profile, ground-20000' at Andenes		Cloudfree conditions.
0917 - 0946	Run at 20000', Andenes - Y,	Hdg. 355°	Since 0917: Flight above cloudfree area. Since 0920: Flight above open cells with As at top of the cell centers.
0946 - 0958	Profile, 20000 - 300', towards Y		Descent starts above area with open cells with cloud tops of about 10000'. 0952: The aircraft crosses a line which separates the area of open cells from an area of 5-7/8 Cu organized in bands with NE-SW orientation. Heights of clouds at the area of cloud bands: Base 1500', top 5300' (most) - 6000' (max). Below 4900': Sometimes inside of clouds. Descent ends below snow shower.
1000 - 1014	Run at 300', Y - Z,	Hdg. 140°	A lot of snow showers with bases touching the surface during the whole run. First the visibility is very bad, since 1004 better visibility.
1017 - 1032	Run at 2200', Z - Y,	Hdg. 340°	First below cloud base, then above it. 1017 - 1026: Area of open cells and two shower bands are crossed. Since 1026: Cloudfree and cloudy sections alternate quickly. 1028: Inside of an intense shower.
1037 - 1040	Profile, 300' - 7500', at Y		6/8 Cu/Sc, base 1800' - 2000', top 5000'. The ascent crosses clouds.
1042 - 1055	Run at 4000', Y - Z,	Hdg. 140°	1042 - 1044: Flight inside clouds. Since 1044: Flight near cloud top. Since 1049: Flight crosses the area of open cells. Here the run crosses the clouds of the cell edge. At cell center the aircraft is flying near top of 0-2/8 Cu.
1057 - 1108	Profile, 300' - 20000' at Z		Ascent out of center of an open cell through 2/8 Cu, base 3500', top 5500' (most) - 8000' (max). N of the line of convergence maximum cloud tops of about 11000' - 13000' are recognizable. S/SE of this line there are also clouds with tops of 12000' - 13000'. From above small open cells embedded at the center of a large open cell are discernible.
1108 - 1121	Run at 20000', Z - Andenes,	Hdg. 170°	Flight above large open cells. First the cell centers are covered by an As-layer, later the cell centers are cloudfree.
1121 - 1138	Profile, 20000' - ground at Andenes		Since 1125: Above cloudfree area.
1138	Landing at Andenes		

Commentary:

For reason of the W/NW - E/NE orientation of the ice edge and of the sea isotherms E of Bear Island the N/NE flow of cold air into the measure area produced two different types of convection: An area of open cells with large top heights was separated by a line of convergence from an area with convection organized in bands and with lower heights of cloud tops. The coastal area was cloudfree because of lee effects.

DO-128: Between Andenes and point B it was cloudfree. NW of point B there was an area of moderate convection activity. The cloud cover increased from 0-1/8 Cu hum, base 2500', top 3000' towards 4/8 Cu, base 2500', top 6000' with slight snow showers. Here the wind was about 10-12 m/s out of NE. NW of this transition zone there was an area of large open cells with diameters of about 50-60 km. The cell edges were marked by Cu con / Cb, base 2500', top 8300'. Below heavy snow showrs the base was lower. As during the mission of 8 March 1991 some clouds at cell edge had sharply marked surfaces while others had diffuse surfaces like St neb. Almost no inversion of temperature or wind veering was registrated. The air-sea temperature difference was about 5-6K. NW of the point A an area of moderate convection activity commenced.

FALCON: The open cells at the SW-section of the measure area rised up to 10000'. At the area of cloud streets the heights of tops were about 5000' - 6000'. At both regions the base heights ranged from 1500' - 2000'. The line of convergence was marked by a wind change: FF 13 m/s, DD 30° NW of this line changed towards FF 6 m/s, DD 50° SW of this line. The convergence rised up towards a height of 3300'. There is a temperature difference of about 3K between Y and Z from ground to 5000' - 6000', which is the height of convection at the area of cloud bands. The air-sea temperature difference decreased from 6-7K at Y towards 4K at Z.

Date: 13 March 1991

DO-128: T/O 1310 UT T/D 1351 UT
FALCON: T/O 1309 UT T/D 1531 UT
Flight No: ARKTIS 17/F1786

Mission: 1. Intercomparison flight.
2. Oceanic convective PBL ahead and behind a cold front.

Synoptic situation: Low over northern part of the Barents Sea. Cold front between N-Norway and Bear Island. A strong NW-flow of about 15-20 m/s transports cold air into the measure area. These wind speeds in connection with the observed air-sea temperature difference of about 10K result in heat fluxes of about 300 W/m^2.

Coordinates of flight patterns: X: 6930 N 1520 E, Y: 7100 N 1600 E, Z: 7400 N 1600 E

Time (UT)	Patterns and Heights		Remarks (Weather etc.)
DO-128			
1310	Start at Andenes		
1310 - 1319	Run at 300', Andenes - X,	Hdg. 300°	1312 - 1314: Flight through shower, bad visibility, heavy turbulences. Wind direction changes after leaving the shower.
1319 - 1329	Profile, 300' - 10000' at X		Ascent through shower with base near ground, top 8000'. Upward vertical wind of 3 m/s inside shower.
1330 - 1338	Profile, 10000' - 300' at X		Descent through snow shower, top 8000', base 1500'.
1338 - 1346	Run at 300', X - Andenes,	Hdg. 150°	1345 - 1346: Flight through shower with increasing wind speed and changing wind direction.
1351	Landing at Andenes		
FALCON			
1309	Start at Andenes		
1311 - 1316	Run at 300', Andenes - X,	Hdg. 300°	Intercomparison run DO-128 - FALCON. Flight crosses shower line. Wind direction changes from 250° to 333° and wind speed decreases after leaving the shower. The air-sea temperature difference is about 5K.
1316 - 1335	Profile, 300' - 30000' at X towards Y		Ascent from 300' to 10000' reached at 1321 UT is intercomparison part of the vertical sounding. Cu fra, base 1300'. 7-8/8 Cu con / Cb, base 3500' - 3800', top 8000' (most). Flight through clouds from 4000' to 7500'. At 7900' short in clouds. Maximum top heights near coast: 10000'.
1335 - 1354	Run at 30000', Y - Z,	Hdg. 0°	Since 1335: Flight above closed cells of large vertical extension. At 1345 near 7158 N 1553 E flight over weak cold front. The front is marked by an Ci/As band at height level of 6000m. At lower level S of this band and parallel to the front line lies a Cb band. N of the Cb band follows a band of flat Sc. N of the front starts an area of intensive convection activity with 6-8/8 Cu con without any convection patterns recognizable.
1354 - 1413	Profile, 30000' - 300' towards Z		Layer of haze at 24000' and between 12000' - 13000'. 6-7/8 Cu con/ Sc, base 4000' (not clearly defined because of many snow showers), top 8000' (most) - 10000' (max). At 6000' aircraft enters cloud. The sea is covered with stripes of white foam in wind direction.
1416 - 1506	Run at 300', Z - Y,	Hdg. 180°	Flight from cold air behind the front into warmer air. 1416 - 1421: Many showers are crossed. FF 17 m/s, DD 320°, air-sea temperature difference of about 10K. 1421 - 1446: 3 areas without showers with diameter of about 50 km are crossed. FF 15 m/s, DD 320°, T_w 5°C, T_L increases from -6°C to -3°C. 1446 - 1450: The cold front is crossed. Strong snow fall without interruption. Air-sea temperature difference of about 7°C to 9°C. The direction of the wind of about 15 m/s changes from 320° to 290°. 1450 - 1506: Areas of broken cloud cover with 4/8 Cu/Sc are crossed.
1506 - 1511	Profile, 300' - 10000' at Y		Cu/Cb, base 2500' - 2800', top 9000' - 9500'. As layer, base 6100', top 7000' (most) - 7500'. From 3000' - 4300' and 4700' - 5000' aircraft crosses clouds. Total cloud cover: 4-6/8.
1511 - 1518	Run at 10000', Y - Andenes,	Hdg. 180°	Flight above open cells with maximum top heights of about 10000'.
1518 - 1531	Profile, 10000' - ground at Andenes		Heading change from 185° to 150° and short holdings of flight level at 5000' and 1500'. At 8400' inside cloud. Between 8000' and 7500' cloudfree and cloudy sections alternate quickly. At 6400' the aircraft leaves a cloud of the edge of an open cell and enters the cell center. As layer at cell center, base 4300', top 4800'. Then a St layer with base height of 2300' is crossed.
1531	Landing at Andenes		Heavy snow shower.

Commentary:

The first part of the mission was an intercomparison flight of the DO-128 and the FALCON. Both aircrafts flew a run of 20 nm at 300' with heading 300° and a vertical sounding from 300' to 10000' with heading 360°. The DO-128 started just after the FALCON. The intercomparison run crossed a line of convergence with a snow shower and heavy turbulence. The wind direction changed from 250° to 330° and the wind speed decreased. The vertical sounding crossed clouds from 4000' to 7500'. Inside the cloud the DO-128 measured a vertical velocity of about 3 m/s. The DO-128 reached the level of 10000' about 5-10 minutes after the FALCON.

The second part of the mission was a flight of the FALCON which crossed a cold front between N-Norway and Bear Island. At Bear Island the temperature decreased from -4°C at 0000 UT to -16°C at 1200 UT. At late morning the satellite picture show cloud streets which were orientated from Spitsbergen S-ward. It was surprising that N of the cold front there was a strong wind of about 20 m/s out of NW while 100 km further N at Bear Island only weak winds from NE were measured. At the measure area one vertical sounding N and one S of the cold front were flown. A horizontal run at 300' was flown in N-S direction to examine the convection N-ward and S- ward of the cold front. During the transit flight at 30000' to the measure area the frontal zone was marked by a line of Ci/As-clouds. At 300' the horizontal diameter of the front was about 20 km. Here a change of wind direction from 320° to 290° was registrated. The wind speed of about 15 m/s remained constant and there was a snow shower at the whole frontal zone. N and S of the front there was no marked difference between the convection patterns of probably open cells partially covered by As-layers. But near point Z more showers were observed than at the other parts of the measure area. The wind direction ranged from 320° to 280°. The air-sea temperature difference was about 10-11K near point Z and 5-6K near point Y. The heat flux calculated from the bulk formula was about 300 W/m^2. This was the largest flux measured during the experiment ARKTIS '91.

It might be of interest to examine the fact, that the N-S orientated cloud streets W of Bear Island were influenced by changing synoptic conditions. The N-wind changed to NW-wind and forced the cloud streets to change their orientation.

5.4. Examples of measurements

5.4.1. Vertical profiles for each flight mission

(B. Brümmer and B. Rump, Meteorologisches Institut der Universität Hamburg)

Figures 5.4 - 5.11 show vertical profiles of temperature T, water vapour mixing ratio m, wind speed FF and wind direction DD up to 5 km height (FALCON-20) and up to 3 km height (DO-128) for each of the eight flight missions, respectively. The profiles are selected to show representatively the vertical structure and its horizontal variation within the operational area. The locations at which the profiles were measured are given in Appendix D.

One striking feature is that the profiles - except for the cold air outbreak on 24/25 February (Figures 5.5 and 5.6) - show no marked temperature inversion at the top of the boundary layer. Instead there are often several layers with an isothermal or weakly stable temperature stratification. These layers mark the tops of the dominating cumulus cloud types. The air-sea temperature difference was unstable in all cases and ranged from -1K to -11K. The sea surface temperature in the area of the flight missions was measured by infrared thermometer and varied between 5 and 6°C.

The temperature and especially the humidity profiles measured by DO-128 are incorrect (see section 7 for details). The temperature is too high by about 1K and the humidity sensor was working incorrectly and gave too high values. In spite of these deficiencies, the profiles are shown because they give at least a correct estimate of the boundary layer height. It is not known so far if the humidity error can be corrected at a later stage.

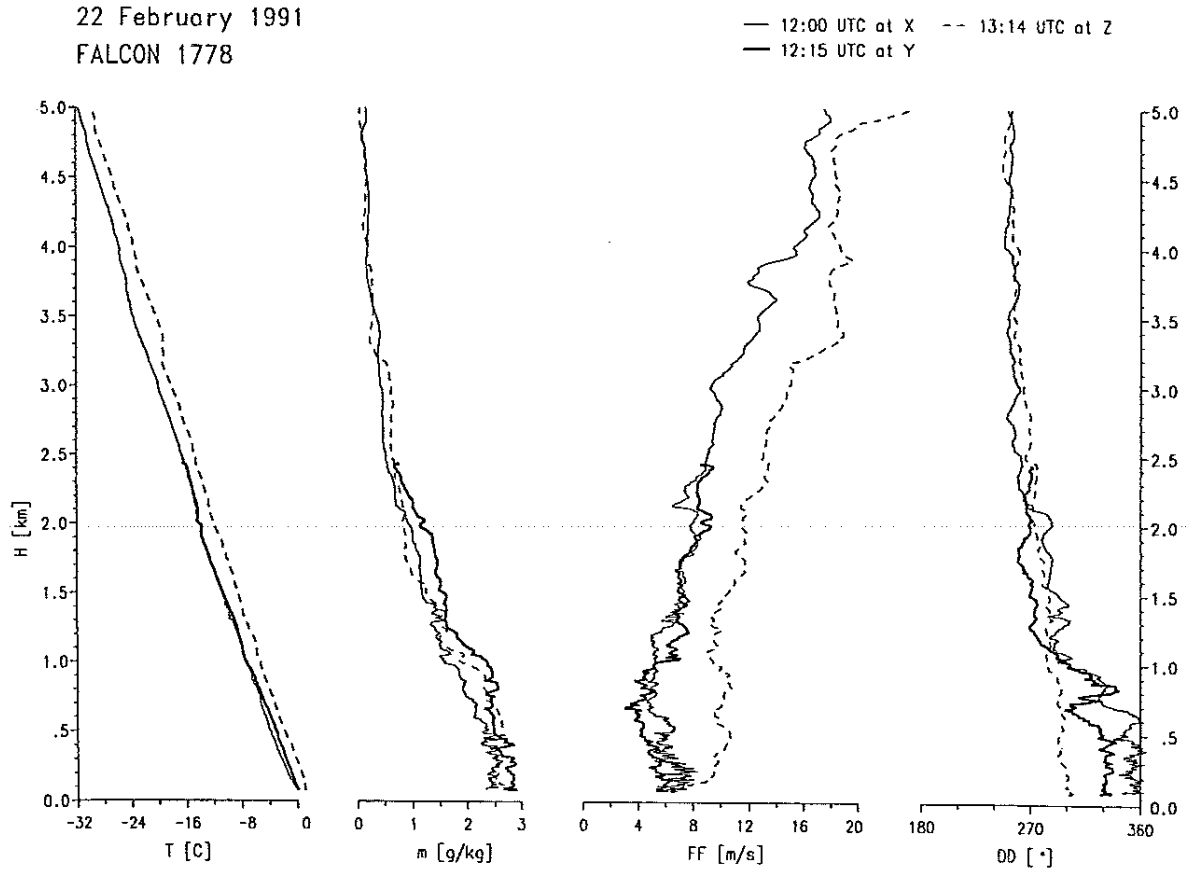

DO-128 data missing.

Figure 5.4: Vertical profiles of temperature T, water vapour mixing ratio m, wind speed FF and wind direction DD measured by FALCON-20 (a) and DO-128 (b) on 22 February 1991. Note that the DO-128 temperature is approximately 1K too high and that the DO-128 moisture is also too high.

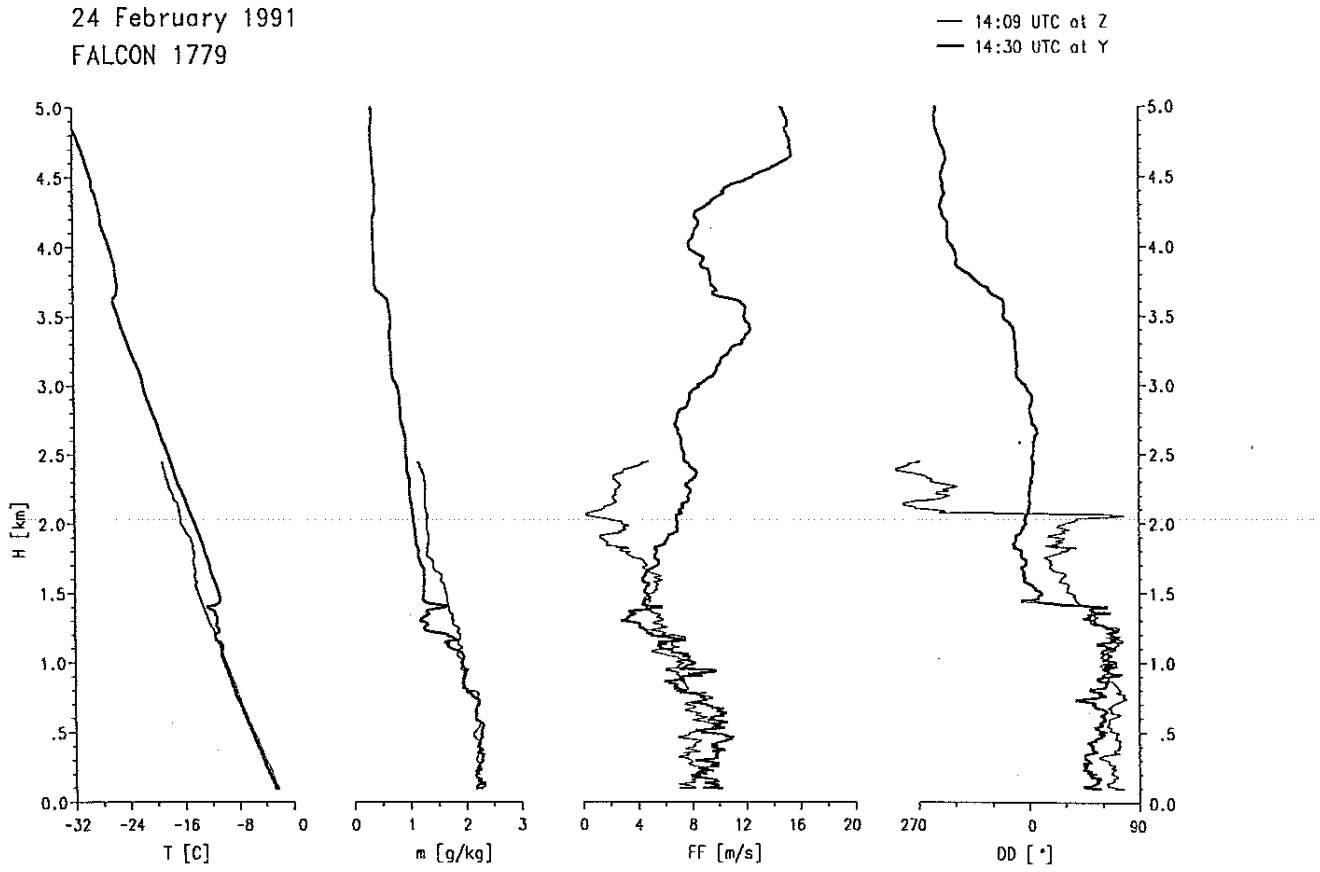

DO-128 data missing.

Figure 5.5: As Fig. 5.4, but for 24 February 1991.

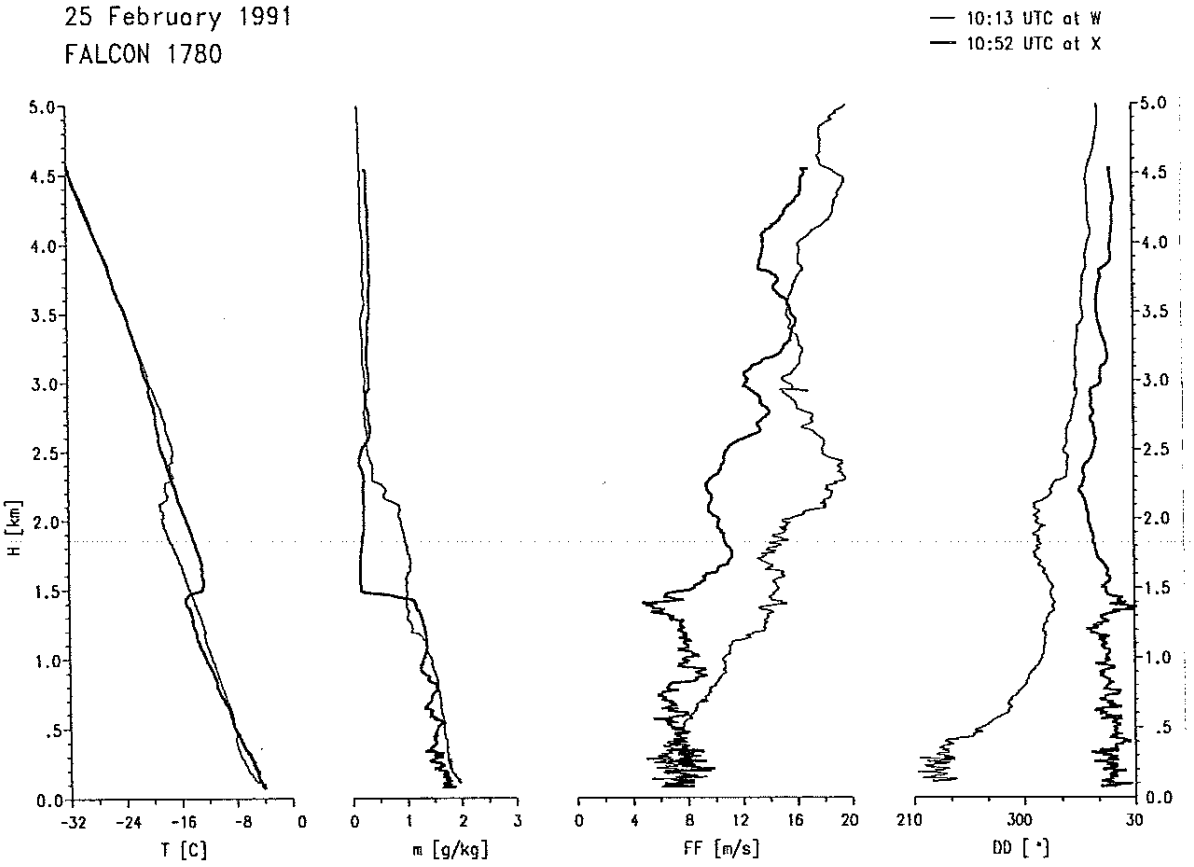

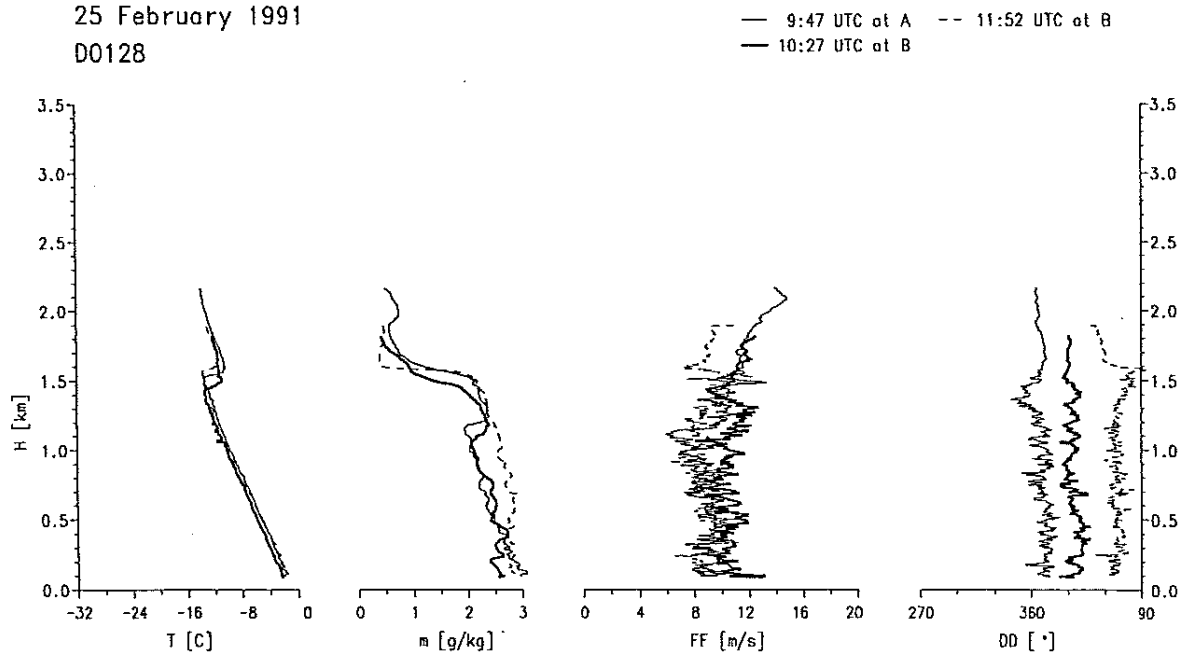

Figure 5.6: As Fig. 5.4, but for 25 February 1991.

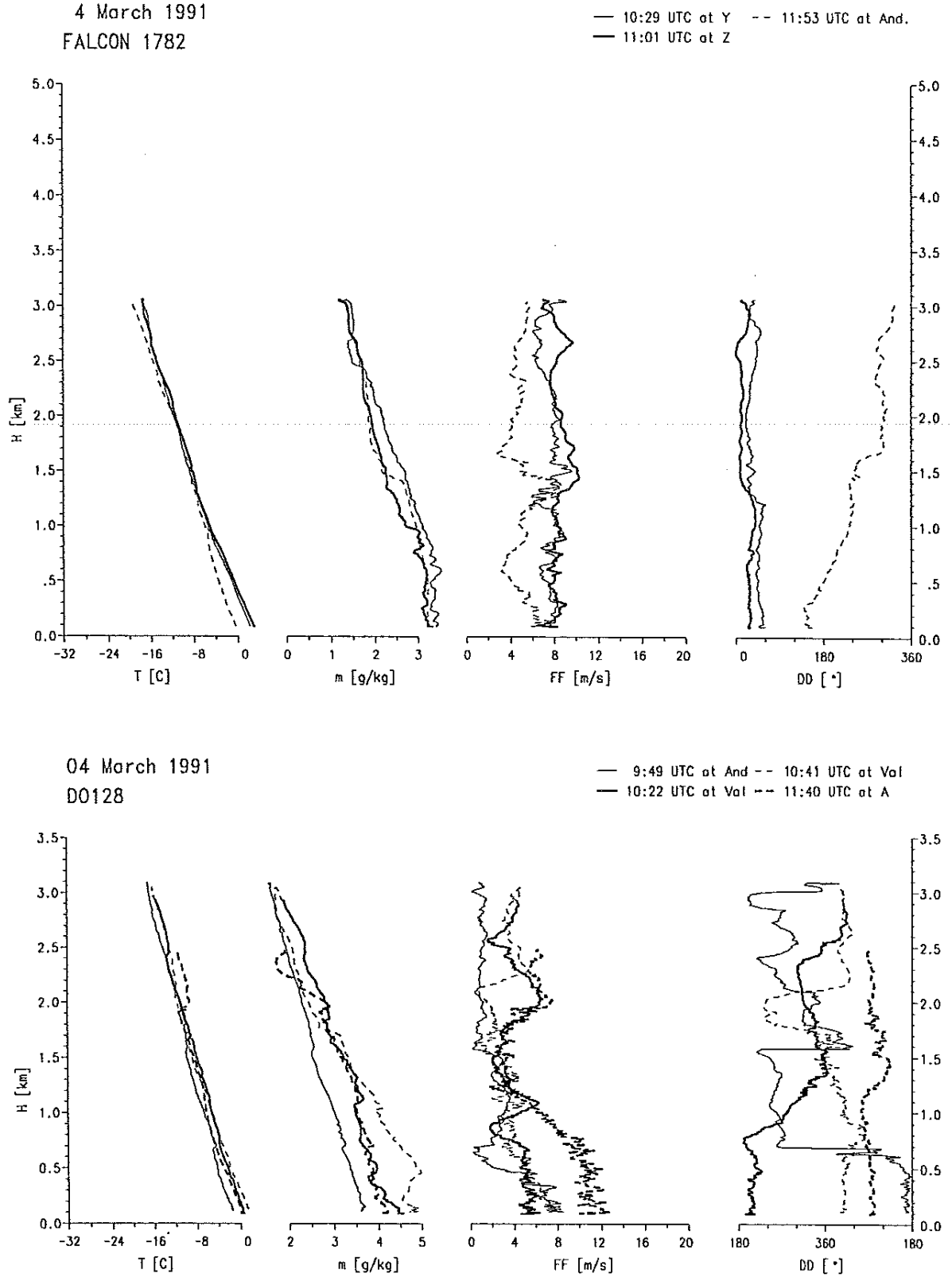

Figure 5.7: As Fig. 5.4, but for 04 March 1991.

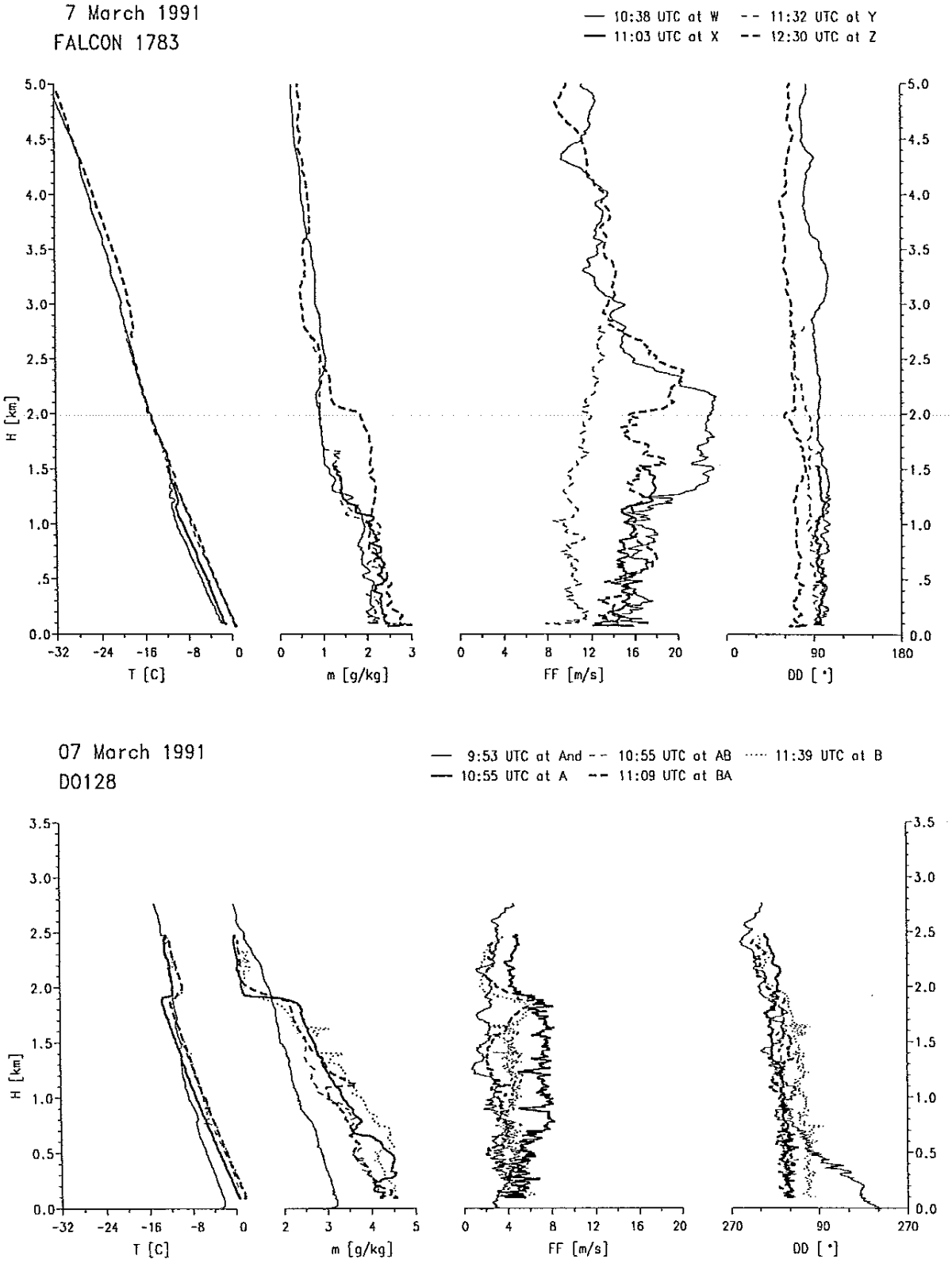

Figure 5.8: As Fig. 5.4, but for 07 March 1991.

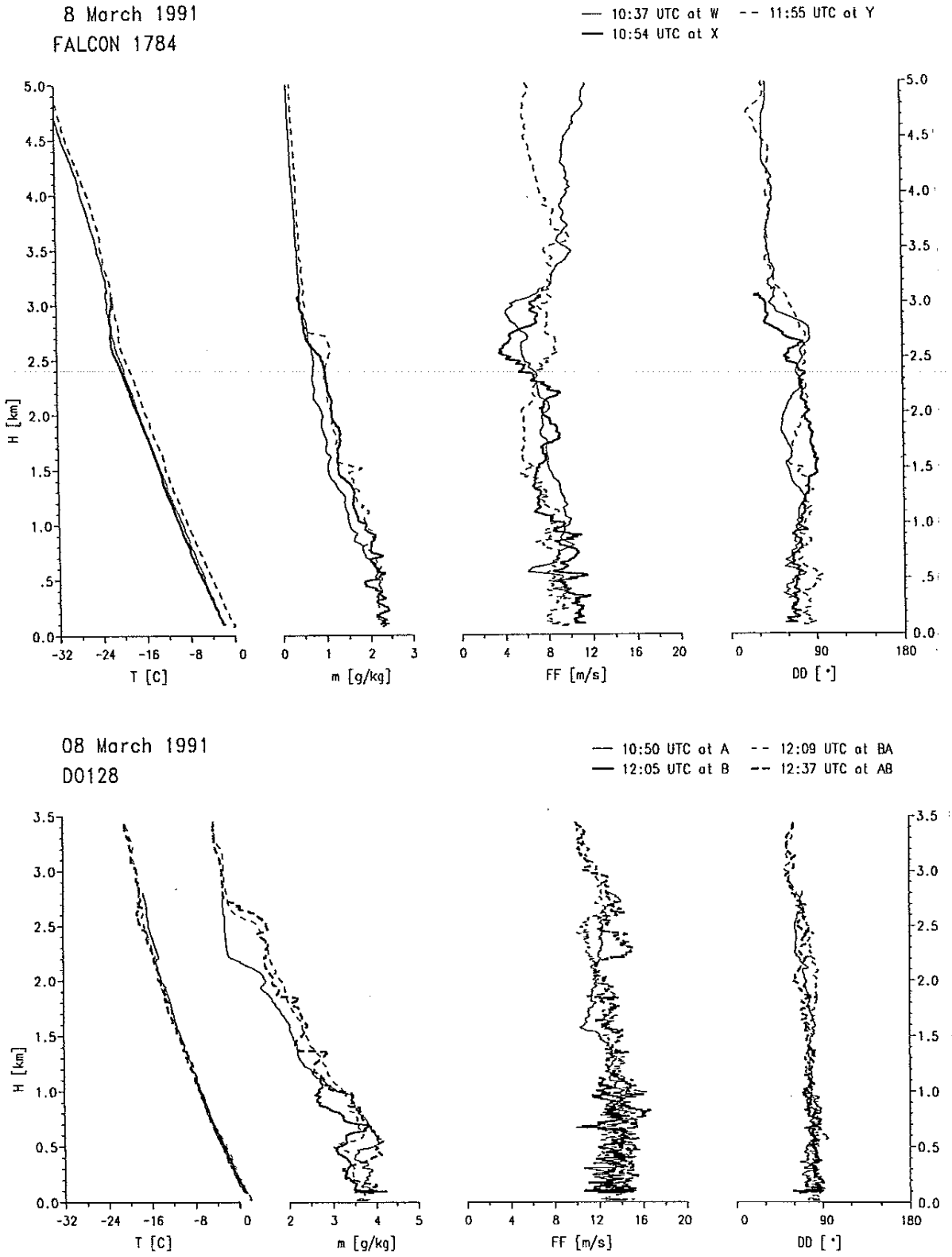

Figure 5.9: As Fig. 5.4, but for 08 March 1991.

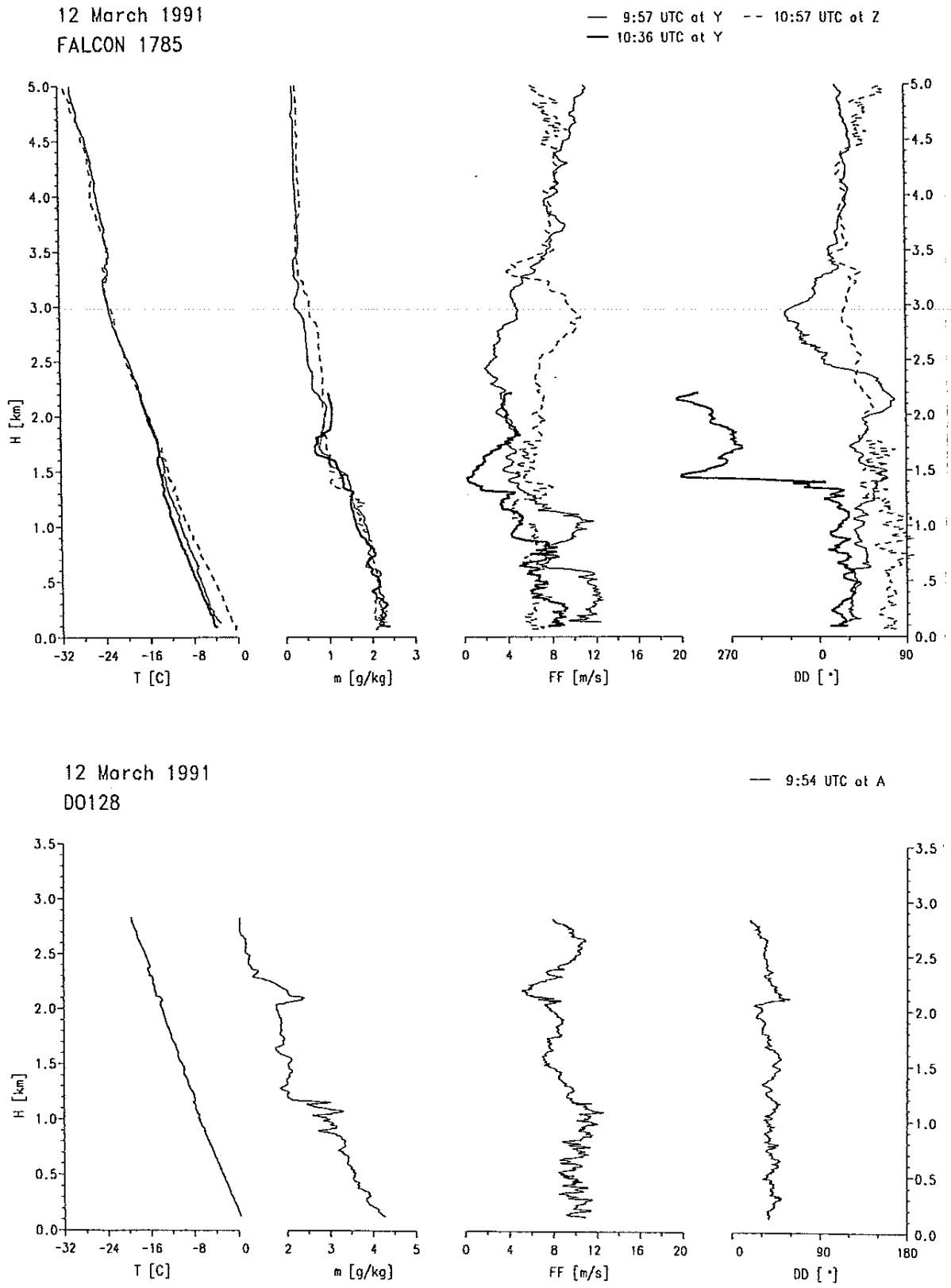

Figure 5.10: As Fig. 5.4, but for 12 March 1991.

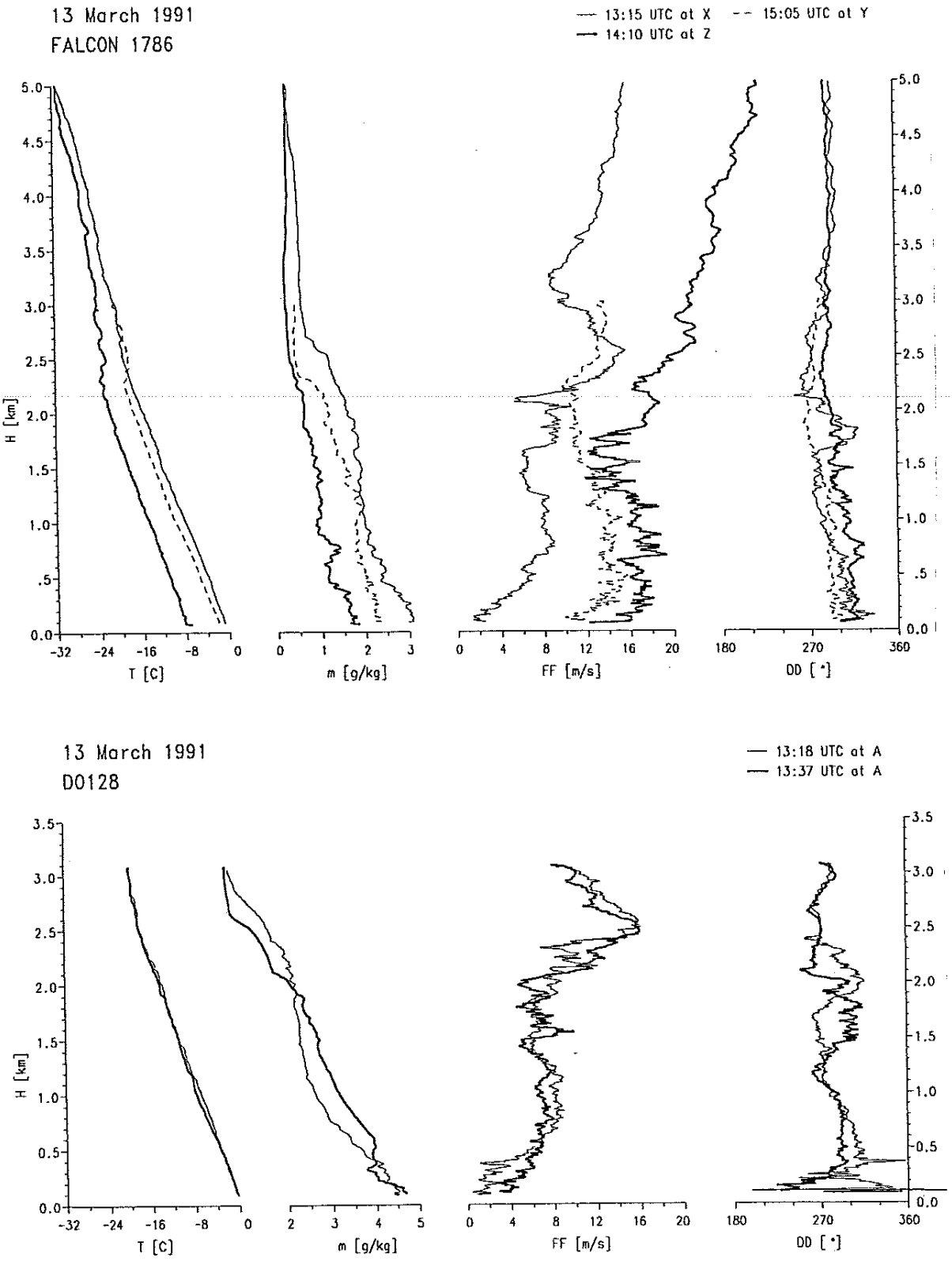

Figure 5.11: As Fig. 5.4, but for 13 March 1991.

5.4.2. *Horizontal traverses through cellular convection*

(B. Brümmer, Meteorologisches Institut der Universität Hamburg)

Each flight mission took place in convective weather situations with air-sea temperature differences between -1K and -11K. Cellular convection was present in all cases, mostly in form of open cells and less frequently in form of closed cells. As an example of horizontal traverses through cellular convection, measurements of the flight on 13 March 1991 are presented below.

The data were taken by FALCON-20 between points Y (71°N, 16°E) and Z (74°N, 16°E) at 9 km and 90 m height. The weather conditions are sketched in Figure 5.12. A weak cold front was situated between Y and Z during the flight mission and moved slowly southward. The low-level wind was WNW south of the front and NW behind the front. The wind speed increased behind the front as well as the air-sea temperature difference ΔT. Deep convection occurred on either side of the front with cloud tops between 2.3 and 2.5 km.

Figure 5.13a shows data sampled at 9 km height during the flight leg from Y to Z. The data presented here are quick-look products which were produced in Andenes immediately after each flight; they are not corrected for any errors and the radiation cuves are not calibrated. This will be part of the final processing at the Meteorological Institute at Hamburg, but was not yet finished. The curves of the short- and longwave radiation from below the flight level, $S\uparrow$ and $L\uparrow$, reflect the pattern of open cells with cell diameters of 25 to 30 km. Together with the above-mentioned convection depth this results into aspect ratios between 10 and 13. A clear relation between the cellular convection below 2.5 km height and the temperature and wind data at 9 km height is not directly obvious. This has to be analysed in detail in the future.

Figures 5.13b, c show the data obtained at 90 m height during the flight from Z to Y. The cloudy parts of the convection cells are marked by "C" in the curve of $L\downarrow$. Most cloudy parts are connected with snow showers which can be seen in the curve of the water temperature T_w because the snow flakes disturb the radiation thermometer measurement.

Near Z, the distance between the showers is very narrow; they were organized in wind-parallel bands. Since the air temperature decreases continuously behind the cold front while the water temperature remains nearly constant, the air-sea temperature difference increases behind the front. The cloudy and open parts of the convective patterns are clearly reflected in the temperature

and humidity curves. The correlation cold/moist occurs in the cloudy parts and warm/dry in the open sections.

To get an idea about the magnitude of the sensible heat flux, the temperature and wind measurements at 90 m height were applied to the bulk aerodynamic formula:

$$H = \rho\, c_H\, FF\, \Delta T.$$

For this estimate we used a constant density ρ of 1.3 kg/m^3, a constant heat transfer coefficient c_H of $1.3 \cdot 10^{-3}$, the measured wind speed FF at 90 m height and an air-sea temperature difference ΔT after adding 1 K to the air temperature at 90 m height. We are aware that this is a poor method, but may give the right order of magnitude. The result is shown in Figure 5.13c. The calculated heat flux is between 100 and 350 W/m^2. The largest values occur near Z in the region of intensive showers where ΔT and FF are largest. These results have to be compared later with accurate calculations of the heat flux via the cross-correlation technique.

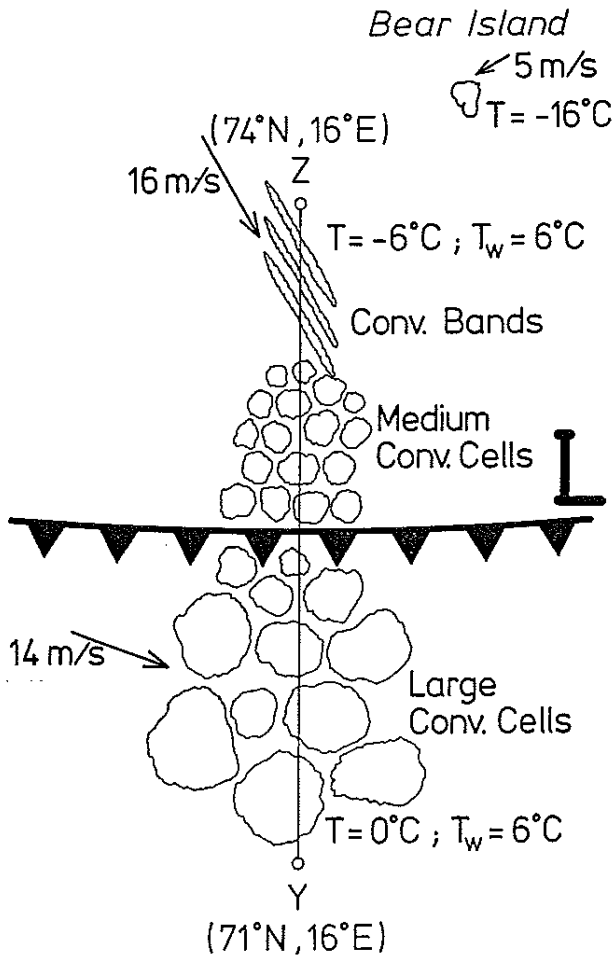

Figure 5.12: Sketch of the weather conditions during the FALCON flight mission on 13 March 1991

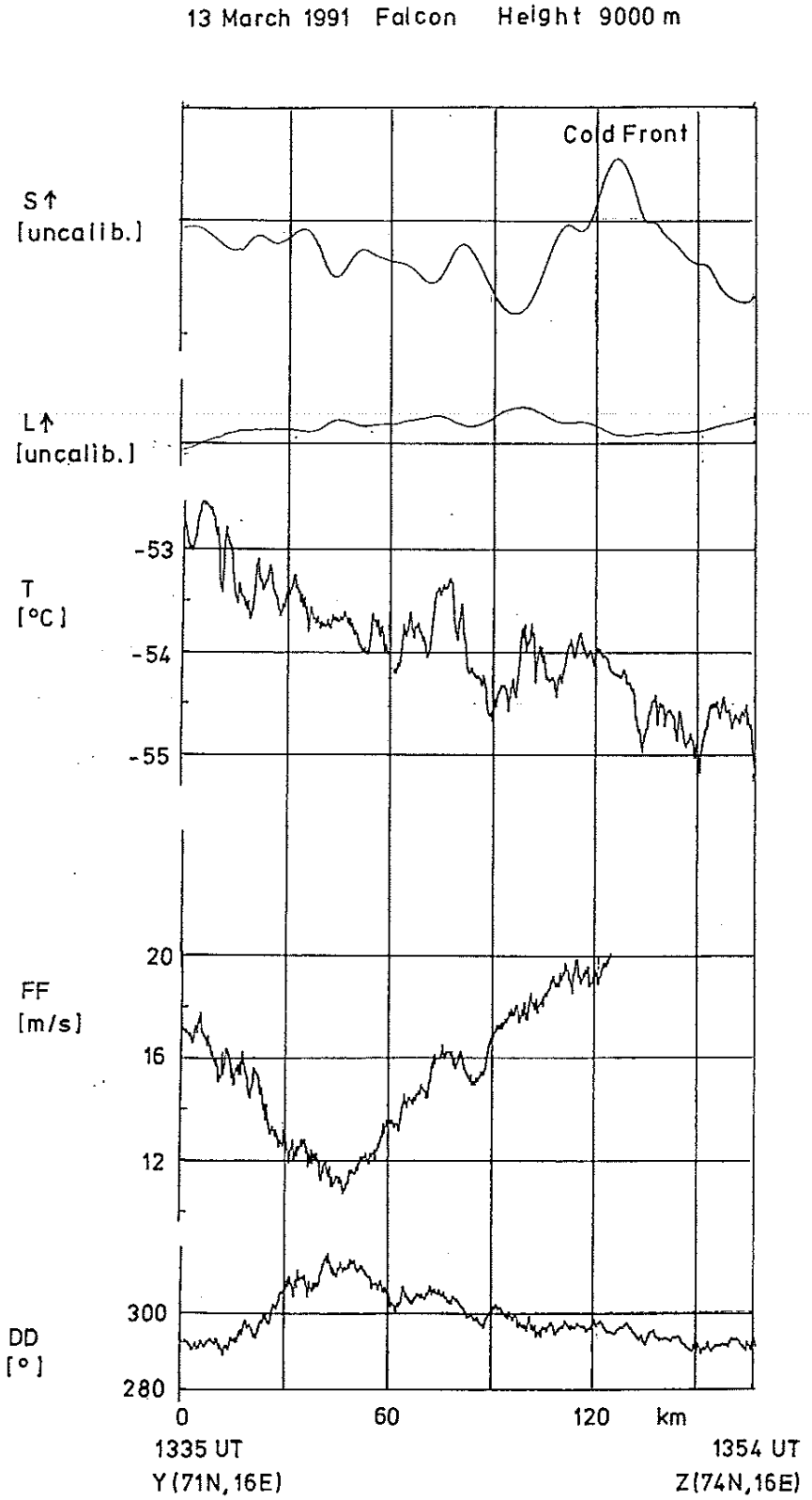

Figure 5.13a: Time series of shortwave and longwave radiation from below, S↑ and L↑, temperature T, wind speed FF and wind direction DD measured during the FALCON flight at 9000 m height from Y to Z on 13 March 1991.

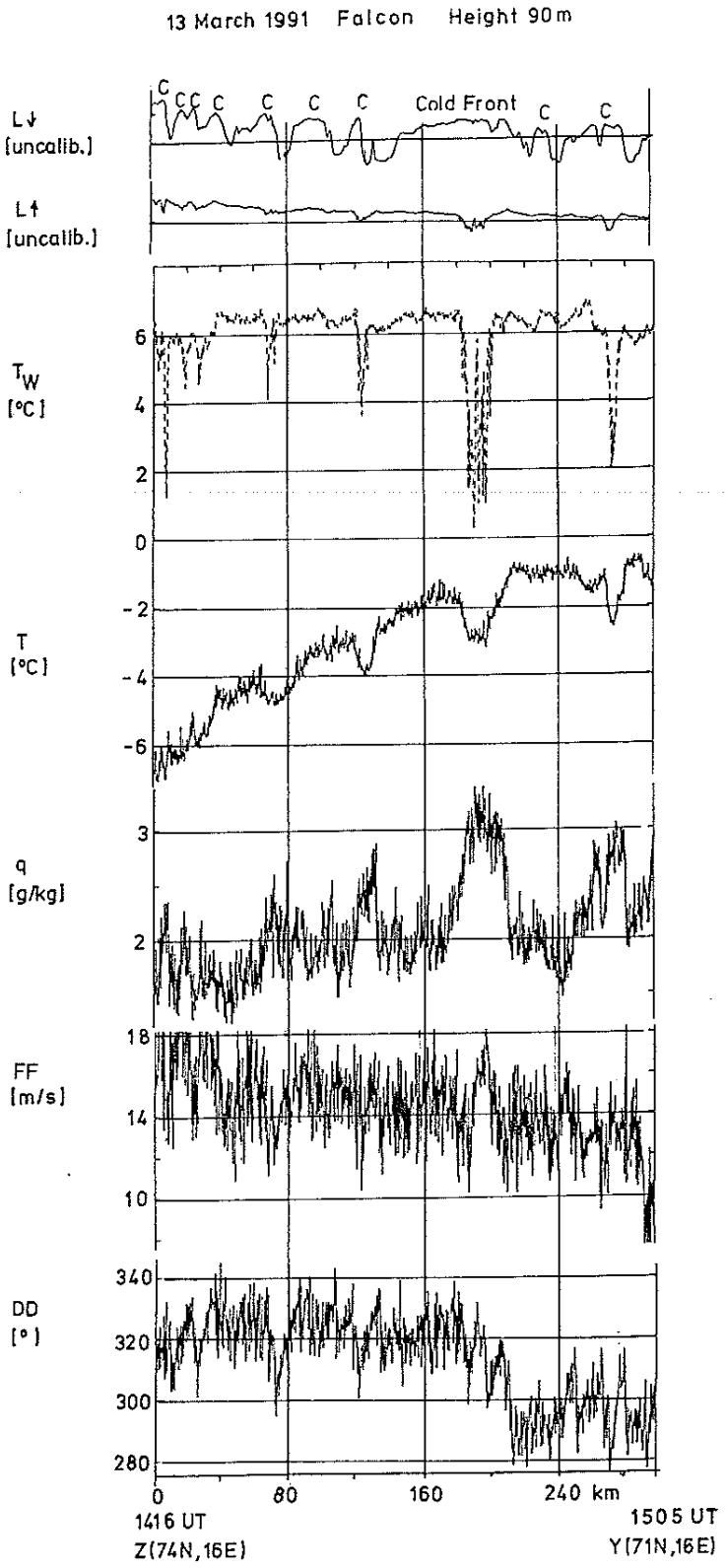

Figure 5.13b: Time series of longwave radiation from above (L↓) and below (L↑), sea surface temperature T_W, air temperature T, specific humidity q, wind speed FF and wind direction DD measured during the FALCON flight at 90 m height from Z to Y on 13 March 1991. The cloudy parts of the convective patterns are marked by "C".

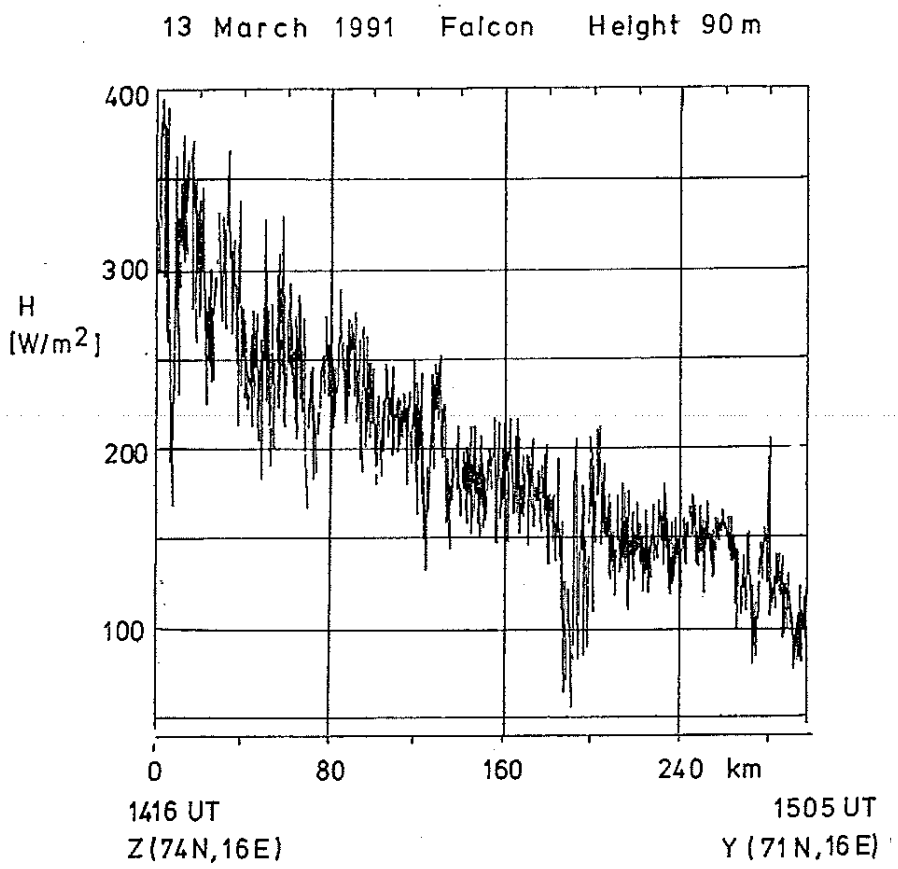

Figure 5.13c: Time series of sensible heat flux H estimated via the bulk aerodynamic formula from the FALCON measurements at 90 m height on 13 March 1991.

5.4.3. *The 2-D Grey Probe for particle measurements on board the DO-128*

(H. H. Brecht, Meteorologisches Institut der Universität Hamburg
S. Bakan, A. Reuter, Max-Planck-Institut für Meteorologie, Hamburg)

a. Function principle and calibration of the 2-D Grey Probe

The Optical Array Grey Probe, manufactured by Particle Measuring Systems, Boulder, Colorado allows airborne measurements of water droplets and ice crystals in the size range of 10 to 600 microns.

The beam of a 4.5 mW He-Ne-Laser, first expanded, two times deflected by mirrors and then amplified by a lens system, illuminates a linear array of 64 photodiodes each of which is 10 µm wide (Figure 5.14). Between the mirrors (which are at a mutual distance of 61 mm) the beam transits the open atmosphere, the sample area. The focus plane of the optical system coincides with the center of this area.

If no particle is passing through the sample area, every diode of the detector array is illuminated by the Laser beam with maximum intensity. The output voltage of the diode is proportional to the light intensity at the input. In case of a particle passing through the sample area, it will be imaged as a shadowgraph onto the photodiodes and darken some of them.

The output of each diode of the linear array is connected to three comparators to discriminate three different shadow intensities. The first comparator switches, if the light intensity reaches at least 75% of the maximum, the second at 50% and the third at 25% of it. The result is a signal representing one of the four grey steps 0 to 25%, 25 to 50%, 50 to 75%, or more than 75% light intensity.

The comparator information of each of the 64 diodes of the array is stored in local memory with a maximum repetition rate of 5 MHz. This frequency is also called "slice rate", because it cuts the particle in several slices of information during its transit through the sample area of the probe. The microprocessor software is able to recognize beginning and end of a particle. After the particle has passed, the data block is sent to the computer, where it is stored on tape as well as reproduced on a PC screen for online presentation as raw image and in accumulated size histograms.

The interpretation of the resulting images is not always simple, as they can be up to ± 30 mm out of focus, which makes the shadow bigger but less dark near the edges due to optical diffraction. This is shown in Figure 5.15, which contains the images of spheric particles of 300 microns diameter at different distances from the focal plane of a 2-D probe (Knollenberg, 1970). The transition from Fresnel diffraction for small distances to Fraunhofer diffraction for larger distances from the focal plane and the increasing intensity peak in the center of the diffraction image (Poisson spot) are the prominent features.

Even if the particle passes right through the focal plane diffraction at the crystal edges and partial transparency create problems for the image interpretation. These might be alleviated somewhat (in comparison to classical 2 D-probes) by using the provided grey level information.

Commonly, calibration of the probe is accomplished with the use of glass beads of known diameter, thrown through the sample area of the probe. To have precise control over the glassbeads, we developed a calibration device mounted on top of the probe tips. It consists of a funnel with an outlet diameter near the size of the beads' diameter and a 2-axis micropositioner to control the trajectory of the beads (Figure 5.17a). Our aim was not only to calibrate the probe, but to investigate diffraction images of known bead size in different distances from the focal plane as well as to get a feeling for the interpretation of the images in later measurements. Figuew 5.16 presents diffraction images of glass beads of 140, 280 and 400 microns diameter falling through the sample area eigher directly through or in specific distances from the focal plane.

The result of our measurements is very similar to those by Knollenberg described above. With increasing distance from the focal plane the distribution of different grey steps changes, the Poisson spot in the center of the image is becoming more intense and the image diameter increases. The interpretation of these calibration data will be used to understand the image geometry more precisely.

There have been some disadvantages in this method:

- Due to adhesion and/or air humidity, the beads tend to clump together, leading to many irregular images.
- Because of this clumping, the outlet of the funnel has to be considerably bigger than the bead diameter itself, making the control of the fall trajectory through the sample area problematic.

- Glass beads with a good precision are very expensive and there is no sufficient sample variability available.

Therefore, we designed an alternative calibration device, which was a rotating glass disk instead of the funnel, driven by a DC-motor. On its surface, there are blackened drill holes of calibrated diameter in concentric tracks (Figure 5.17b). This device was used successfully for calibration purposes before the ARKTIS '91 field phase and the experience gained during the field phase suggests further development of this calibration system.

b. The 2-D Grey Probe during the field phase

During the field phase, the probe was mounted under the left wing about 1.5 m from the wing tip of the Dornier DO-128 two engine turboprop aircraft of the Technische Universität Braunschweig (Figure 5.18). Connection with the data acquisition and power supply inside the plane is through high-noise-immunity twisted pair airborne cable.

The DO-128 flew a total of eight missions from February 22 to March 13, 1991 mostly in situation of convective cloudiness in moderately cold air flow. Concerning the 2-D probe, the first three flights were necessary to resolve inflight problems with sonde alignment and temperature drift under in situ conditions. During the next five missions a total of 12 h 07 min of data of good quality, 2 h 17 min of data disturbed by temperature drift, start or landing effects, and 32 min of data disturbed by deicing effects (large drops of melting water from the probe tips) were sampled.

The bulk of data stems from horizontal flight legs below 1000 m, occasionally also from profile ascents up to 3000 m. The total temperature range encountered was between about +3 and -16°C. The moisture range is not yet completely clear, as the Humicap calibration curve drifted obviously during the field phase.

c. Preliminary results

(i) General remarks

During the successful flights a wealth of ice crystal images of widely different sizes and occasional cloud water droplets have been sampled. In a preliminary analysis it was attempted to classify the cloud particle structure according to their environmental temperature and humidity. Several attempts of such a classification, evaluating laboratory generated ice crystals are sited by Pruppacher (1978) from that book a somewhat simplyfied version is reproduced in Figure 5.19.

A few essential points have to be kept in mind for the following:

- As mentioned, the humidity measurements of the DO-128 of the Technische Universität Braunschweig were corrupt due to an unrecognized drift of the calibration curve which could not yet be corrected for. Therefore, the following results can only be given in relative humidity units.
- In addition, the temperature range encountered was only from -3 to -16°C due to the confinement of the DO-128 flight level to the lowest 10000 feet.
- In contrast to laboratory generated ice particles only few particles observed during such a flight are locally generated. Most of the larger particles should be fallen down from heights above. Therefore, the observed particles represent different growing conditions and different fall histories. Especially in low levels the bulk of recorded data stems from layers above.

(ii) Precipitation particles

During the field phase a lot of flight time was spent below cloud base height, resulting in extensive samples of precipitation particles. Most of these resembled rather large melting snow complexes. Occasionally, the fine structure acquired in cloud is conserved, which may be possible if these particles fall into cold and relatively dry air. Figure 5.20 shows several typical samples of these types.

(iii) Cloud particles

In the upper cloud regions the particle structure was usually quite uniform. In the lower layers, however, quite different particle sizes and forms are frequently encountered within a short time interval. In a preliminary analysis those particles were ignored, that can be assumed to stem from levels above. Also particles smaller than about 100 μm are ignored. From the remaining images typical crystal forms are derived by subjective judgement. These have been arranged as a function of environmental humidity (in relative units due to the mentioned problems) and temperature in Figure 5.21. A rough correspondence of the particle shapes to those in Figure 5.19 is evident. Nevertheless, the subjective nature of the present procedure has to be stressed.

(iv) Benefits of grey levels

The special feature of our 2-D-probe is the availability of 4 grey levels, which introduces more details into the 2-D-images. No real use could be made of this additional feature till now.

For most of the observed particles the intermediate grey levels only mark the particle boundary, while the bulk of the particle image is black. Sometimes the bulk of the image shows a lighter grey shade, indicating, probably, that the particle passed out of focus.

A few particles of roughly circular, elliptical or hexagonal structure exhibit a brightening of the central ares (see examples in Figure 5.22). This could either be a result of a thin translucent ice plate or of the Poisson spot due to Fraunhofer refraction on a spherical particle out of focus. If the latter were true, the interpretation of the corresponding image at low humidities and -12 to -16°C as a thin plate is wrong.

(v) Outlook

The data collected proved to be of excellent quality, despite some disturbance in the optical path alignment due to temperature effects. Elongated particles (needles, columns) are often observed to be oriented from bottom left to top right of the images (see two examples in Figure 5.21). The reason for this is not yet clear.

The mentioned preliminary analysis was already time-consuming. Standard programs shall in near future be used to derive droplet size distributions and cloud water or ice content.

References

Knollenberg, R.G. (1970): The optical array: An alternative to scattering or extinction for airborne particle size determination. J. Appl. Meteor., 9, 86-103.

Albers, F. (1989): Flugzeugmessungen der Eiskristallkonzentration und -größenverteilung mittels optisch abbildender Sonden in Cirrus-Wolken. Institut für Geophysik und Meteorologie der Universität Köln.

Pruppacher, H.R., J.D. Klett (1978): Microphysics of clouds and precipitation. Reidel Publ. Co., Dordrecht, 714 pp.

Table 5.4: Time and quality of sampled data for the five missions.

Date	Time (UTC) from	total (min)	Remarks
March 04,1991	09:28-09:30	2	data failures
	09:30-10:36	66	data o.k.
	10:36-10:38	2	temperature effects
	10:38-10:43	5	data failures
	10:43-11:02	19	temperature effects
	11:02-11:15	13	data o.k.
	11:15-11:24	9	temperature effects
	11:24-11:43	19	data o.k.
	11:43-11:54	11	data failures
	11:54-12:47	53	data o.k.
	12:47-12:58	11	temperature effects
March 07, 1991	09:51-10:16	25	data disturbed due to take off
	10:16-10:38	22	data o.k.
	10:38-10:39	1	data with temperature failures
	10:39-10:48	9	data o.k.
	10:48-10:49	1	data failures due to deicing
	10:49-13:20	151	data generally o.k., occasional temperature failures
March 08, 1991	10:27-10:32	5	data o.k.
	10:32-10:40	8	data with deicing failures
	10:40-11:40	60	data o.k.
	11:40-11:45	5	data with deicing failures
	11:45-12:03	18	data o.k.
	12:03-12:11	8	data o.k., few deicing failures
	12:11-12:36	25	data o.k.
	12:35-12:43	7	data disturbed by landing effects
March 12, 1991	09:31-12:02	143	data o.k.
March 13, 1991	12:55-13:11	16	data failures due to take off
	13:11-13:26	15	data o.k.
	13:26-13:27	1	temperature effects
	13:27-13:48	21	data o.k.

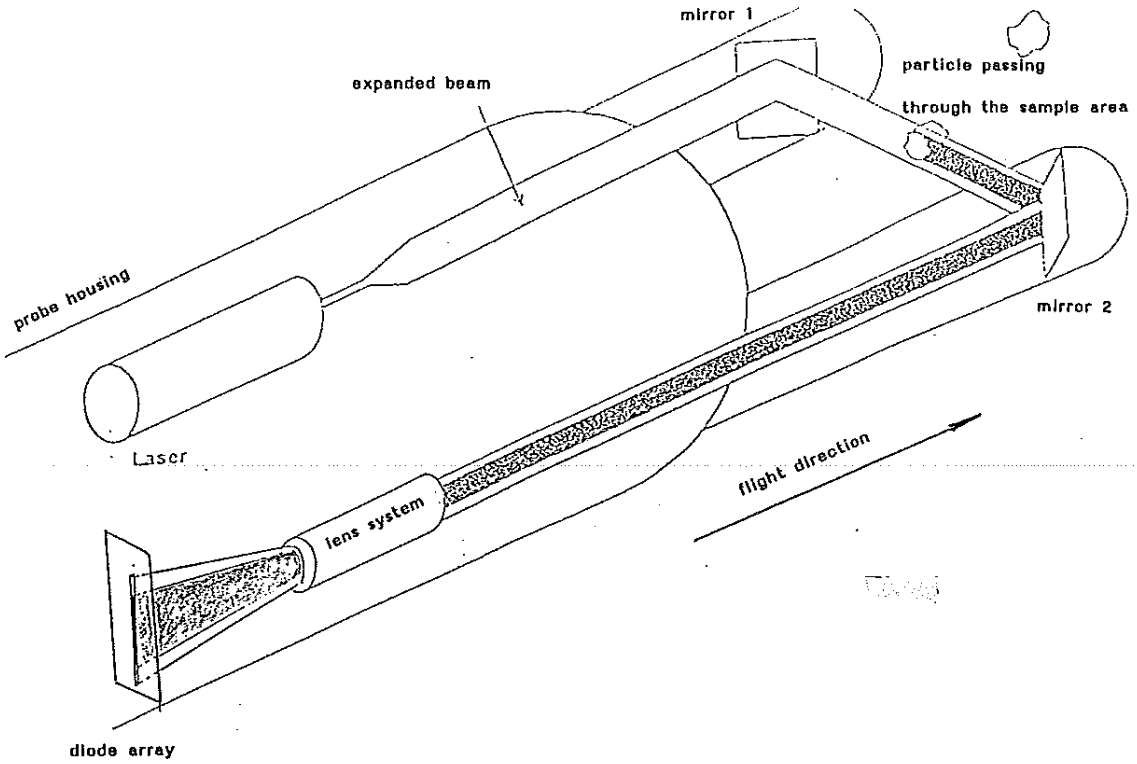

Figure 5.14: Scheme of the 2-D grey probe (Albers, 1989).

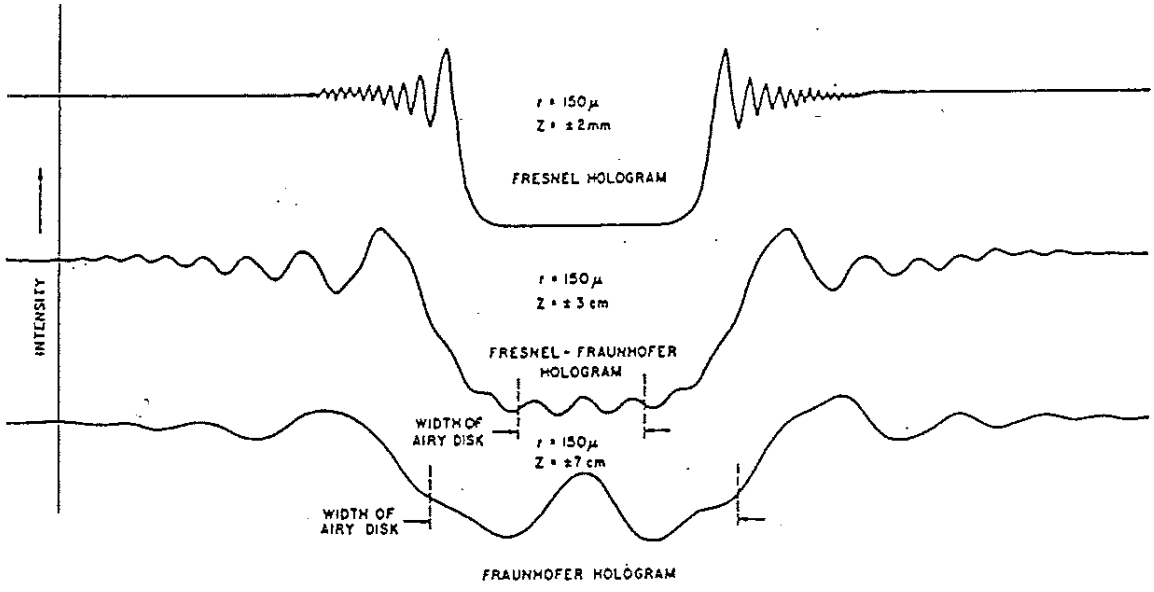

Figure 5.15: Intensity distribution for diffracted particles in different distances from the focus plane (Knollenberg, 1970).

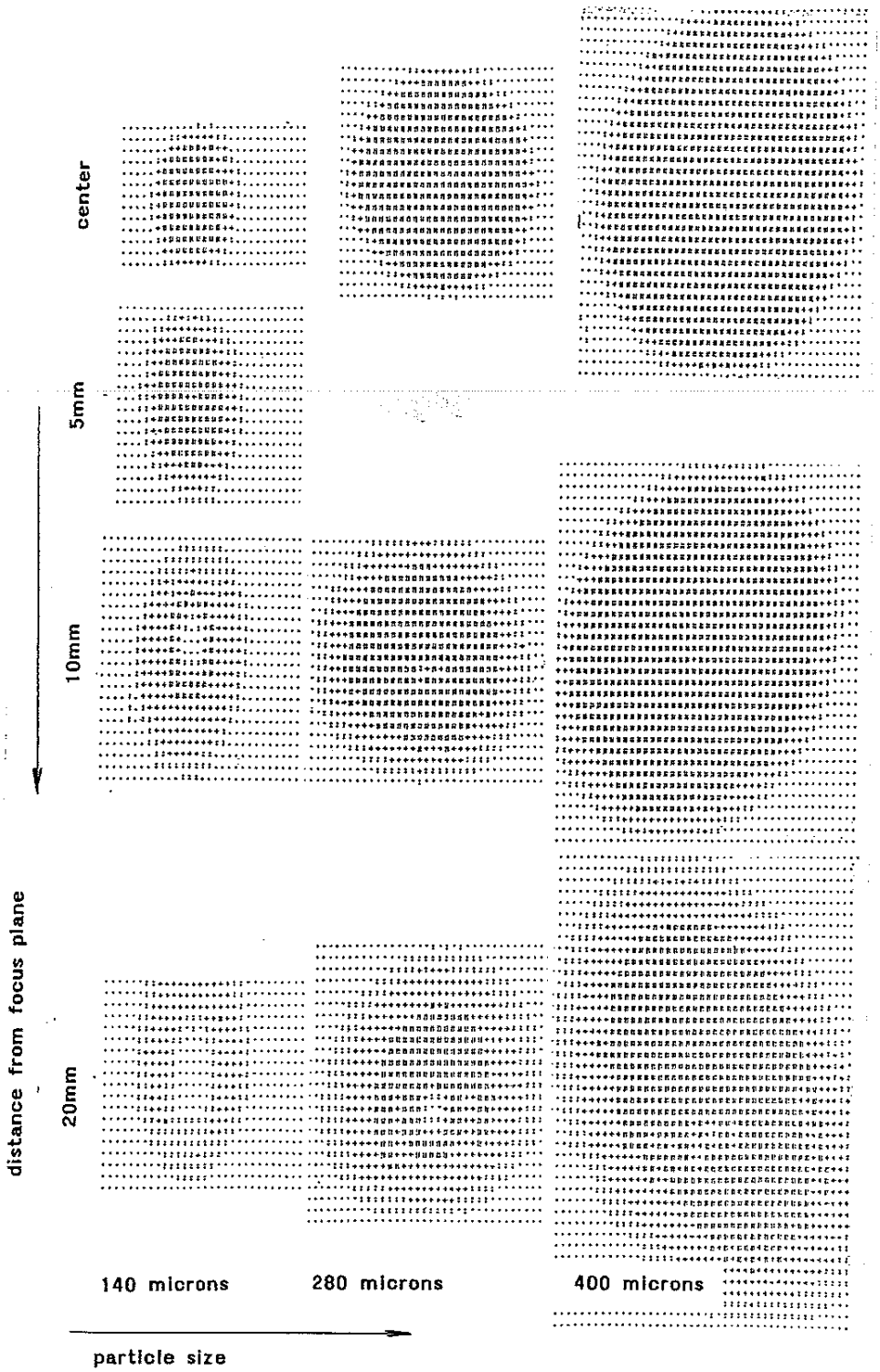

Figure 5.16: Diffraction images of glass beads (140, 280, 400 micron diameter) in different distances from the focal plane, displayed from the Exabyte tape with the PMS Dump-it routine (F = 0 - 25%, + = 25-50%, : = 50-75%, . > 75% of maximum light intensity).

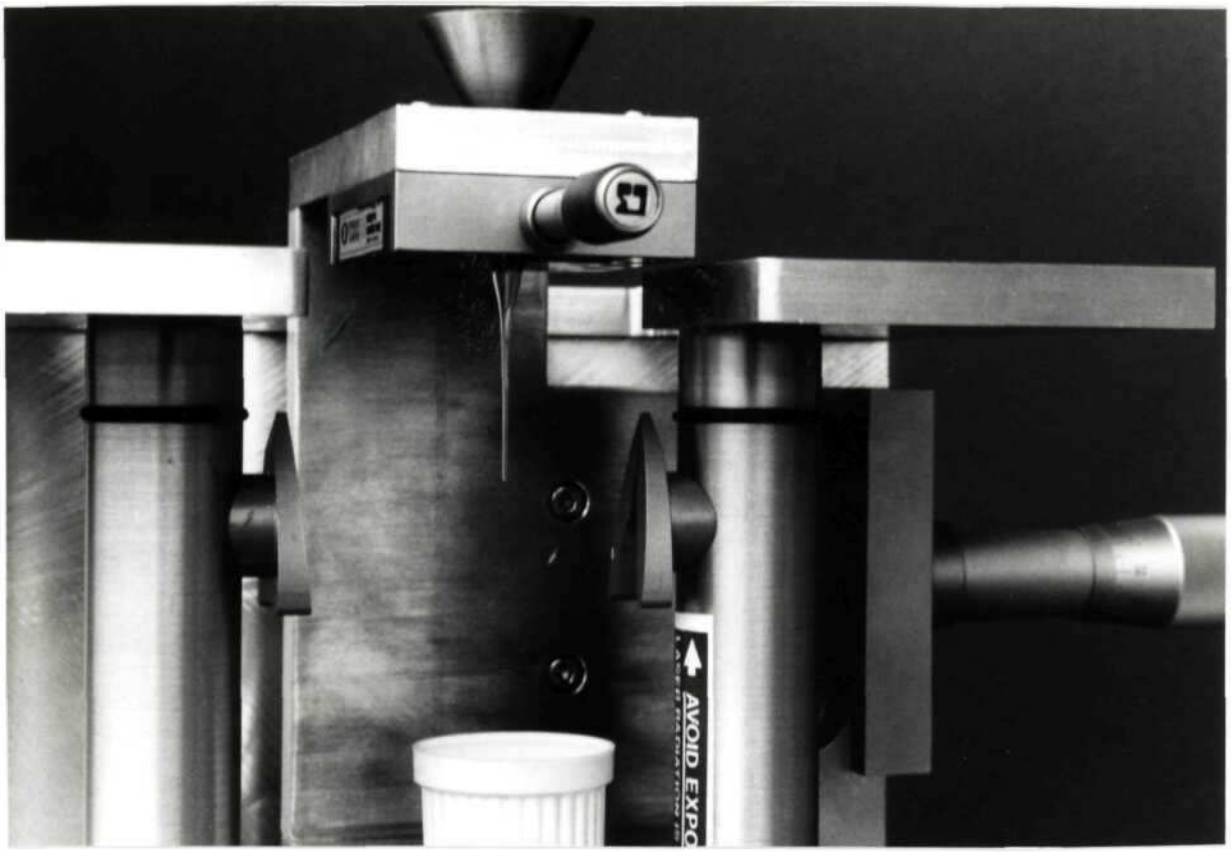

Figure 5.17a: 2-D-grey probe calibration device with glass beads.

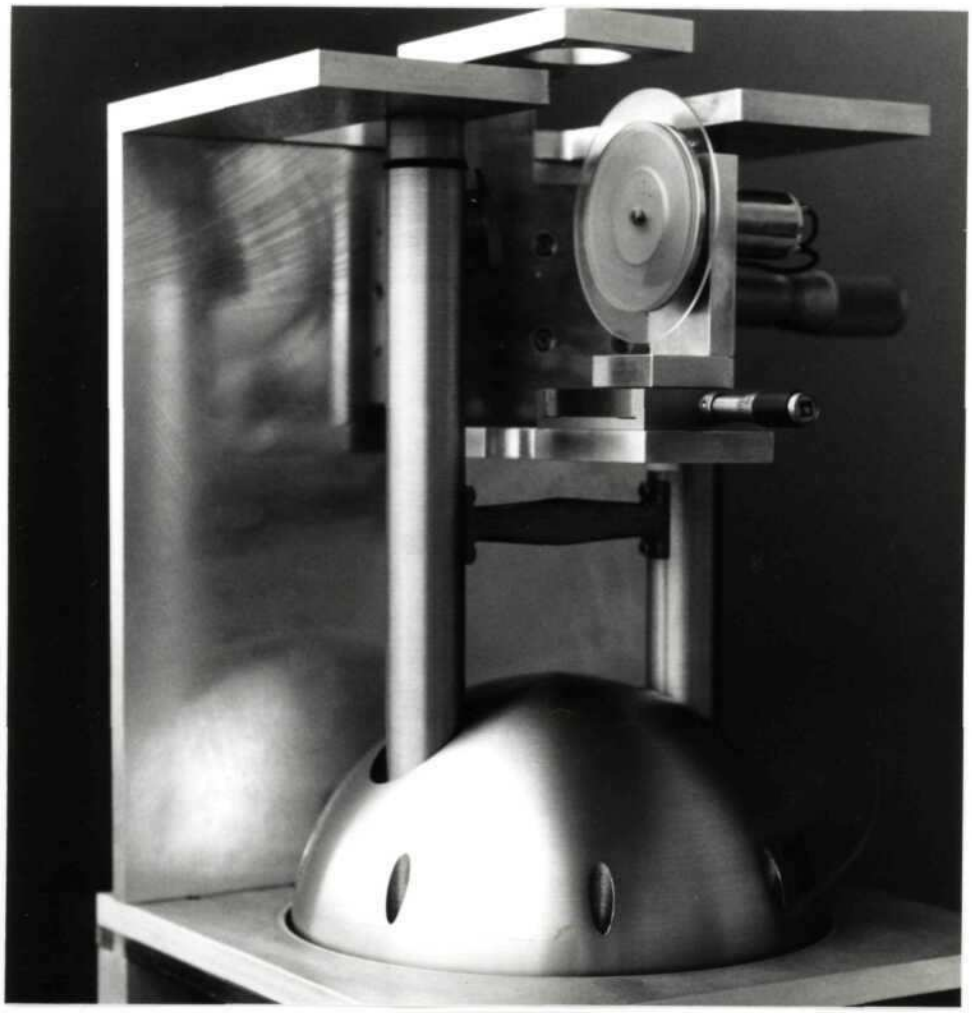

Figure 5.17b: 2-D-grey probe calibration device with rotating disk.

Figure 5.18: The research aircraft DO-128 of the Technische Universität Braunschweig showing the location of the 2-D-grey probe under the left wing.

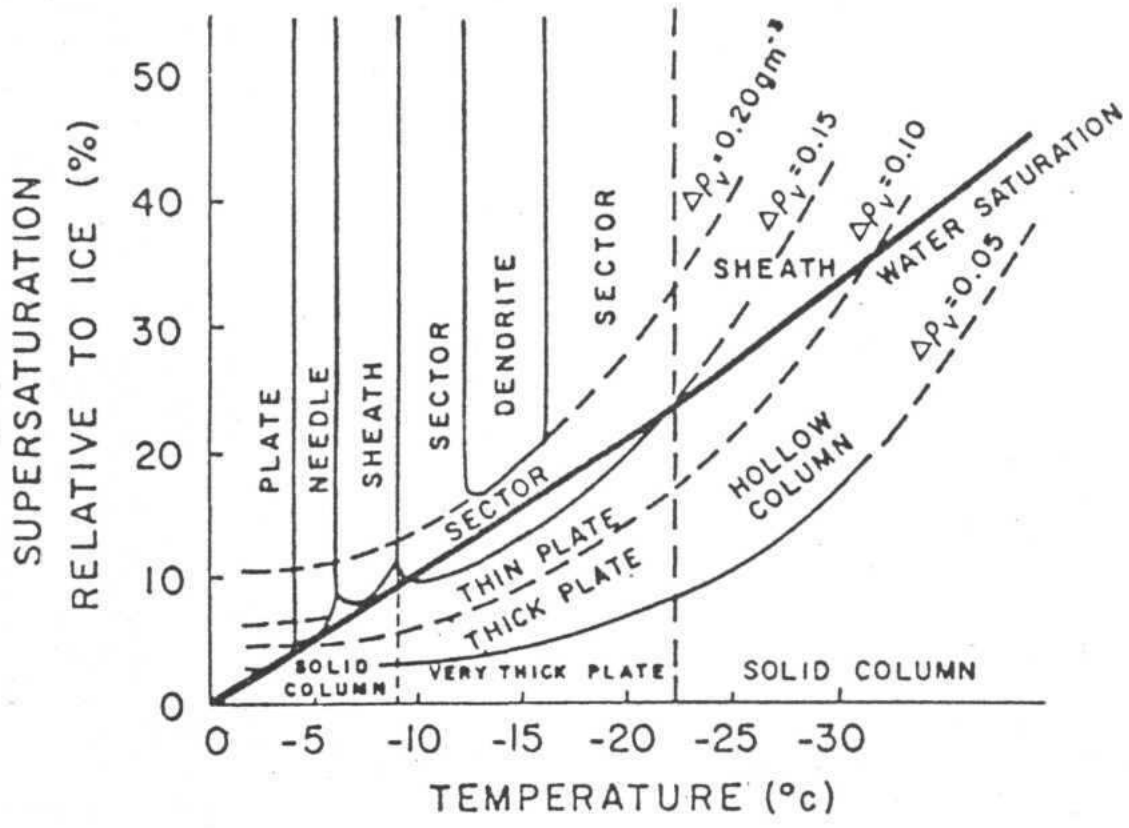

Figure 5.19: Variation of ice crystal habit with temperature and supersaturation (from Pruppacher, 1978, Fig. 2-25a).

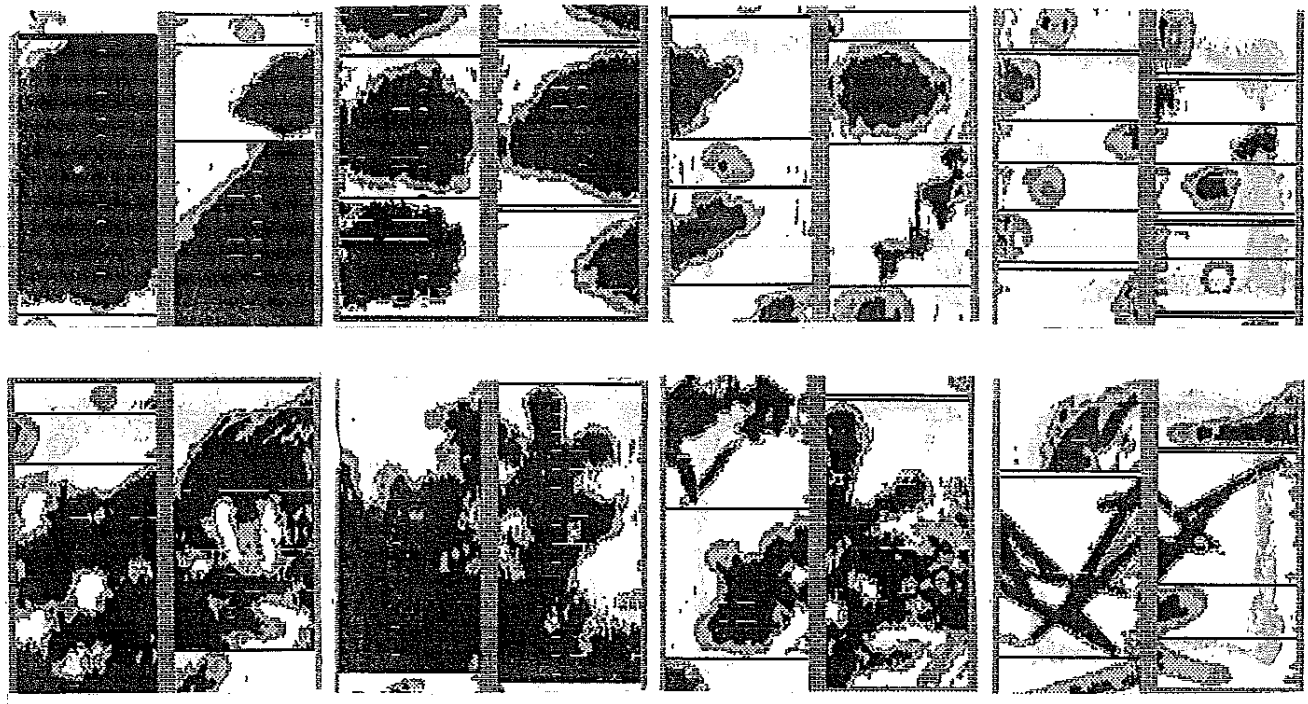

Figure 5.20: Typical samples of precipitation particles as collected during flight legs below cloud base.

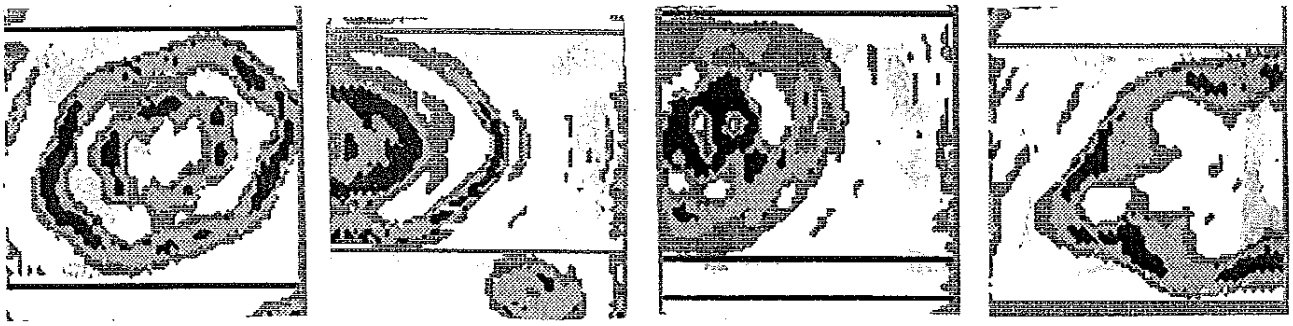

Figure 5.22: Examples of cloud particles with bright spot in the central part.

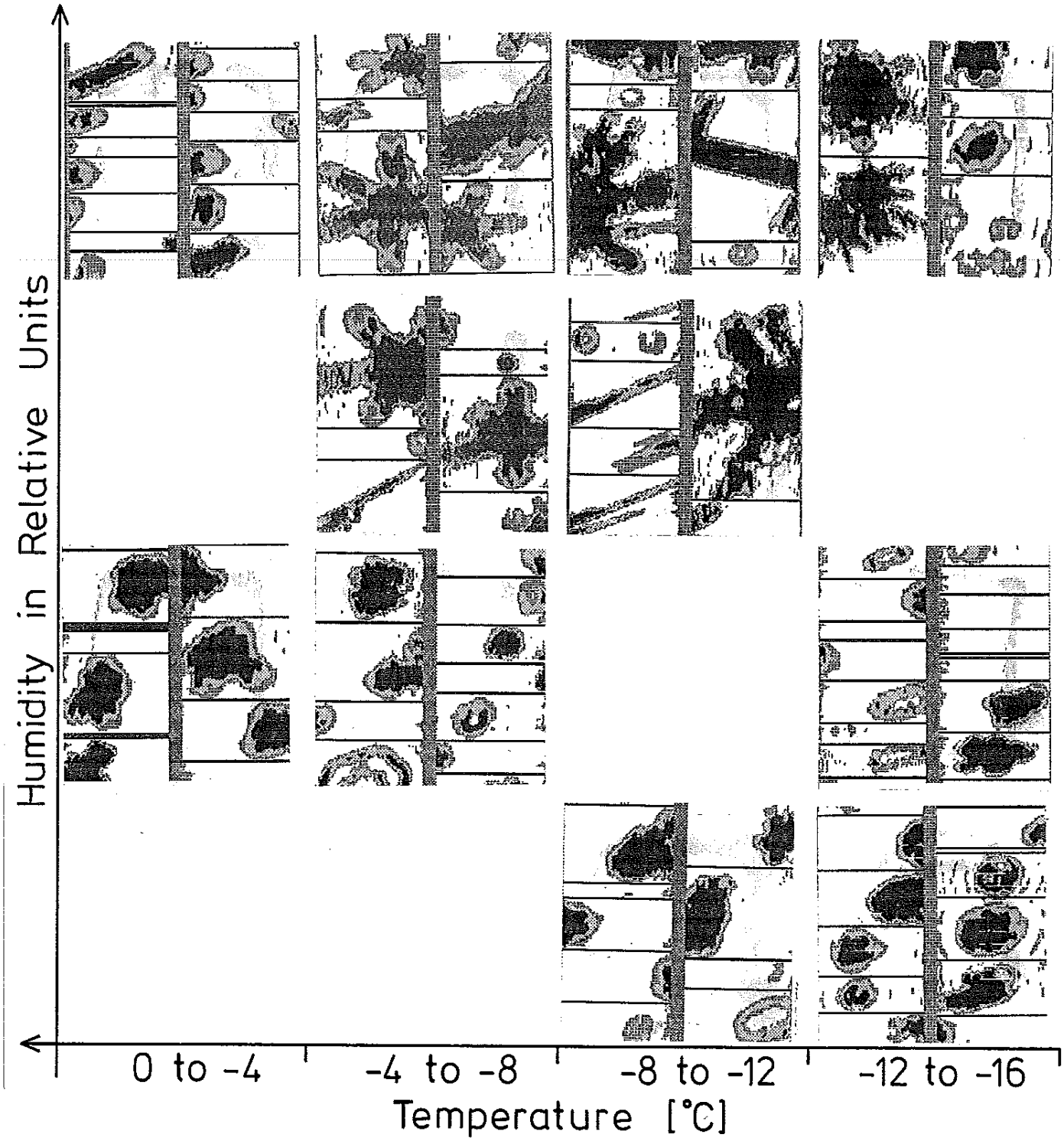

Figure 5.21: Typical cloud particle samples at various humidity-temperature combinations.

5.4.4. *Experience with in situ measurements of contrail properties*

(S. Bakan, Max-Planck-Institut für Meteorologie, Hamburg)

a. Motivation

The increasing number of contrails in the upper troposphere may have a profound influence on the Earth's radiation budget by increasing the global cirrus cloud cover. In addition, recent work (Betancor-Gothe, 1991) suggests different microphysical and optical conditions in contrails or contrail generated cirrus as compared to ordinary cirrus. As these differences are not well documented nor understood, studies in this direction will be conducted at the Universität Hamburg. On the experimental side these studies will include combined surface and airplane investigations.

The ARKTIS 1991 campaign provided the opportunity to gather first experience with contrail intersection by airplane. After February 26 the large scale weather condition was characterized by a ridge over Scandinavia and a trough line between Iceland and Spitsbergen. At the location of the experiment, this situation led to supression of boundary layer cloudiness (the central target of ARKTIS 1991) but to extended fields of thin cirrus. As in the afternoon of February 27 an extended contrail was visible for 1/2 hour, a test flight to produce and later on intersect such a contrail was planned for the following day. Although, such a mission was not foreseen in the original experiment plan the conditions seemed to be nearly ideal, as most of the necessary equipment and logistics was available.

b. Flight decision

In the morning of February 28 the final decision to use the DLR-FALCON-20 for such a mission was made, based on the following facts:

- The general weather situation with advection of rather warm and moist air from SW into the experiment area has been stable for two days and would continue, according to forecasts, throughout the 28th. This stable situation had made possible an extended discussion of the basic ideas to be tested, and a careful mission planning.
- The radiosoundings from VALDIVIA at position 71.2 N, 13.5 E (Figure 5.23) showed a moisture maximum near the tropopause, indicating the upper part of the visible cirrus layer. The tropopause at 04 UT was at about 11300 m height with a temperature of -67°C. This temperature is about 13° less than the critical temperature for contrail appearance

according to the nomogram of Appleman (1953). This profile was very similar to those on the day before, where we could observe a long-living contrail over Andoya.

- The flight weather forecast from Bodö expected cirrus between 7500 and 12000 m and a good chance for long-living contrails above 7500 m.
- At the Andoya Rocket Range a NdYg-laser system of the Universität Bonn showed during the night between February 27 and 28 clear evidence of the observable cirrus layer with backscatter maxima between 7000 and 12000 m height.
- The visible cirrus layer was rather thin, which would allow to see (and document) the expected contrail by a surface observer as well as in the satellite image.

The mission was planned to proceed in the following manner (Figure 5.24):

- Ascent to 35000 feet to define the vertical profile of temperature and moisture as well as the cirrus cloud level. Final decision about the operation height.
- Level flight along two tracks into the direction of the wind (B → C) and (after a turn) against this direction (D → E) to produce a well defined contrail pattern that would provide minimum problems to be picked up again for measurements.
- After way point E a procedure turn should bring the FALCON into the youngest part of the contrail. Following a path E → D1 → C1 → B1 (where D1, C1, B1 are the way points corresponding to D, C, B if wind drift is accounted for) successively older parts of the contrail will be passed (~30 minutes at B1).
- Throughout the flight the turbulence instruments should work as well as the FSSP (unfortunately, the 2-d probe was not available under these flight condition).
- The data from the final descent to Andoya should again document the vertical profile.
- The flight pattern was selected such, that an observer at the coast between Bleick and Andenes could follow the whole mission. He was supposed to document the maneuvers (photos, report) and give advice to the pilots by radio contact.

c. The mission

As is documented in the plot of the real flight pattern (Figure 5.24) the mission differed considerably from the planned. This was initially due to misunderstandings with the pilots, lateron due to unexpected problems in the flight situation. As planned, the initial ascent, starting at 1130 UT, was made with heading W up to 7500 m (1144 UT) and with heading SE up to 9000 m (1150 UT, flight level 300).

In this last part we may have passed a few cirrus streaks, but they were very faint and hard to detect. The measured relative humidity was very low and not near to saturation, not even over ice (see Figure 5.23). Till 1156 UT several maneuvers were flown in this height in order to recognize the hopefully produced contrail. At 1155 UT the surface observer confirmed that we were creating only a very short contrail of about 100 meters length. After this, height was gained during a left turn and a following straight leg from points B towards C. Flight level 330 (≈ 10000 m) was reached at 1202 UT. The surface observer could still recognize only a very short contrail. As we should have been already very near to the tropopause, and given the slow ascent speed of the FALCON in this height, it was decided not to try greater heights.

Below that flight level cirrus became visible (compare Figure 5.25 for Ci layer to the north of Andenes) and it was decided to measure at least some cirrus particles during descent. Therefore, the northbound leg was taken beyond the planned way point C and the FALCON sank down to 8500 m (flight level 280) at 1208 UT. Unfortunately, at this northernmost point of the flight pattern we were still above clouds. After a 180° left turn we proceeded with sinking and entered a very faint cloud layer at about flight level 220 (~7000 m height). But as this was near the south edge of the cloud field, we left this cloud very soon and crossed a cloud free region.

At this point the flight was interrupted, as we were obviously not able to produce a contrail (which was our major goal) and as further measurements in cirrus would have required an inappropriate amount of additional time.

d. Preliminary data analysis

Turbulence data have been recorded throughout the whole flight, but only a few level flight legs exist for a sensible evaluation of turbulence features. The following data products have been prepared after the flight:

- A plot of the planned and real flight pattern (Figure 5.24) was prepared as well as plots of height and heading versus flight time.
- Wind speed and direction, temperature, and moisture were plotted versus time. It turned out that the Lyman-α-humidity record is essentially useless at these low temperatures. This would be of importance if turbulence data of high frequency are of interest.
- Two vertical profiles (from the initial ascent and the final descent) of wind speed and direction, of temperature, and of moisture were plotted.
- The particle counter (FSSP) showed very few particles with preferred radii of about 15 μm and maximum radii of about 30 μm. Due to a misunderstanding, these data were not recorded and are, therefore, not available for any further evaluation.

For the interpretation, critical maximum temperature values for the appearance of contrails as given in a nomogram by Appleman (1953) are added to the observed profiles in Figure 5.23. According to this, contrails should be expected on February 27 as well as on February 28. In the afternoon of February 27 the tropopause was found at about 12000 m height at -70°C, which was about 15° colder than T_c. Under these conditions we observed at least one rather permanent contrail near Andenes (where not too many flight operations take place daily). The tropopause was lower on February 28, at about 10000 m height during the flight mission. As the tropopause temperature varies approximately with the dry adiabatic gradient, but T_c varies slower than that, the maximum temperature difference between tropopause and T_c was only 5-7°C during the flight mission. Although this should lead to visible contrails according to Appleman (1953), during the CLOUD TRAIL experiment (1956/57) it was found that under these conditions in 5% of the time no contrail could be observed (Pilié and Jiusto, 1958).

e. Conclusions

Although the primary aim of this mission was not reached, it was a good opportunity to get experience with a contrail hunting flight mission type.

The following list of problems and recommendations to avoid or enable them summarizes the lessons learned with this mission:

- The large flight speed (~200 m/s) of the FALCON in these heights creates problems for operations in strongly limited regions, if many in flight decisions are necessary. Way points may be reached or passed before decisions can be made. It turned out that flying a 360° circle provides some time to reach at conclusions before entering the measurement track.
- Ascent rates are very small near the tropopause. Together with the large flight speed this leads to large horizontal travel distances during a height change manoeuvre. Unplanned hight changes are, therefore, very disturbing to the mission progress.
- All necessary measurement devices should be active from a very early stage and resulting data should be recorded throughout the whole flight.
- Profile information, especially of temperature and humidity, above about 5000 m, should be immediately available to the mission scientist to be checked against the mentioned T_c-nomogram for a rapid estimation of the actual chances to produce a durable contrail.
- The surface observer was very helpful in reporting length and intensity of the produced contrail, which is difficult to assess for the flight crew. Therefore, a flight mission should be planned within a radius of less than 30 km around such a surface observer. He could be best positioned on an island or ship, as satellite images in these cases allow a rather simple contrail detection over the sea surface.
- Thin cirrus is hard to detect in flight by eye. Maybe the signal of the FSSP would be helpful to define the cirrus level. Additional problems are provided by the spatial inhomogeneity of cirrus streaks. As these streaks are not necessarily all in one height, the selection of the best flight level (given the high flight speeds) is very difficult.
- A detailed planning of the flight profile before the mission start is vital. This mission plan has to account for possibly necessary additional inflight decisions by providing time for that (e.g. define possible flight positions for 360° turns). For this planning the most actual satellite images are vital.

A prerequisit for a realistic estimate of the chance to observe durable contrails would be a known connection between contrail life time and the difference between environmental and the critical maximum temperature (or any other simply observable quantity). Short horizontal legs in different heights could allow a surface observer to document the resulting contrail length, which could then be correlated with the observed vertical profiles.

References

Appleman, H. (1953): The formation of exhaust condensation trails by jet aircraft. Bull. Am. Met. Soc., 34, 14-20.

Betancor-Gothe, M. (1991): Einfluß von Kondensstreifen auf den Strahlungshaushalt der Atmosphäre. Diplomarbeit, Universität Hamburg, pp. 72.

Pilié, R., J. Juisto (1958): A laboratory study of contrails. J. Met., 15, 149-154.

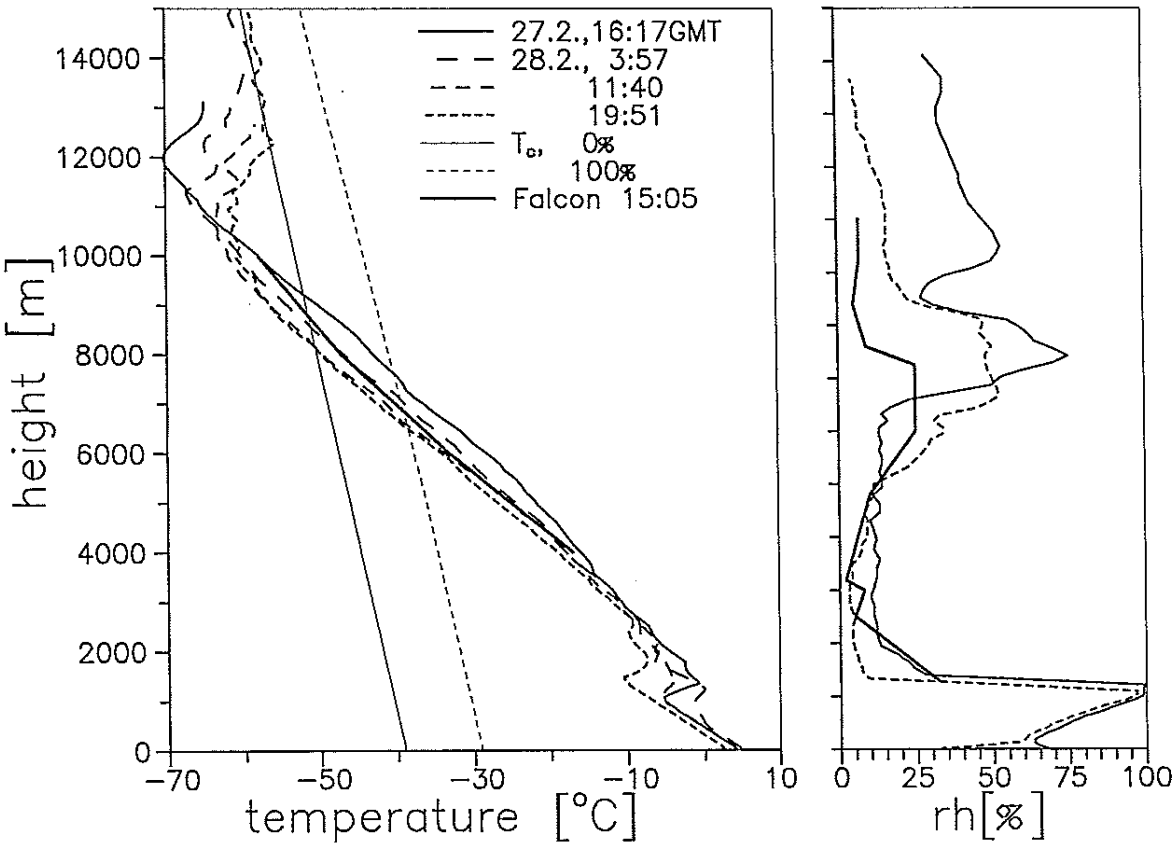

Figure 5.23: Vertical profiles of temperature and relative humidity (over water) from RV VALDIVIA (position 71.2°N, 13.5°E) and from FALCON flight, as well as the critical maximum temperature for contrail appearance at 0 and 100% relative humidity according to Appleman (1953).

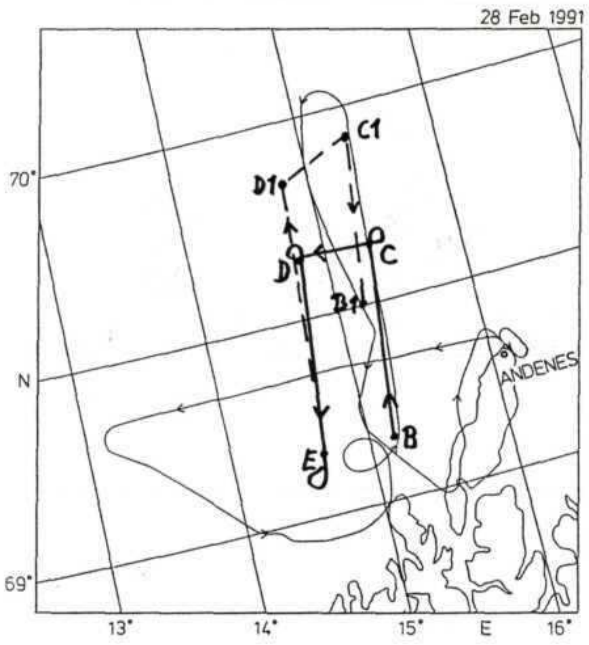

Figure 5.24: Planned (thick line) and real (thin line) flight pattern.

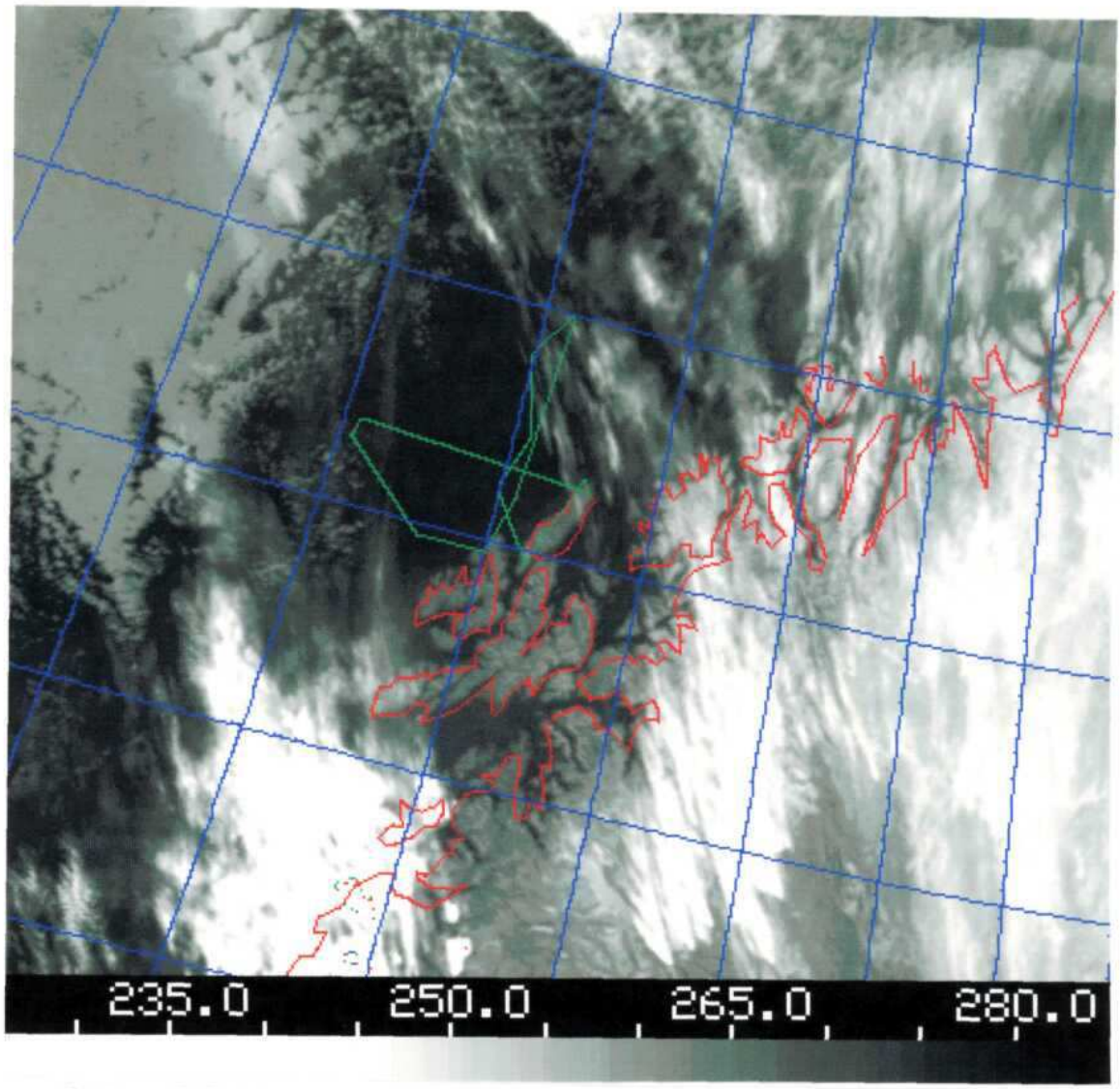

Figure 5.25: NOAA 11 / AVHRR Channel 5 image (brightness temperature) from 1230 UT, with flight path indicated.

6. *Satellite data analysis*

(A. Manschke, Meteorologisches Institut, Universität Hamburg,
S. Bakan, Max-Planck-Institut für Meteorologie, Hamburg)

6.1. *General remarks*

High quality satellite images proved to be very helpful for the planning of research flight missions. The general overview of the actual weather conditions, but also the location of interesting phenomena like cold air outbreaks and the associated cloud types, can only be provided by satellite images not older than a few hours.

The satellite data used in this report stem from the AVHRR radiometers onboard the satellites NOAA-9, 10, and 11. Due to the rather high resolution of about 1 km in the subsatellite point, the near polar orbit, and the AVHRR sensor characteristics, those data seemed to be most promising for the campaign. They were acquired and processed for the experiment purposes by a group from the Meteorologisches Institut der Universität Hamburg (A. Manschke, T. Martin, H.-H. Brecht) and Max-Planck-Institut für Meteorologie (S. Bakan).

6.2. *Satellite data acquisition*

The satellite data processing during ARKTIS '91 may be divided in three sections:

- An **A**utomatic **P**icture **T**ransmission (APT) receiver took down the most actual images of the weather situation, but with low spatial resolution.
- High resolution satellite data were received, processed, and stored by **T**romsø **S**atellite **S**tation (TSS).
- Image transfer, further processing and printout was performed by our experiment group at **A**ndøya **R**ocket **R**ange (ARR), Andenes.

6.2.1. *APT-images at Andenes*

The APT data consist of subsampled AVHRR raw data (resolution reduced from 1 to 4 km) of channel 4 (~11 μm), which are transmitted as online video signals. A Technavia APT ground station was first operated at ARR to receive the data and display them for an immediate overview of weather situations. Due to unexplained but unacceptable disturbance of images received at the location of ARR (signal shielding by mountains around the station?) only very few satellite passes could be recorded. Therefore, the ground station was moved

to Andenes airport. There, the image quality was initially much better, but later on this was only occasionally true. Due to unknown electromagnetic disturbances (perhaps from the airport operations?) and some hardware problems, the amount and quality of the images was poor, but still helpful in some situations. A problem was posed by the unreliable grid computer which highlighted the importance of the availability of a grid in the APT-images for orientation.

6.2.2. Tromsø Satellite Station

The satellite receiving station in Tromsø is still developing. We had access to the available satellite data products with an interactive ordering system for satellite products, which was in a test phase during the campaign period. Two of these products were of special interest:

a. Quicklooks:
The raw data of AVHRR channel 4 are geometrically corrected and the radiometer data are transformed from the original 10 to 8 bit/pixel such, that maximum contrast is provided for each image. Unfortunately, there is no information about the grey values (like e.g. a greywedge) in the output image available. Therefore, no quantitative interpretation of these images is possible, and the intercomparison between two images is very difficult. Grid and coast lines are superimposed to the image, but were sometimes considerably misplaced. The quick look images of one satellite pass were available in three chunks of 360 image lines with 512 pixels per line, each of these containing a header for identification.

b. High Resolution Picture Transmission (HRPT) data:
The HRPT data contain the original digital counts measured by the AVHRR in all channels. Only channels 3 (central wavelength at ~3.7 μm), 4 (~11 μm) and 5 (~12 μm; for NOAA-9 and 11 only) were available from TSS. The calibration data necessary to transform digital counts to radiances or brightness temperatures were stored in a separate file by TSS.

Due to problems with the catalogue system it was not possible to order HRPT data interactively. Instead, operators from TSS cut our predefined area of interest out of the raw satellite data. These data were stored together with information about relative location of the cutout area on a separate computer (TSS-SUN 4 in Figure 6.1), from which we transferred them via an X.25 network.

Problems which sometimes occurred within this procedure were:
- not all requested passes recorded and processed by TSS;
- image navigation not possible due to wrong position of the cut-outs or wrong geographical informations;
- not all channels available;
- incorrect calibration data;
- network problems.

Table 6.1 gives an overview of the available HRPT and quicklook data with indications of their quality.

6.2.3. Computer facilities at ARR

Two SPARC-Workstations were carried to ARR in order to receive, process and store the satellite data delivered by TSS. A sketch of the hardware configuration is given in Figure 6.1. The workstations were plugged into the Local Area Network (LAN) of ARR. A disk drive of 1 GByte capacity and an Exabyte tape drive (2 GByte) were installed as mass storage devices. Image output was produced on a Canon color printer. The connection to TSS was provided by an X.25 interface on the ARR-LAN.

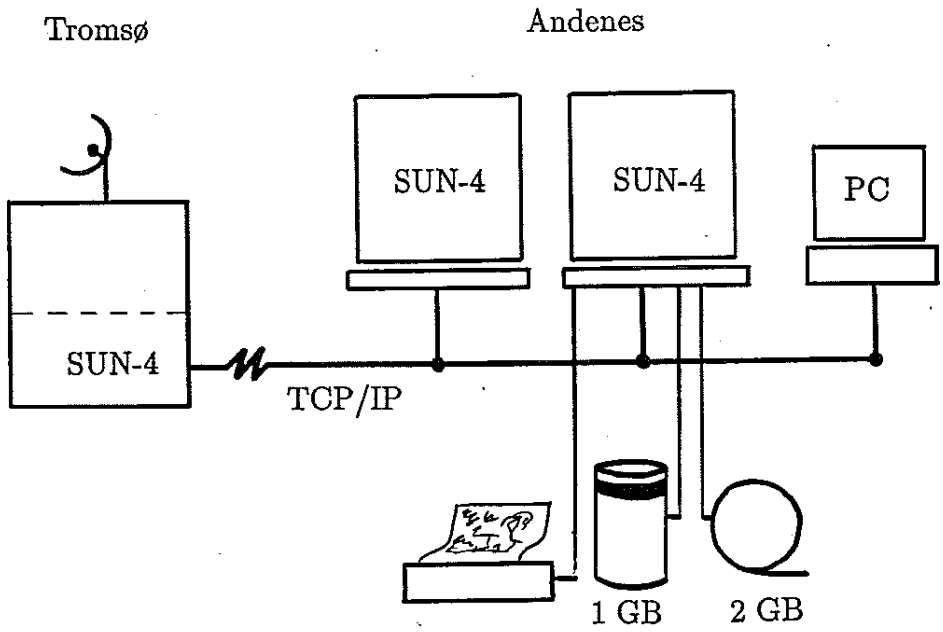

Figure 6.1: Sketch of the hardware equipment and network connections for satellite image processing at Andøya Rocket Range.

6.3. *Satellite data products during the campaign*

Only few operations had to be performed on the quicklook data after receiving them via network. Since the full satellite passes were divided into three different files (of 360 lines each) by TSS, they were recombined and the area of interest was cut out. After adding a header containing date, time and satellite orbit number the images were ready for printing. See appendix A for examples. Within the first week of the campaign all procedures were developed well enough to ensure the availability of a printed image within 3 hours after the satellite pass.

Much more care had to be taken of HRPT data. Due to the large amount of data the network transmission took up to half an hour for all three channels. Then, the data had to be checked and processed further. It turned out that it was not possible to deliver HRPT products during the campaign on a routine basis, but only a few example results could be provided during that period. This was due to the problems of TSS listed in chapter 6.2.2, and the initial occupation of the satellite data group with production and correction of quicklooks.

The HRPT products produced during the campaign were maps of satellite derived sea surface temperature (SST) and images of cloud brightness temperatures. For these, the digital counts had to be converted to radiances and brightness temperatures according to Lauritson (1979) using actual calibration coefficients. The SST is then obtained from AVHRR channels 4 and 5 by equation (1):

$$SST = a_o + a_1 \cdot T_4 + a_2 \cdot (T_4 - T_5) \qquad (1)$$

Values of coefficients a_i depend on the radiometers actual viewing angle. They were computed following the procedure of Schlüssel (1986). In Eq. (1) the SST will be in Kelvin, when mean values a_0 = 1.53 K, a_1 = 0.993 and a_2 = 3.17 are used and T_4 and T_4 - T_5 are given in K. Eq. (1) can give reasonable results for cloudless regions only. Those were detected by the algorithms of Saunders and Kriebel (1988).

Figure 6.2 shows, as an example, the mean SST in the area between 6 and 12 March 1991 composited of nine different satellite passes. The warm tongue of atlantic water reaching into the Fram Strait and towards the Barents Sea are clearly depicted as well as the rather well expressed oceanic polar front. White areas in the image represent either ice areas (as in the left and right upper

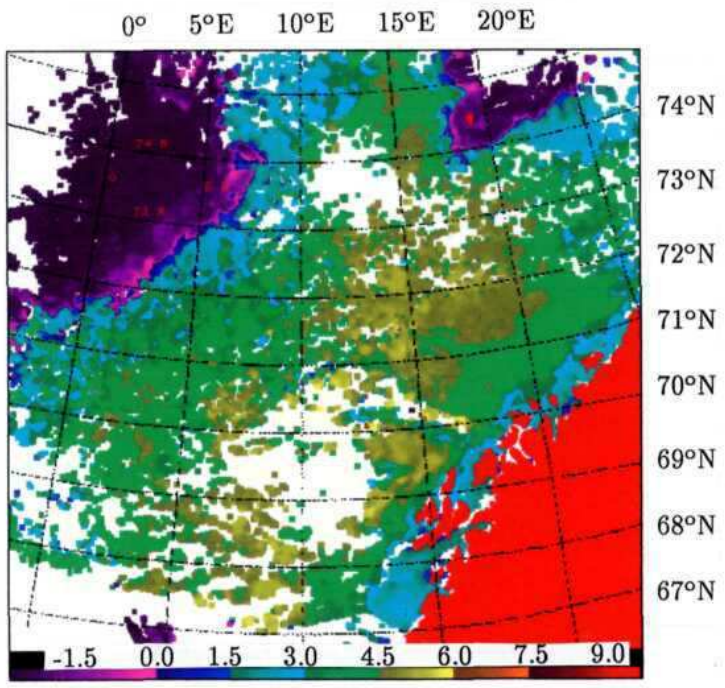

Figure 6.2: Mean values of the sea surface temperature (°C) for the period 6 March to 12 March 1991. The SST values derived from nine different satellite passes were averaged at those locations with multiply measurements available. Areas left blank were detected cloudy in all scenes. The Norwegian coast and the Bear Island are marked red. The geographical grid has distances of 1 degree latitude and 5 degrees longitude.

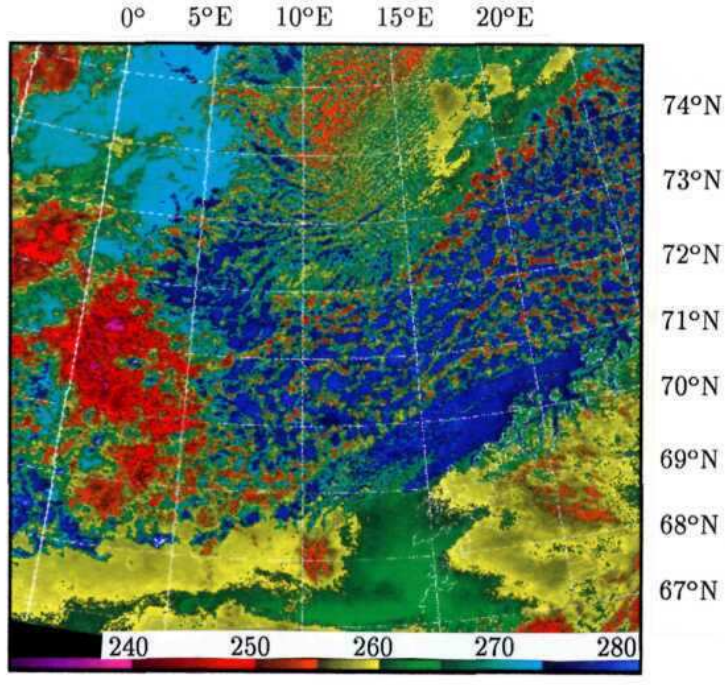

Figure 6.3: Temperatures in K as derived with the SST-algorithm for a single pass (12 March 1991) without masking of cloudy areas (coastlines are in white).

corners of the image) or pixels, that were not cloud free during the whole time. Each pixel was averaged over all cloud free pixels of a 9 x 9 pixel surrounding.

To estimate cloud top temperature (CTT) as well as SST equation (1) was applied to the whole scene without cloud removal (Figure 6.3). This procedure was, for simplicity, applied to each pixel in the image and guarantees correct SST's. It should also give realistic CTT values for boundary layer clouds, as their brightness temperatures should be influenced by atmospheric water vapour in a similar way as that of the sea surface. This numerical procedure introduces, however, slightly erroneous CTT's for large cloud top heights of up to 2 K. But as the problem of partially filled image pixels and varying cloud top height within a pixel does not allow all too accurate cloud top height estimates anyway, especially in convective situations, this error was assumed small enough to be tolerable. No algorithms were used to eliminate semitransparent or partly cloudy pixels. Therefore, it is not possible to derive top temperatures of low clouds, because pixels totally covered with low (warmer) clouds tend to show similar brightness temperatures as pixels partly filled with high (colder) clouds.

6.4. Future data evaluation

The HRPT data gathered during the campaign contain a lot of information not evaluated until now. Several points are of interest for future investigations with the data collected:

- comparison of the SST measurements made by ship and plane with the satellite derived values in order to validate the coefficients used in Eq. (1);
- derivation of temperature fields for cloud tops and bases to derive cloud thickness by help of radio sounding measurements. The vertical development of boundary layer clouds along cold air outbreaks could be studied from the results;
- derivation of simple statistics of cloud types, extensions and frequencies by help of cloud analysis algorithms.

During the campaign an interesting phenomenon in the surrounding of Bear Island lead to misinterpretations of the quicklook images. As shown in Figure 6.4 the water surrounding the island is warmer (darker) than the island itself but still colder than open water. This pattern is clearly seen on several successive satellite passes on March 8 and 9, but was not observable on the early passes on March 10. As this region became cloud covered during that day, the further development is unknown. The most likely interpretation seems to be

the building and vanishing of new ice. But since research flights into this area reported low level cloudiness, further investigation of this problem is necessary.

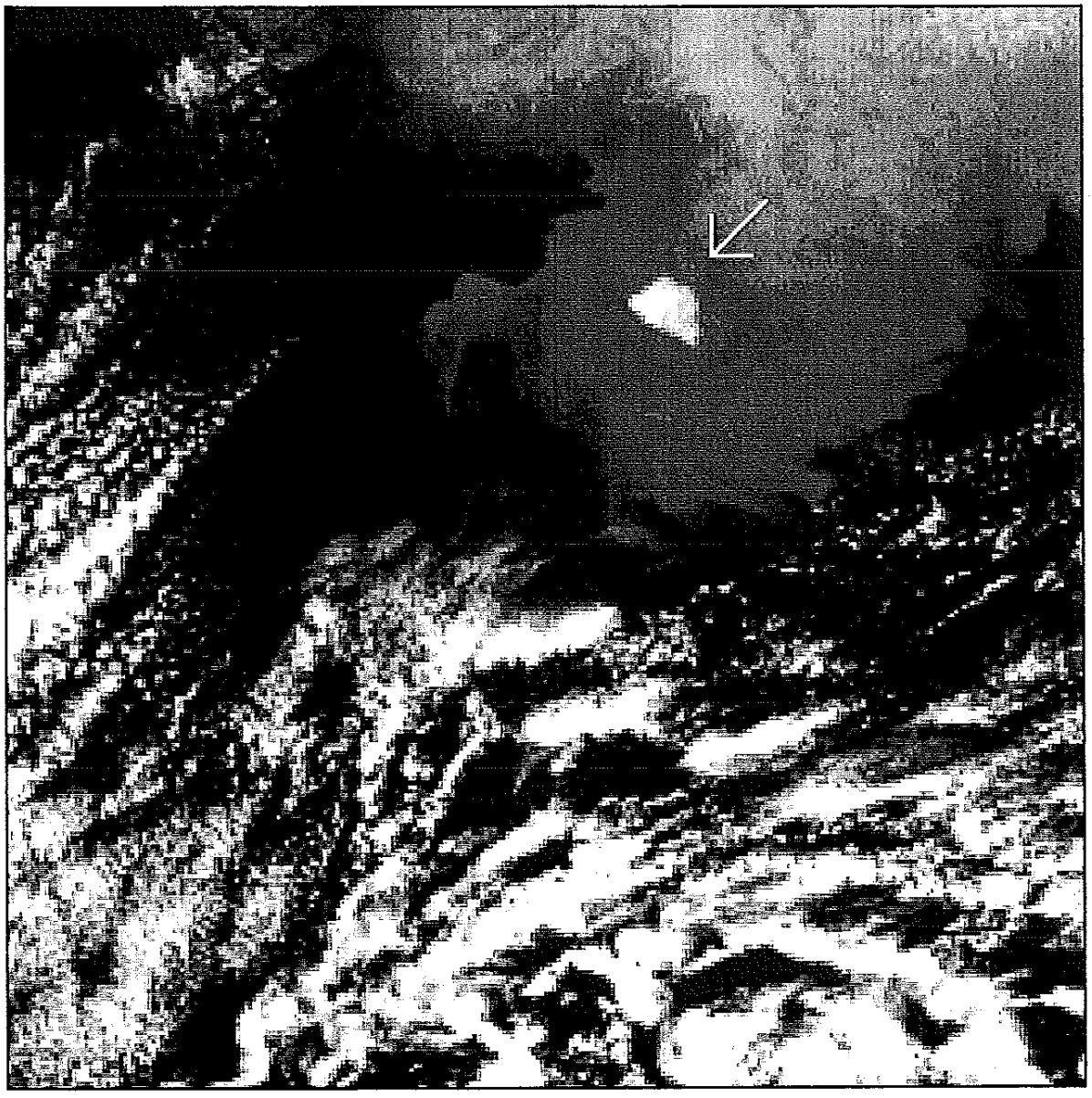

Figure 6.4: Brightness temperatures of AVHRR channel 3 for the area of Bear Island (white arrow) on 10 March 1991, 0222 UTC. The grey scale used is nonlinear to show maximum contrast. High brightness temperatures (warm) are dark and low ones are bright.

6.5. Conclusions

The experiences from the campaign and first off-line evaluations have shown, that the following points should be kept in mind for the next experiment:

- Satellite based products requiring clear sky conditions (SST, water vapour content, etc.) will only be available as weekly averages, because individual scenes are mostly too cloudy to obtain enough interpretable information.
- All algorithms for products needed during a campaign should be tested and verified prior to the beginning, since the time for development is severely limited by routine tasks as data sampling, transmission, printout, and the associated on-line problems.
- The satellite data group should install all hardware at least one week before the beginning of the campaign, because hard- and software must be adopted to data transmission facilities, possible changes in satellite data format at the receiving station, etc.
- For computing intensive tasks, like geometrical corrections, workstations with at least the power of a SUN/SPARC-station 2 are necessary.

References

Lauritson, L., G.J. Nelson, F.W. Porto (1979): Data extraction and calibration of TIROS-N/NOAA radiometers. NOAA Technical Memorandum, NESS 107, Washington.

Saunders, R.W., and K.T. Kriebel (1988): An improved method for detecting clear sky and cloudy radiances from AVHRR data. International Journal of Remote Sensing, Vol. 9, No. 1, 123-150.

Schlüssel, P. (1986): Infrarotfernerkundung von Oberflächentemperaturen sowie atmosphärischer Temperatur- und Wasserdampfstrukturen. Dissertation, Universität Kiel. 132 pp

Table 6.1: Overview of AVHRR products delivered by TSS. The TIP data files contain the calibration informations for HRPT data.

Date	Satellite	Orbit	Time	Quicklook chunks	Rawdata channels	TIP	Remarks
19.2.1991	N11	12380	02.38	1 2			
	N11	12381		1 2			
	N11	12386	12.42	1 2 3			
20.2.1991	N11	12394	02.32	1 2	4 5	x	
	N11	12395	04.13	1 2			
	N10	22992	09.00				
	N11	12400	12.23	1 2 3	3 4 5		no navigation
	N10	22997	17.15				
21.2.1991	N11	12408	02.11	1 2			
	N11	12409	03.52	1 2	3 4 5	x	no navigation
	N10	23006	08.26	1 2	4		
	N11	12414	12.22	1 2 3	3 4 5		
	N10	23011	16.43				
22.2.1991	N11	12422	01.59	1 2	4	x	
	N11	12423	03.40	1 2 3		x	
	N10	23020	08.03	1 2			
	N11	12428	12.01	1 2 3	3 4 5		
	N10	23025	16.19				
23.2.1991	N11	12436	01.49	1 2			
	N11	12437	03.30	1 2	3 4 5	x	
	N10	23035	09.21	1 2			
	N11	12443	13.31	1 2 3	3 4 5		no navigation
	N10	23039	15.56	1 2			
24.2.1991	N11	12450	01.38	1 2			
	N11	12451	03.19	1 2	3	x	
	N10	23049	08.58	1 2			
	N11	12456	11.39	1 2 3	3 4 5	x	
	N10	23054	17.13	1 2 3			
25.2.1991	N11	12464	01.27	1 2			
	N11	12465	03.08	1 2	3 4 5	x	
	N10	23063	08.35				
	N11	12471	13.08	2 3	3 4 5	x	QL useless
	N10	23068	16.51				
26.2.1991	N11	12479	02.56	1 2	3 4	x	
	N11	12480	04.37	1 2	3 4 5		
	N10	23077	08.12	1 2		x	
	N11	12485	12.57	2 3		x	
	N10	23082	16.27	1 2			
27.2.1991	N11	12493	02.44	1 2	3 4 5	x	
	N11	12494	04.35	1 2			
	N10	23091	07.48	1 2			
	N11	12499	12.55	2 3	3 4 5	x	
	N10	23096	16.14	1 2 3			
28.2.1991	N11	12507	02.43	1 2	3 4 5	x	
	N11	12508	04.24	1 2			
	N10	23106	09.05	1 2			
	N11	12513	12.34	1 2 3	3 4 5	x	
	N10	23111	17.31	1 2		x	

Date	Satellite	Orbit	Time	Quicklook chunks	Rawdata channels	TIP	Remarks
1.3.1991	N11	12521	02.22	1 2	3 4 5	x	
	N11	12522	04.03	1 2			
	N10	23120	08.42	1 2	3 4	x	
	N11	12527	12.23	1 2	3 4 5	x	
	N10	23125	16.57	1 2			
2.3.1991	N11	12535	02.10		3	x	
	N11	12536	03.51	1 2			
	N10	23134	08.18	1 2 3			
	N11	12541	12.11	1 2 3	3 4 5	x	
	N10	23139	16.35	1 2			
3.3.1991	N11	12549	01.59	1 2			
	N11	12550	03.40	1 2		x	
	N10	23148	07.55	1 2			
	N11	12555	12.10	1 2 3	3 4 5	x	
	N10	23153	16.11				
4.3.1991	N11	12563	01.48	1 2 3			
	N11	12564	03.29	1 2 3	3 4 5	x	
	N10	23163	09.12	1 2 3			
	N11	12569	11.49	1 2 3			
	N10	23168	17.28	1 2 3			
5.3.1991	N11	12577	01.34	1 2			
	N11	12578	03.15	1 2	3 4 5	x	
	N10	23177	08.47	1 2 3			
	N11	12584	13.17	1 2 3			
	N10	23182	17.03	1 2 3	3 4 5		
6.3.1991	N11	12591	01.23	1 2			
	N11	12592	03.04	1 2	3 4 5	x	
	N10	23191	08.24	1 2 3			
	N11	12598	13.06	1 2	3 4 5	x	no navigation
	N10	23196	16.40	1			
7.3.1991	N11	12606	02.53	1 2	3 4 5	x	Rawdata useless
	N11	12607	04.34	1 2	3 4 5	x	no navigation
	N10	23205	08.01	1 2	3 4		
	N11	12612	12.54	1 2 3	3 4 5	x	
	N10	23210	16.17	1 2 3		x	
8.3.1991	N11	12620	02.42	1 2			
	N11	12621	04.22	1 2	3 4 5	x	no navigation
	N10	23220	09.18				
	N11	12626	12.43	1 2 3	3 4 5	x	no navigation
	N10	23224	15.53	1 2 3			
9.3.1991	N11	12634	02.32	1 2	3 4 5	x	
	N11	12635	04.13	1 2			
	N10	23234	08.56	1 2			
	N11	12640	12.33	1 2 3	3 4 5	x	
	N10	23239	17.10	1 2 3			
10.3.1991	N11	12648	02.21	1 2	3 4 5	x	
	N11	12649	04.02	1 2			
	N10	23248	08.43	1 2			
	N11	12654	12.22	2 3	3 4 5	x	
	N10	23253	16.49	1 2			
11.3.1991	N11	12662	02.10	1 2	3 4 5	x	
	N11	12663	03.51	1 2			
	N10	23262	08.10	1 2		x	
	N11	12668	12.1		3 4 5	x	
	N10	23267	16.26				
12.3.1991	N11	12676	01.58	1 2	3 4 5	x	
	N11	12677	03.39	1 2			
	N10	23276	07.47	1 2			
	N11	12682	12.00	1 2 3			
	N10	23281	16.03				
	N09	32184	08.31		3 4 5		

7. *Intercomparisons*

(B. Busack, Meteorologisches Institut der Universität Hamburg)

7.1. *General remarks*

In the course of the ARKTIS '91 experiment only one formal intercomparison between the FALCON-20 and the DO-128 took place on 13 March 1991. However, there were incidential intercomparisons between aircraft and platforms, when VALDIVIA and Bear Island were incorporated into the flight pattern on several flight missions. Table 7.1 gives a summary of formal (f) and incidental (i) intercomparisons during the experiment. Further details can be obtained from Appendix C and the flight catalogues in section 5.2.

Table 7.1: Summary of formal (f) and incidental (i) intercomparisons during the ARKTIS '91 experiment.

Date	Time	Platforms, resp. aircraft	Measurements	IC
22.02	130210 - 130300	Valdivia - Falcon	level 90 m	i
24.02	141940 - 142015	Valdivia - DO-128	level 45 m	i
25.02	095240 - 101300	Falcon - Bear Island	profile	i
04.03	104500 - 104700	Valdivia - DO-128	level 110 m	i
	105200 - 105400	Valdivia - DO-128	level 50 m	i
13.03	131030 - 131545	Falcon -	level 90	f
	131040 - 131900	DO-128		
	131600 - 132150	Faclon -	profile	f
	131900 - 132900	DO-128		

Since a detailed analysis of the data of the platforms and the aircraft has not been finished yet, only some preliminary results from the formal intercomparison flight between FALCON-20 and DO-128 are presented below.

7.2. *Aircraft-aircraft intercomparison (FALCON-20 / DO-128)*

On 13 March at the beginning of a regular flight mission of the FALCON-20, both aircraft performed a level run of about 20 nm at 90 m height and a final profile up to 3500 m in the comparison area between Andenes and way points A/X and Y (see Appendix D). Unfortunately these flight sections were not flown simultaneously, because both aircraft cannot fly side by side due to different flight speeds (see section 5.1). However, the DO-128 followed the FALCON-20

immediately and was 7 minutes left behind at the end of the intercomparison mission.

Figure 7.1 shows vertical profiles of temperature, humidity, wind speed and direction measured by both aircraft at B1. Since they flew only one profile for intercomparison it is difficult to work out systematic errors and to distinguish them from local air mass inhomogeneities. That goes for the horizontal flight leg, too. Nevertheless, the temperature profiles differ considerably and moreover these differences vary with height. They are about 0.5°C on the lower hundred meters and come up to 1.5°C above 1500 m. These varying differences may be caused by icing up of the DO-128 in the strong turbulent showers of snow intersected by both aircraft during the profile ascent, but a final statement requires a more intense data evaluation.

A comparison of the Vaisala Humicap sensors of the FALCON-20 and the DO-128 is useless at the moment, because the DO-128 humidity sensor drifted throughout the experiment and a definite relation between relative humidity and voltage has not been found until now.

The profiles of wind speed and direction agree in a remarkable way, although the height of the wind direction maxima differs by about 200 m which might be effected by the locally different cloud structures.

One second average data from the horizontal intercomparison flight at 90 m height are shown in Figure 7.2. The time series of both aircraft are translated to distance in order to present the same length interval. The horizontal leg crossed a convergence line with heavy snowfall and strong turbulence (not to be seen in these one second average data). There is a strong wind shift from 230° to 330°, while the wind speed decreases from 12 to 3.5 m/s. The temperature difference is 1°K. These changes are represented by both aircraft.

Table 7.2 shows the horizontal averages of wind speed, direction, horizontal wind components (parallel and normal to the mean wind direction in the planetary boundary layer), temperature, humidity and pressure on this flight leg.

Table 7.2: Mean values of wind speed FF, wind direction DD, horizontal wind components u and v, temperature T, water vapour mixing ratio m and pressure p during the horizontal intercomparison flight of FALCON-20 and DO-128.

	DO-128	FALCON
p [hPa]	1002.93 ± 0.20	1002.51 ± 0.02
T (°C]	-0.93 ± 0.56	-1.54 ± 0.50
m [g/kg]	4.21 ± 0.43	2.87 ± 0.24
v [m/s]	4.40 ± 6.30	2.64 ± 6.14
u [m/s]	3.07 ± 1.60	2.75 ± 1.22
DD [deg]	275.37 ± 50.93	293.12 ± 55.46
FF [m/s]	7.22 ± 4.34	6.25 ± 3.83

The differences in air temperature are 0.61°C and in the same sense as observed during the profile flight (Fig. 7.1). The averages of wind speed differ by about 1 m/s, which appears to be within the absolute accuracy limits of wind sensors on aircraft. The differences in the wind direction are two-handed. The FALCON measured a 105° wind shift whereas the DO-128 measured a 90° veering. Moreover the horizontal flight leg of the FALCON behind the wind shift is longer than the DO-128 one, which leads to a higher mean value.

A final conclusion concerning the accuracy of the aircraft measurements is not possible as long as the detailed data analysis has not been finished.

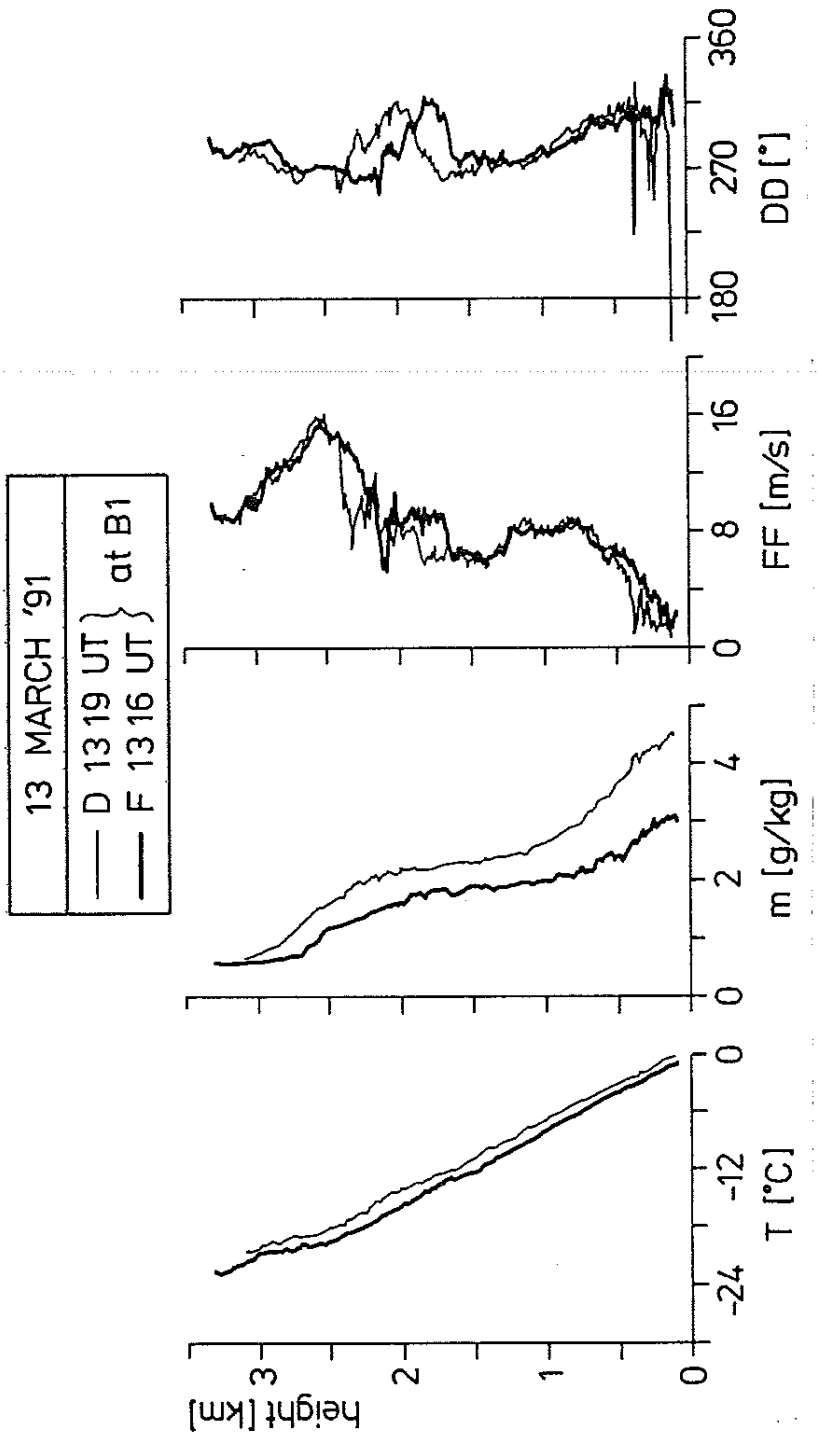

Figure 7.1: Vertical profiles of temperature (T), water vapour mixing ratio (m), wind speed (FF) and direction (DD) measured by FALCON (F) and DO-128 (D) in the intercomparison area between A/X and Y on 13 March 1991.

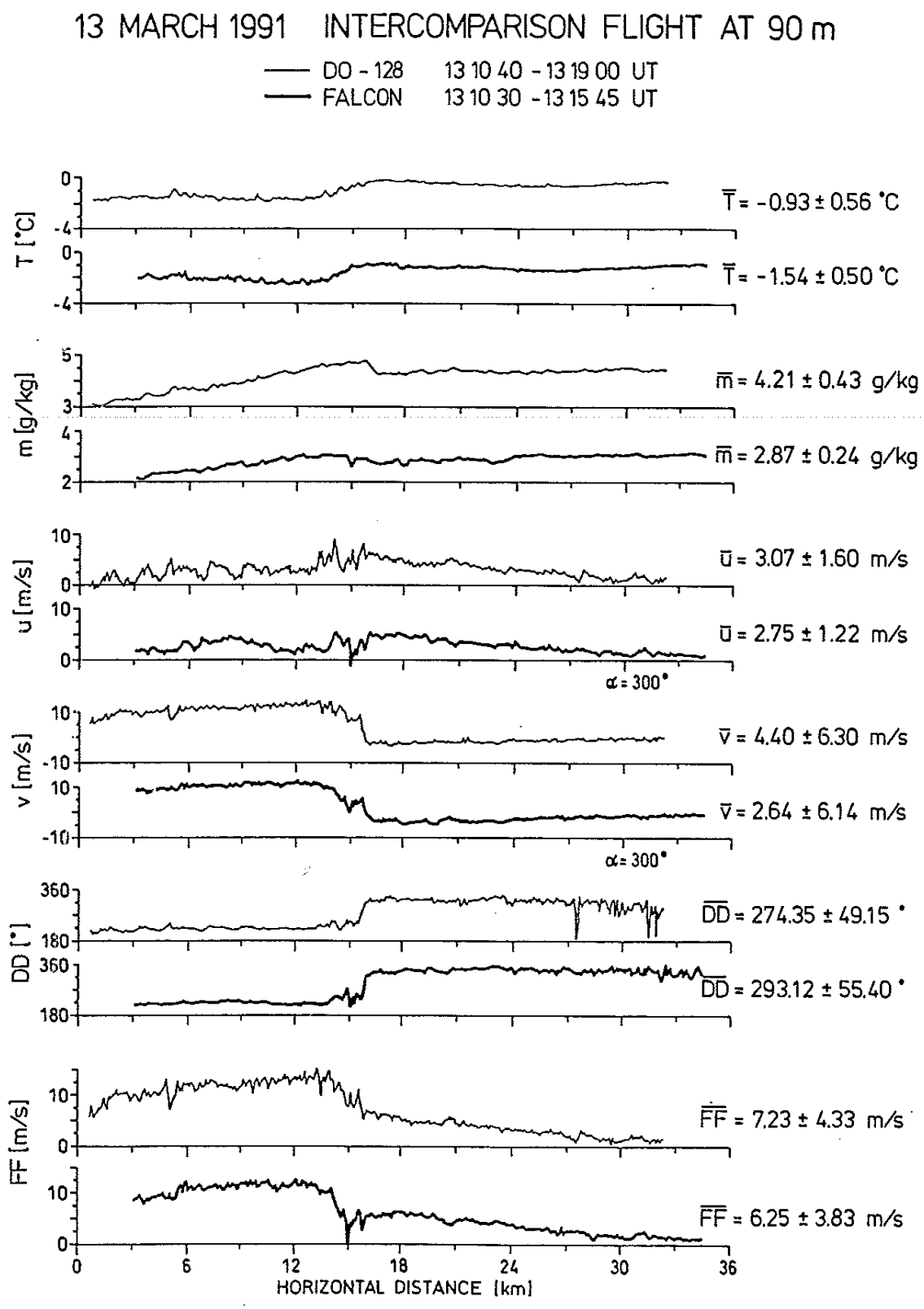

Figure 7.2: Time series of air temperature (T), water vapour mixing ratio (m) measured by Vaisala humicaps, wind components parallel (u) and normal (v) the the mean boundary layer wind (α = 300°), wind speed (FF) and direction (DD) measured by FALCON (F) and DO-128 (D) at 90 m height in the intercomparison area between Andenes and A/X on 13 March 1991.

8. *Concluding remarks*

(B. Brümmer, Meteorologisches Insitut der Universität Hamburg)

In this final section we attempt to assess the degree to which the logistical and technical part of the experiment was successful and to which the scientific objectives have been met.

8.1. *Assessment of logistical and technical success*

Altogether the logistical structure worked out well and the data collection of most of the systems was successful. This is due to the engagement of all participants doing excellent jobs on the ship, on the aircraft and on the ground stations: Particularly mentioned and acknowledged is the organizational support by the Andøya Rocket Range.

However, also some weak points should be mentioned because this may help to improve these shortcomings in futures experiments.

The communication links to and from VALDIVIA turned out as one weak point. The communication facilities on board the VALDIVIA should be improved to obtain better links between VALDIVIA on one side and the operation center, the aircraft or the international meteorological networks on the other side. Although promised to the synoptic servies, the VALDIVIA data could not be submitted on-line to the meteorological networks to be used for the routine analyses and prognosis programmes.

Another weak point was the humidity measurement on board the DO-128 aircraft. For some, still unknown reason the relative humidity sensor did not indicate values larger than 89%, so that in large parts of each flight mission the humidity is missing.

8.2. *Assessment of scientific success*

The scientific success of field experiments like ARKTIS 1991 which have to be planned for a fixed place and a fixed period, heavily depend on the weather conditions which really occur. In this regard the experimentators were lucky. The weather conditions were favourable, so that all three topics, namely cold air outbreaks, arctic marine stratus clouds and subsynoptic-scale vortices, could be investigated.

In all eight flight missions open or closed cellular cloud structures were met in situations of cold air advection. A marine stratus/stratocumulus situation lasted for several days in the region of VALDIVIA and could be observed extensively. Two subsynoptic-scale vortices could be detected by aid of the NOAA satellite images; both were documented by the measurements at VALDIVIA and one vortex could be intersected by both aircraft.

As already mentioned in the introduction, the field experiment ARKTIS 1991 is a continuation of the research which began with the field campaign ARKTIS 1988 in May in the area west of Spitsbergen. According to the earlier season, much larger air-sea temperature differences and consequently larger heat fluxes were met this time. Whereas the largest sensible heat fluxes were around 60 W/m^2 in May 1988, fluxes up to around 250 W/m^2 were measured in this experiment. Furthermore, due to the larger heat flux from the surface and the longer distance from the ice edge, the top of the boundary layer in cellular convection situations was between 1500 and 3000 m height compared to 500 to 1200 m in May 1988.

Beside aircraft traverses through cellular convection at different levels, also flights above the convective layer could be made. From the latter ones we shall obtain the radiation balance and hope to get an answer to the question whether the cellular pattern is also reflected in form of gravity waves in the air above the convective layer.

Not in all cases of cold air outbreaks the air flow over the experimental area originated from the region around Bear Island. In these cases the initial conditions of the cold air outbreak are not exactly known and have to be extracted as good as possible from the synoptic weather charts by interpolation techniques.

Basically, the two ground stations, Bear Island and VALDIVIA, only allow a two-dimensional analysis of the cold air outbreak. This is a major shortcoming because effects of divergence, vorticity or baroclinicity on the boundary layer development cannot be taken into account. We hope to overcome this shortcoming - at least partly - by using other routine weather observations in the surrounding or the results of three-dimensional mesoscale routine forecast models.

We are aware that this can only be a compromise, because the needed resolution of these fields is clearly smaller than the distance between the routine

weather stations. For future experiments in this area it is therefore necessary to set up a fine-mesh network of ground stations, i.e. ships and buoys. The plannings of the next experiment, which is scheduled for March 1993, take these requirements into account.

Acknowledgement

The authors thank Mrs. B. Zinecker for typing with patience the various versions of the manuscript and Mr. M. Lüdicke and Mrs. M. Grunert for preparing graphical representations and modifying several of the computer diagrams.